NOVA SCHOOL OF
SCIENCE & TECHNOLOGY

DEPARTAMENT OF
<NAME OF THE DEPARTMENT>

VICTOR FEIJÓ DE CARVALHO
Master in Scientific Illustration

LATE JURASSIC MICROFOSSILS FROM CAMBELAS BONEBED, WESTERN PORTUGAL

PALAEOECOLOGY AND PALAEOENVIRONMENTAL ASPECTS

MASTER IN PALAEONTOLOGY
NOVA University Lisbon
September, 2024

NOVA SCHOOL OF SCIENCE & TECHNOLOGY

DEPARTAMENT OF
DEPARTMENT OF EARTH SCIENCES

LATE JURASSIC MICROFOSSILS FROM CAMBELAS BONEBED, WESTERN PORTUGAL

PALAEOECOLOGY AND PALAEOENVIRONMENTAL ASPECTS

VICTOR FEIJÓ DE CARVALHO

Master in Scientific Illustration

Adviser: Lígia Nunes de Sousa Pereira de Castro
Assistant Professor, NOVA School of Science and Technology/NOVA FCT

Co-advisers: Bruno Camilo Silva
Centro de Paleobiologia e Paleoecologia da Sociedade de História Natural de Torres Vedras

Examination Committee:

Chair: Paulo Alexandre Rodrigues Roque Legoinha,
Full Professor, NOVA School of Science and Technology/NOVA FCT

Rapporteurs: Fátima Lopes da Silva,
NOVA School of Science and Technology/NOVA FCT

Adviser: Lígia Nunes de Sousa Pereira de Castro,
Assistant Professor, NOVA School of Science and Technology/NOVA FCT

Members: Kenneth Angielczyk,
Full Professor, The University of Chicago

MASTER IN PALEONTOLOGY

NOVA School of Science and Technology/NOVA FCT
September, 2024

Late Jurassic microfossils from Cambelas bonebed, western Portugal. Palaeoecology and palaeoenvironmental aspects

Acknowledgements

I want to express my deepest gratitude to the individuals listed below, whose invaluable support and contributions made this work possible:

My advisor Prof. Lígia Castro, and my co-advisor Bruno Camilo Silva. I wouldn't have words to describe how important you were on this long journey.

I would like to express all my gratitude to Ricardo Araújo, from Instituto Superior Técnico, for his priceless and essential help.

A huge special thanks to Marcelle Feijó de Carvalho, Darja Dankina, and Mariana Branco.

I would like to thank my fellow master's students who made this task easier: Sofia Patrocínio, and Pedro Andrade, who gladly helped me to screen wash the sediments, André Burigo, Beatriz Mascarenhas and Pedro Costa. I also thank my dear colleagues from Sociedade de História Natural (SHN): Hilde Desmet, Ignace Nerinckx and Verena Fuchs. A special thanks to Graça Ramalheiro, for finding this amazing quarry.

I would also like to thank Sílvia Carvalho, from Instituto Superior Técnico, Carlos Natário, Jorge Sequeira, from the Geological Museum of Lisbon, Carlos Galhano, from NOVA School of Science and Technology/NOVA FCT, and the team of technicians from the HERCULES Laboratory of the University of Évora.

To finish I would like to thank those who, even though they were far away, were of great help: Dr. Roger Malcolm Harris Smith, from the University of the Witwatersrand, Jacob Van Veldhuizen, from the University of Colorado Museum of Natural History, Matthew Miller, from the Department of Paleobiology of the National Museum of Natural History, Smithsonian Institution, Prof. Gregory Wilson Mantilla and Dr. David DeMar from the Burke Museum of Natural History and Culture, Ulrike Hermes, from the Universität Hamburg and the Geosciences Library Team from the Freie Universität Berlin.

Thank you all once again!

Abstract

Understanding the evolutionary trajectory and phylogenetic relationships of the Multituberculata order, an extinct group of nontherian mammals with a fossil record spanning from the Middle Jurassic to the Late Eocene, remains a significant challenge due to substantial gaps in the fossil record. Recent excavations at the Ulsa quarry, within the Freixial Formation, dating from Tithonian (Upper Jurassic), in Torres Vedras Municipality (Portugal), have yielded a notable discovery: the partial jaw of an odontologically immature multituberculate exhibiting distinct morphology and a rare alternate posteroanterior tooth replacement pattern, a trait previously identified in only two other species. Detailed morphological and phylogenetic analyses have confirmed this specimen as a new species of Pinheirodontidae, providing the first detailed insights into the jaw anatomy and tooth replacement pattern of this family. The origin from a fossiliferous multi-taxonomic bonebed is particularly significant, as it includes rare articulated post-cranial bones of Mesozoic multituberculates, offering a unique view of these ancient mammals. The taphonomic study of both macro- and microfossils, combined with palynological and geological analyses of the Ulsa quarry strata, has provided significant insights into the paleoenvironment and paleoclimate, depicting a semiarid to arid climates, with excessive evaporation and water scarcity. In the low-energy depositional settings of the Ulsa quarry, the limited availability of water in the form of springs and seeps likely turned that environment into deadly traps. Animals already weakened by extended dry seasons, probably became entrapped and perished in the mud. The entombed remains, now exposed in the layers on the coasts of western Portugal, reveal the richness of the Lusitanian Basin and its significant paleontological potential. This discovery not only enriches the understanding of the phylogenetic relationships of this obscure family of multituberculates but also

underscores the importance of the Portuguese fossil record. The findings extend beyond taxonomy, offering a deeper comprehension of the evolutionary and ecological dynamics that shaped the ancient environments of the Iberian Peninsula.

Keywords: Multituberculata, Pinheirodontidae, Teeth Replacement, Lusitanian Basin, Tithonian, Paleoenvironment, Paleoclimate

RESUMO

A compreensão da trajetória evolutiva e das relações filogenéticas da ordem Multituberculata, um grupo extinto de mamíferos não-Theria com um registo fóssil que abrange desde o Jurássico Médio até ao Eocénico Final, continua a ser um desafio significativo devido a lacunas substanciais em seu registo fóssil. Escavações recentes na jazida da Ulsa, Formação de Freixial, datada do Titoniano (Jurássico Superior), em Torres Vedras (Portugal), resultaram numa descoberta notável: a mandíbula parcial de um multituberculado odontologicamente imaturo, exibindo uma morfologia distinta e um raro padrão posteroanterior alternado de substituição de dentes, uma caraterística previamente identificada em apenas duas outras espécies. Análises morfológicas e filogenéticas detalhadas confirmaram este espécime como uma nova espécie de Pinheirodontidae, fornecendo os primeiros detalhes sobre a anatomia da mandíbula e os padrão de substituição de dentes desta família. A sua origem de um leito ósseo fossilífero multi-taxonómico é particularmente significativa, uma vez que inclui raros ossos pós-cranianos articulados de multituberculados mesozóicos, oferecendo uma visão única destes antigos mamíferos. O estudo tafonómico dos macro e microfósseis, combinado com análises palinológicas e geológicas dos estratos da jazida da Ulsa, forneceu informações significativas sobre o paleoambiente e o paleoclima, descrevendo um clima semiárido a árido, com evaporação excessiva e escassez de água. Nos ambientes de deposição de baixa energia da jazida da Ulsa, a disponibilidade limitada de água sob a forma de nascentes e poços provavelmente transformava aquele ambiente numa armadilha mortal. Os animais, já enfraquecidos pelas longas estações secas, provavelemente ficaram presos e pereceram na lama. Os restos sepultados, agora expostos nas camadas da costa ocidental de Portugal, revelam novamente a riqueza da Bacia Lusitânica e o seu importante potencial paleontológico. Esta descoberta não só enriquece a compreensão das

relações filogenéticas desta obscura família de multituberculados, como também denota a importância do registo fóssil português. Os resultados vão para além da taxonomia, oferecendo uma compreensão mais profunda das dinâmicas evolutivas e ecológicas que moldaram os ambientes antigos da Península Ibérica.

Palavras chave: Multituberculata, Pinheirodontidae, Troca Dentária, Bacia Lusitaniana, Titoniano, Paleoambiente, Paleoclima

CONTENTS

List of Figures

List of Tables

ACRONYMS

BMNH	British Museum of Natural History
DORCM	Dorset County Museum
IPFUB	Institute of Palaeontology of the Free University of Berlin
HCL	Hydrochloric acid
HF	Hydrofluoric acid
LACM	Natural History Museum of Los Angeles County
NHMUK	Natural History Museum (London)
SHN	Sociedade de História Natural
UCM	University of Colorado Museum
USNM	Smithsonian National Museum of Natural History

1

INTRODUCTION

1.1 Microfossils and their Relevance for Palaeontology

The evidence of the existence of any deceased organism, its remains or its activity, which is susceptible to integrating the geological record due to natural processes, is referred to as a fossil (Behrensmeyer *et al.*, 2000; Milsom & Rigby, 2009). Among the different forms of relationship classifications, fossils are frequently divided into two groups according to their size: microfossils (including calcareous nannofossils) and macrofossils (Armstrong & Brasier, 2005; Kanungo *et al.*, 2017). Following this premise, microfossils are any fossils that require a binocular magnifier, microscopes (optical or electron) or computed tomography scans to be effectively studied due to their size and distinctive features (Armstrong & Brasier, 2005; Saraswati & Srinivasan, 2016). Since this classification is based solely on size criteria and all the six living kingdoms (Archaebacteria, Eubacteria, Protista, Fungi, Plantae and Animalia) have microscopic life forms, it makes microfossils extremely heterogeneous. Besides the remains of unicellular and multicellular microorganisms (microbiota), microfossils also include dissociated elements and skeletal fragments of larger organisms (macrobiota) of unrelated distant fossil groups (mammal teeth, fish teeth and scales, pollen, etc.) (Bignot, 1985; Milsom & Rigby, 2009). From a geological point of view, the most useful microfossil groups are those that provide the most information when utilised in palaeoenvironment interpretations. For this reason, they are best studied. This utilitarian view of microfossils has already been criticised (Lipps, 1981),

since most of the time these fossils are conveniently used as biostratigraphic markers in applied Geology, with little concern for the Palaeobiology and Evolution of these microfossils as living organisms. In addition, most of the research carried out is done by companies and industries with an economic focus, rather than by researchers linked to laboratories and universities (Lipps, 1981; Bignot, 1985).

The main groups of microfossils (Fig. 1.1) are, among others: Foraminifera, Ostracoda, Pteropods, Radiolaria, Diatoms, Chitinozoa, Conodonts, Spores and Pollen (Saraswati & Srinivasan, 2016). The chemical nature of the fossilisable parts of these ancient life forms can vary from silica to carbonate or phosphate, and sometimes even non-mineralized organic compounds like chitin, sporopollenin and pseudochitin (De Wever, 2020). Considering this chemical composition, the methodology used for the treatment and laboratory preparation of microfossils may vary depending on the study. Generally, these particles of organic origin are found in deposits in which the sedimentary structure is composed of very thin grain size, mainly silt and clay (Carvalho, 2004). However, the measurements that define a microfossil are somewhat arbitrary and may vary depending on the author. For example, according to Drewes (2006), the size of microfossils can range from 0.001 mm (= 1 micron) up to 1-2 mm. For Carvalho (2004), the microfossils size would not exceed 5 mm, except for some foraminifera. Their microscopic dimensions also demand different techniques for collecting, preparation, processing and analysis, culminating in their method of study – Micropalaeontology (Armstrong & Brasier, 2005). However, some authors may argue that the principles of Micropalaeontology are nothing more than the principles of Palaeontology itself (Kleinpell, 1971; Lipps, 1981). The employment of the term "Micropalaeontology" for the study of tiny ancient organisms was used for the first time in 1883 by Arthur H. Foord in an article called "Contributions to the micropaleontology of the Cambro-Silurian rocks of Canada" (Croneis, 1941). Nevertheless, an arbitrary tendency has emerged over the years to limit the use of the term "Micropalaeontology" to the study of microfossils with mineral walls, like foraminifera and ostracods, whereas the study of microfossils with organic walls, such as pollen grains and spores, dinoflagellate cysts, and acritarch cysts is often called Palynology or Palaeopalynology (Armstrong & Brasier, 2005).

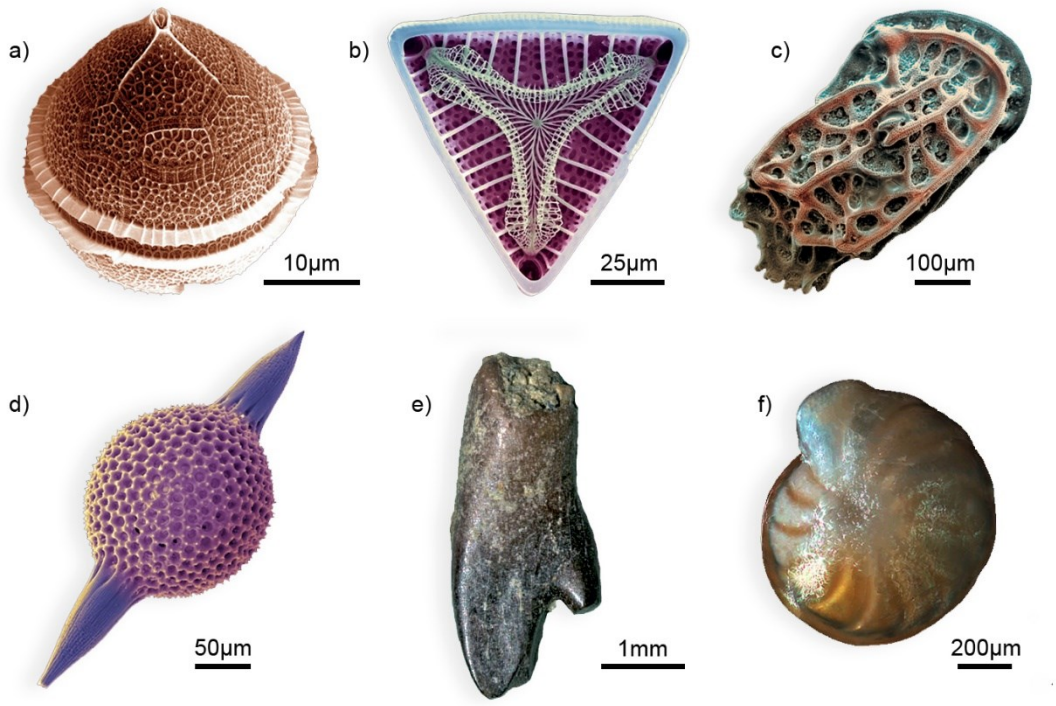

Figure 1.1 — An example of the heterogeneity found within the various groups of microfossils and their different chemical compositions: a) organic-walled microfossil: dinoflagellate cyst *Protoperidinium* sp. (Wever, 2020); b) photosynthetic siliceous algae: diatom *Entogonia* cf. formosa (Wever, 2020); c) calcareous ostracod microfossil *Bosasella elongate* (Wever, 2020); d) siliceous plankton, radiolarian *Spongatractus* sp. (Wever, 2020); e) phosphatic microfossils: incisor of the multituberculate *Meniscoessus* sp. in lingual view (De and Brand *et al.*, 2022); f) calcareous foraminifera *Cibicidoides kullenbergi* (Holbourn & Henderson, 2002).

Micropaleontology is arguably the area of Palaeontology that offers the most information about defining and comprehending the age and depositional conditions of a sedimentary basin when it comes to Geology (Carvalho, 2004). That is because microfossils occur in almost every type of sediment, covering different environments, from marine, brackish water, fresh water and terrestrial, from different ages and in more quantity than macrofossils, making them a better representation of the overall biological diversity of that ecosystem. Besides that, their durability through fossil diagenesis and worldwide distribution makes microfossils an essential agent of biostratigraphy (Milsom & Rigby, 2009). This subject relies on the taxonomy of microfossils and their temporal and spatial distribution to delineate geological periods and establish standardised biostratigraphical units. These biozones are defined by the occurrence of specific fossil *taxa* or narrow stratigraphic intervals characterised by *taxa* with overlapping

ranges, which are used in dating, correlating stratigraphic sequences and determining the environment of the deposits (Saraswati & Srinivasan, 2016). The use of microfossils in stratigraphic analysis was mainly initiated in the 1920s by workers from American and Russian oil companies (Lipps, 1981). Later, in the 1960s, with the improvement of radiometric techniques, the inference of absolute ages began, giving rise to biochronology (Carvalho, 2004). This made it possible to correlate biozones with numerical age information via radiometric dating, contributing to the refinement of the Geological Time Scale (https://www.iugs.org/ics).

Beyond Biostratigraphy, Micropaleontology plays a crucial role at various stages of basin analysis and palaeoenvironmental reconstructions. The understanding of past climates has been greatly enhanced by microfossils as their sensitivity to environmental conditions provides crucial insights. The tiny size of microfossils allows a small sample to contain a complete ecosystem of microorganisms, thus enabling the reconstruction of factors such as climate, water depth and salinity, among others (Bercovici & Vellekoop, 2017). In the meantime, basin analysis establishes the stratigraphic framework and provides essential data for reconstructing the palaeogeography and subsidence history of these basins through microfossils for an effective exploration of their mineral and fuel resources (Saraswati & Srinivasan, 2016).

1.2 Palynology and Palynomorphs

The term "Palynology" was coined by Hyde and Williams (1944) to replace the designations "pollen science" or "pollen analysis", branches of botanical science that studied pollen (Traverse, 2007; Bercovici & Vellekoop, 2017). However, over time, Palynology came to refer to the study of palynomorphs, a term introduced by Tschudy (1961), which groups all the organic-walled microfossils (dinoflagellate cysts, acritarchs, pollen and spores) (Halbritter *et al.*, 2018), according to their shared preparation technique: maceration (Sorkhabi, 2020). It is important to emphasise that this designation is given within Palaeontology, in which this area of study is often referred to as “Palaeopalynology”, since the term "Palynology" is also used for the study of present-day pollen and spores, for example in Forensic Palynology (Milne *et*

al., 2004; Bryant & Jones, 2006; Mildenhall *et al.*, 2006). Although geological interest in fossilised pollen developed in the 20th century, the study of these organisms predates it. The first description of pollen grains and spores was done by Göppert (1837), who also made their first depiction by pencil illustrations (Fig. 1.2).

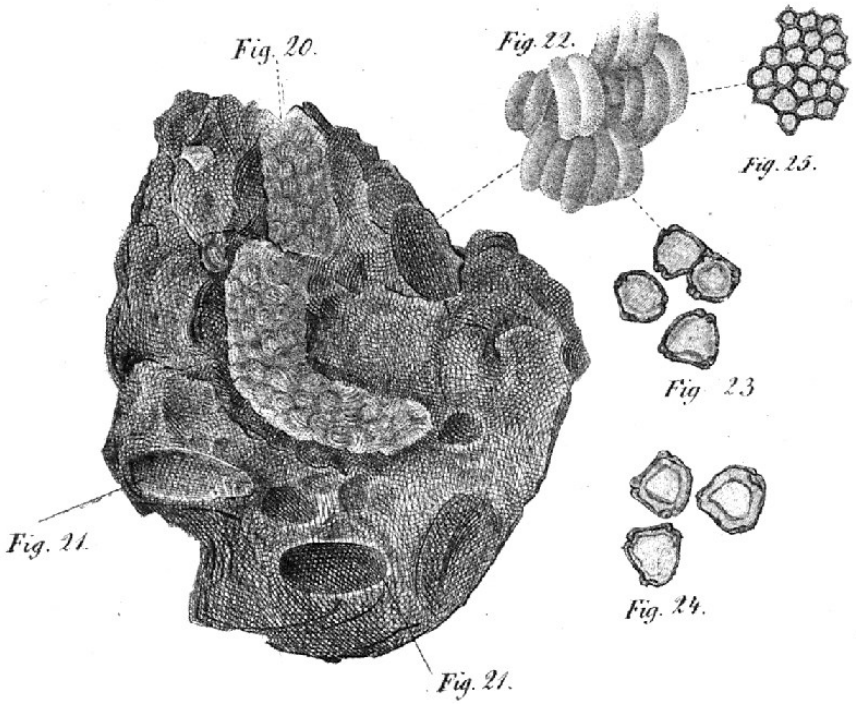

Figure 1.2 — The first depiction of fossilised seeds of a certain pine species and fossil pollen grains (amplified 270x) (Göppert, 1837: Pl. 2, Figs. 20 to 25).

Palynomorphs include pollen, spores, fungi, and planktonic microorganisms with non-mineralized cellular walls, such as dinoflagellates cysts, colonial algae, acritarchs, and chitinozoa (Castro, 2006). They have a typical size range of 5 to 500 μm and are found in the residue of palynological samples after the maceration processes of sedimentary rocks by strong inorganic acids, generally HCl and HF (Sorkhabi, 2020). Once the mineral matrix has dissolved, it is possible to observe these microfossils composed, at least in part, of very resistant organic molecules like chitin, or "pseudochitin" or sporopollenin (Bercovici & Vellekoop, 2017). The latter is probably the most resistant, durable and inert organic material of biological origin found in nature and geological samples (Feagri & Iverson, 1964).

1.2.1 Morphology and Biology

Unlike most microfossils, pollen and spores are not individual organisms but rather reproductive structures that plants produce as part of their life cycle (Armstrong & Brasier, 2005). Although they are the most significant group of microfossils in terrestrial environments, predominantly originating from continental vegetation, they play significant roles as biostratigraphic indicators in terrestrial and marginal marine environments. Since terrestrial plants are attached to their substratum, they rely on pollen and spores for reproduction and dispersal. For that reason, pollen and spores are produced in large quantities and released into the environment, where they travel great distances quickly through wind dispersal or the outflow from deltaic regions (Sorkhabi, 2020). The size of these microscopic structures, which do not exceed 200 μm, helps their transportation until they are deposited on land surfaces and in bodies of water, including places where preservation is more likely to occur, such as the bottoms of ponds, lakes, rivers and oceans (Bercovici & Vellekoop, 2017). Nevertheless, it is relevant to stress that their usefulness in marine sediment is limited precisely due to this allochthonous nature (Saraswati & Srinivasan, 2016). On the other hand, the vast and complex morphological variety of pollen and spores helps in the identification of different organisms which, combined with their production in large numbers, facilitates the development of statistical research (Castro, 2006). In addition, the resilient nature of sporopollenin, besides being resistant to microbial attack (Jain, 2020), allows spores and pollen to remain preserved unalterably in sediments that have endured numerous changes for hundreds of millions of years, which makes them a useful fossil group for environmental reconstruction, palaeoecology and as biostratigraphic markers (De Wever, 2020).

1.2.1.1 Spores

Spores are the reproductive cells of asexually reproducing cryptogam organisms (Sorkhabi, 2020). At specific periods of the year, or under specific stresses, haploid spores are generated through meiosis by a structure called sporangium (pl. sporangia) (Rost *et al.*, 1998),

which is found in non-vascular plants like bryophytes, pteridophytic vascular plants, such as ferns and horsetails, fungi and algae (Bercovici & Vellekoop, 2017; Jain, 2020).

The presence of spores in the fossil record is associated with the profound ecological shift of the land incursion by terrestrial vegetation. However, it predates the first widespread forest ecosystems that became established between the Devonian and Carboniferous periods (416–299 Ma), dating from the Middle Cambrian (ca. 500 Ma) (DiMichele *et al.*, 2007 in Garwood & Edgecombe, 2011; Bercovici & Vellekoop, 2017).

Since spores have a wide morphological variety, they can be classified based on different characteristics, such as their size, which varies between 1 μm and 2 mm, the average being 50-100 μm. (Castro, 2006). Other distinctive traits are their apertures, wall structure and shape, the latter being inherently connected to the nature of the meiotic divisions that occur inside the sporangium (Armstrong & Brasier, 2005). Spores are encountered individually or in aggregations known as tetrads, comprising four spores derived from a single parent cell. The configuration of spores or pollen grains within tetrads can assume two distinct geometries: a tetrahedral arrangement, forming a tetrahedron tetrad, and a planar arrangement, termed a tetragonal tetrad. Towards the centre, in the proximal portion of the spore, there is a slit-like suture called *laesura* (pl. *laesurae*). This aperture marks the contact area between it and the other three spores of the tetrad and defines the proximal and distal poles. According to the *laesura* configuration, which can be absent, single or triradiate the spores are divided into alete, monolete or trilete, respectively (Saraswati & Srinivasan, 2016).

The trilete spores have three *laesurae* (Fig. 1.3) forming a Y-mark on the proximal pole (Armstrong & Brasier, 2005), resulting from their position within the tetrad. They represent the basic spore morphology, originating during the Late Ordovician period (458–443 Ma). The monolete spores have only one proximal *laesura*, deriving it from the trilete spores in the Silurian (Saraswati & Srinivasan, 2016). This spore morphotype is generally less common than the trilete spores, being more abundant in Palaeogene-Quaternary assemblages. The alete spores lack a *laesura*, a condition that probably was derived from monolete or trilete spores (Traverse, 2007).

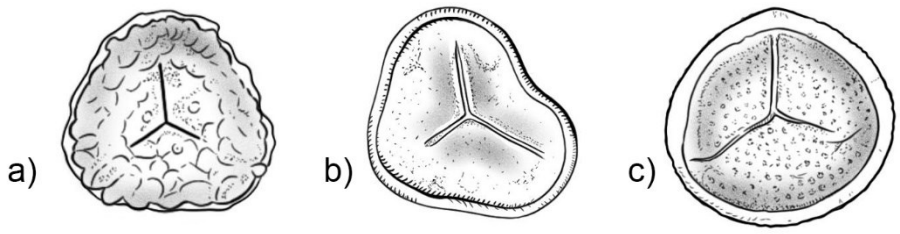

Figure 1.3 — The morphological diversity of trilete Mesozoic spores: a) *Ischyosporites crateris*, ornamented by heavy ridges; b) the smooth *Cyathidites australis*; c) Carnisporites *spiniger* showing a circular outline.

In addition to morphological structure, the arrangement of ornamental elements on the superficial sculpture of the exine layer (Fig. 1.6) plays a crucial role in the description and classification of both spores and pollen (Armstrong & Brasier, 2005; Castro, 2006). According to Traverse (2007), the exine, or shell, of palynomorphs is composed of sporopollenin, including other compounds present in the interstices and on the surface that are typically lost during fossilisation.

Spores have proven to be significant in determining the age and correlation of coal seams in terrestrial sedimentary strata. In hydrocarbon exploration, the colour shift observed in spore walls serves as a reliable indicator of the thermal maturity of source rocks (Saraswati & Srinivasan, 2016), responsible for the generation of hydrocarbons (Ferriday & Montenari, 2016).

1.2.1.2 Pollen

Pollen is the male gametophytes developed from microspores of spermatophytes (seed plants), such as Pteridospermatophyta (extinct seed-producing ferns), gymnosperms and angiosperms (Jain, 2020). The spermatophytes first appeared in the Late Devonian (382–372 Ma) (Milsom & Rigby, 2009), as a response to their progression towards the terrestrial environment, they had to adapt to the scarcity of water, developing what Farjon (2017) calls the "seed habit", i.e., an integument to protect the gametophyte. Angiosperms, also known as flowering plants, are characterised by bearing seeds within a fruit. In contrast, gymnosperms, which include conifers, cycads and ginkgo, produce exposed seeds without an enclosing fruit. In the sexual reproduction of seed plants, the two primary stages are pollination, which involves the transport of pollen grains from the anther or microsporangia to the ovule or stigma, and fertilisation, the fusion of sperm with egg (Simpson, 2010). The evolution and optimisation of these

processes in response to biotic and abiotic factors of transport, lead to a vast diversity in pollen morphology and a more efficient pollen transfer among different seed plant species.

The pollen morphology (Fig. 1.4) is incredibly intricate and extensive (Jain, 2020), especially in angiosperm pollen (Castro, 2006). Their morphology varies from small, simple, spherical organisms with no opening to larger ornate grains that have a wing-like structure called a *saccus* (pl. *sacci*), which can be present alone (monossacate), in pairs (bissacate) or groups of three (trissacate) (Armstrong & Brasier, 2005; Saraswati & Srinivasan, 2016).

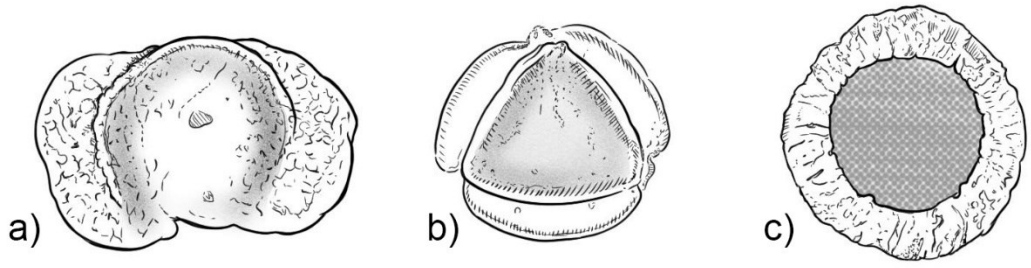

Figure 1.4 — The morphological diversity of pollen: a) *Alisporites grandis*; bissacate pollen; b*) Callialasporites trilobatus*, trissacate pollen; c) *Plicatipollenites densus*, monossacate pollen.

Before fertilisation, during the meiotic division, the produced pollen grain units can be classified as individual grains called monads, pairs known as dyads, groups of four like the spores, termed tetrads, sets of eight named octads, or multiple grains in a formation called polyads, which can have up to 64 cells that stay connected post-maturation. The monads and dyads are already separate grains from tetrads after they mature. According to the disposition of the grains in the units, they can be classified as tetrahedral, tetragonal, rhomboidal, decussate, T-shaped, linear, cryptotetrad, and either a pseudomonad or pollinia (Fig. 1.5). The latter involves releasing the entire content of an anther as a single entity or even the anther locule being expelled by once as one united mass of pollen (Traverse, 2007; Jain, 2020).

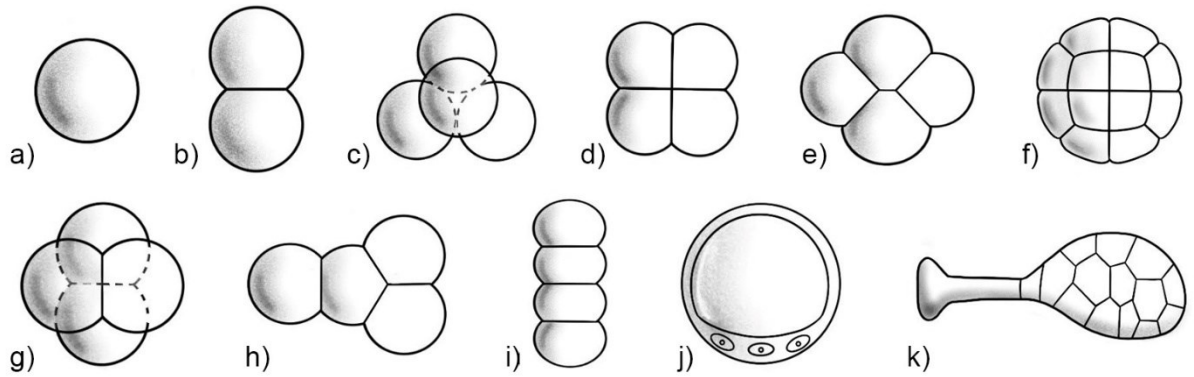

Figure 1.5 — Pollen units: a) Monad; b) Dyad; c) Tetrahedral tetrad; d) Tetragonal tetrad; e) Rhombohedral tetrad; f) Polyad; g) Decussate tetrad; h) T-shaped tetrad; i) Linear tetrad; j) Cryptotetrad; k) (modified from Jain, (2020)).

As previously mentioned, the pore and pollen exine ornamentation (Fig. 1.6) are diagnostic phylogenetically. Exine ornamentation comes in two distinct forms: sculpturing and structure (also called texture). Sculpturing includes every geometric element on the outside without considering its internal structure, whereas the structure, as the name says, comprises all the internal structural characters (Jain, 2020).

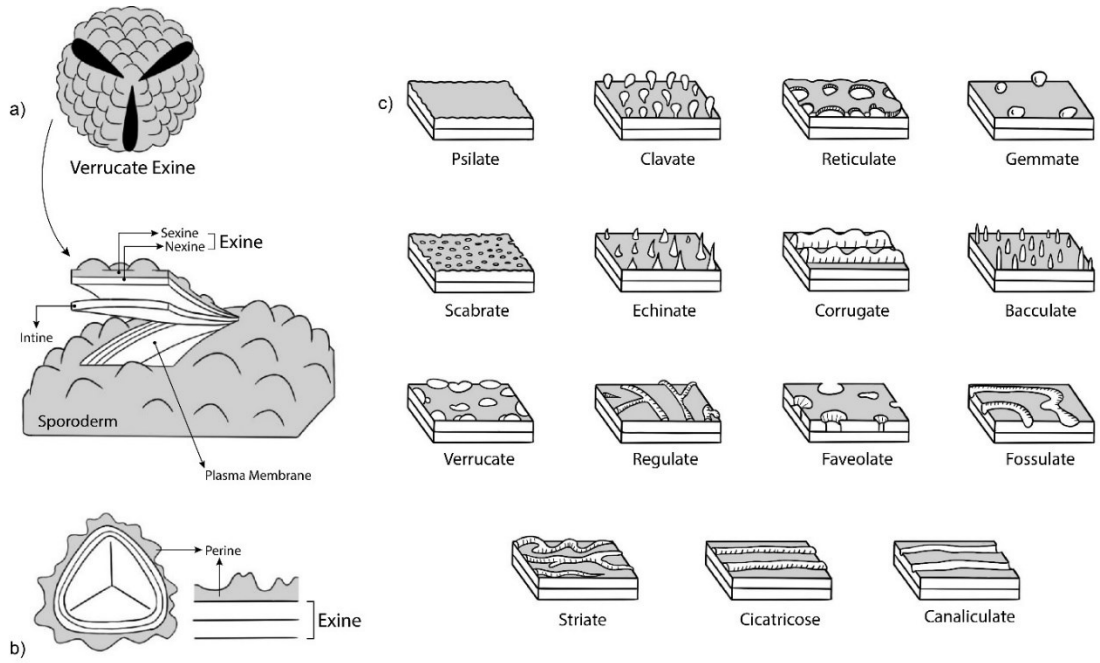

Figure 1.6 — The sporoderm and exine ornamentation: a) The sporoderm is the outer layer surrounding spores and pollen. Consisting of two layers, the intine and the exine, it plays a crucial role in protecting the genetic material; b) The spores of bryophytes and pteridophytes may present perine, which is the outermost layer of the sporoderm; c) The exine is known for its toughness and resistance to chemical degradation. It is often highly ornamented with patterns that can be species-specific, being extremely relevant for phylogeny (modified from Jain, (2020)).

1.3 Microvertebrates

In the fossil record, small-sized vertebrate organisms are characterised by microvertebrate fossils, usually requiring magnification for detailed study due to their tiny size, which does not exceed 12.5 mm. According to Rogers *et al.* (2008), vertebrate microfossils are specimens with a size limit smaller than 5 cm in maximum dimension. In most cases, these fossils are isolated material like scales, bones and teeth (Heckert, 2004). Within the geological record, teeth stand out as some of the most abundant and resilient forms of fossils, especially the mammalian teeth (Ungar, 2010). The reason behind this is largely due to their composition; mammalian teeth enamel consists predominantly of minerals (98%), mostly in the form of hydroxyapatite. Consequently, teeth have a greater resistance to chemical and physical wear, as well as to various diagenetic processes, compared to bones (Smith, 2021).

The microvertebrate fossils are found in deposits called microfossil bonebeds, also known as vertebrate microfossil (microvertebrate) assemblages or microsites (Rogers & Brady, 2010). A microfossil bonebed is defined as an accumulation of vertebrate skeletal remains, originating from multiple individuals, where at least 75% of these elements do not exceed a maximum size of 5 cm, whether this bone concentration is of a single species (monotaxic) or multiple species (multitaxic). Disarticulated and completely dissociated skeletal parts along with fragments of bones and fully articulated skeletons will be categorised as microfossil bonebeds under this size-based classification (Eberth *et al.*, 2007). Typically, terrestrial microvertebrate fossils accumulate in a variety of settings, such as channel lags and bars, a prevalent occurrence among mesozoic specimens, as well as in small, oxygen-rich lakes, springs and seeps, caves, beneath layers of volcanic ash, and originating from predatory activity (scatological deposits) (Fraser & Sues, 2018; Rogers & Brady, 2010; Jurigan *et al.*, 2023). Additionally, these remains are also found within middens and similar structures, and preserved in pedogenic carbonate nodules (Behrensmeyer, 1992; Heckert, 2004). While the small bodies of

microvertebrates provide a great opportunity to study the most profound evolutionary changes, those that lead to the establishment of new clades, the microsites are essential for reconstructing the community-level of terrestrial vertebrate paleofaunas, providing taphonomic and environmental data, and estimates regarding the relative abundance and diversity of species (Clark, 1992; Carroll, 1997; Heckert, 2004; Vullo, 2009).

1.4 Mammals: a Brief History and Definitions

The exact definition of Mammalia is substantially influenced by the phylogenetic tree topology (Benton, 2014). Authors such as Luo *et al.* (2002), Kielan-Jaworowska *et al.* (2004), Benton (2014), and Brusatte (2022) opt for the definition of mammals as any descendants of the earliest cynodont (therapsid) that evolved a strong dentary-squamosal jaw articulation, i.e., a clade united by the shared common ancestor of *Sinoconodon*, morganucodontans, docodontans, Monotremata, Marsupialia, and Placentalia, as well as any extinct *taxa* included within this group. Another definition (Rowe, 1988) proposes that stem-mammals that developed a squamosal-dentary jaw articulation, which diverges from the common ancestor of monotremes and therians (placental mammals and marsupials) before these two groups split (ca. 166 Ma), are classified as Mammaliaformes. i.e., Mammaliaformes comprises the last common ancestor of morganucodontans and Mammalia and all its descendants. In its turn, the crown-group Mammalia would be smaller, defined only by the most recent common ancestor of all currently existing mammals (monotremes, marsupials, and placentals) and all its descendants. Nevertheless, mammaliaforms and mammals belong to a broader clade known as Synapsida, which includes mostly permian forms such as biarmosuchians, eothyrids, dinocephalians, sphenacodontians or dicynodonts (Zachos & Asher, 2018).

At the end of the Carboniferous period (ca. 315 Ma), synapsids, the forerunners of mammals, are thought to have originated (Smith, 2021). They diverged morphologically from their sister clade, the sauropsid lineage, around 318 to 332 Ma (Benton *et al.*, 2015). Dating from the Middle Permian, the oldest undisputed evidence of a more advanced synapsid clade called Therapsida emerged, displaying a high diversity of *taxa* already in their earliest occurrence in the fossil record (Kemp, 2005). Featuring a mammal-like bauplan with a more upright posture, the potential presence of hair and a remarkable morphological variety in their teeth, tailored

for ecological specialisation, the therapsids dominated the terrestrial ecosystems during the Permian. Subsequently, this immense diversity was drastically reduced by the extinction event at the end of the same period. The surviving therapsid lineage paved the way for the emergence of mammaliaforms around 225 Ma, setting the stage for the rise of mammals (Smith, 2021).

As previously mentioned, mammaliaforms are distinguished by an apomorphy: a secondary jaw articulation. In addition to the primary jaw joint between the quadrate and articular bones, mammaliaforms possess a squamosal-dentary articulation. Following this definition, *Morganucodon* from the Late Triassic and *Sinoconodon* from the Early Jurassic period represent the most basal mammaliaforms (Zachos & Asher, 2018). Although the earliest appearance of basal mammaliaforms dates back to the Upper Triassic, their fossil record is very fragmentary, making the morganucodonts from the Early Jurassic period the earliest mammaliaforms to be reasonably well-preserved. The divergence of morganucodonts from the cynodont lineage occurred when a more robust secondary jaw joint was developed between the dentary and squamosal bones. Through this conventional perspective, palaeontologists place the origin of the Mammaliaformes clade at this point (Benton, 2014). However, determining the boundaries of clades often generates considerable discussion, primarily because, although grounded in morphological evidence, the extant delineation remains arbitrary. It's no different with the node point of mammaliaforms since the jaw of *Morganucodon*, although reduced, still displays traits of its non-mammalian ancestors (Sánchez, 2012). These plesiomorphic, or "reptilian", characteristics consist of a more complex jaw composed of more bones, such as the angular, prearticular, surangular, coronoid and articular bones. Over time, the dentary became larger and deeper, whereas the quadrate and articular bones diminished in size to the point where they had no function in mouth opening. As a result, they continued to shrink until they finally became disconnected from the mandible and the rest of the skull. These postdentary bones transitioned completely into a separate auditory passage, originating two of the three mammalian ear ossicles: the malleus (former articular) and incus (former quadrate), with the third ossicle being the stapes (Fig. 1.7). This new hearing mechanism gave mammaliaforms and mammals the ability to hear a wide range of sounds, compared to birds, reptiles, and amphibians (Benton, 2014; Brusatte, 2022).

Endothermy, or warm-bloodedness, is another fundamental characteristic of mammals, closely linked to other defining traits such as the presence of sweat glands and fur (Benton,

2021). According to Lovegrove (2019), endothermy in mammals is the ability of these organisms to generate internal heat on demand, allowing them to maintain a stable body temperature despite external conditions and stay warm during cold periods. This ability evolved abruptly in the Mammaliamorpha clade, around 233 Ma, during The Late Triassic Carnian Pluvial Episode (Araújo *et al.*, 2022). It allowed mammals to maintain high levels of activity over longer periods, improve their muscle efficiency and reaction times, adapt to a wider range of environments, have constant metabolic rates and improve their cognitive function (Lovegrove, 2019). All these factors were significant in the evolutionary success of mammals, providing them with the ability to thrive in a wide array of ecological settings.

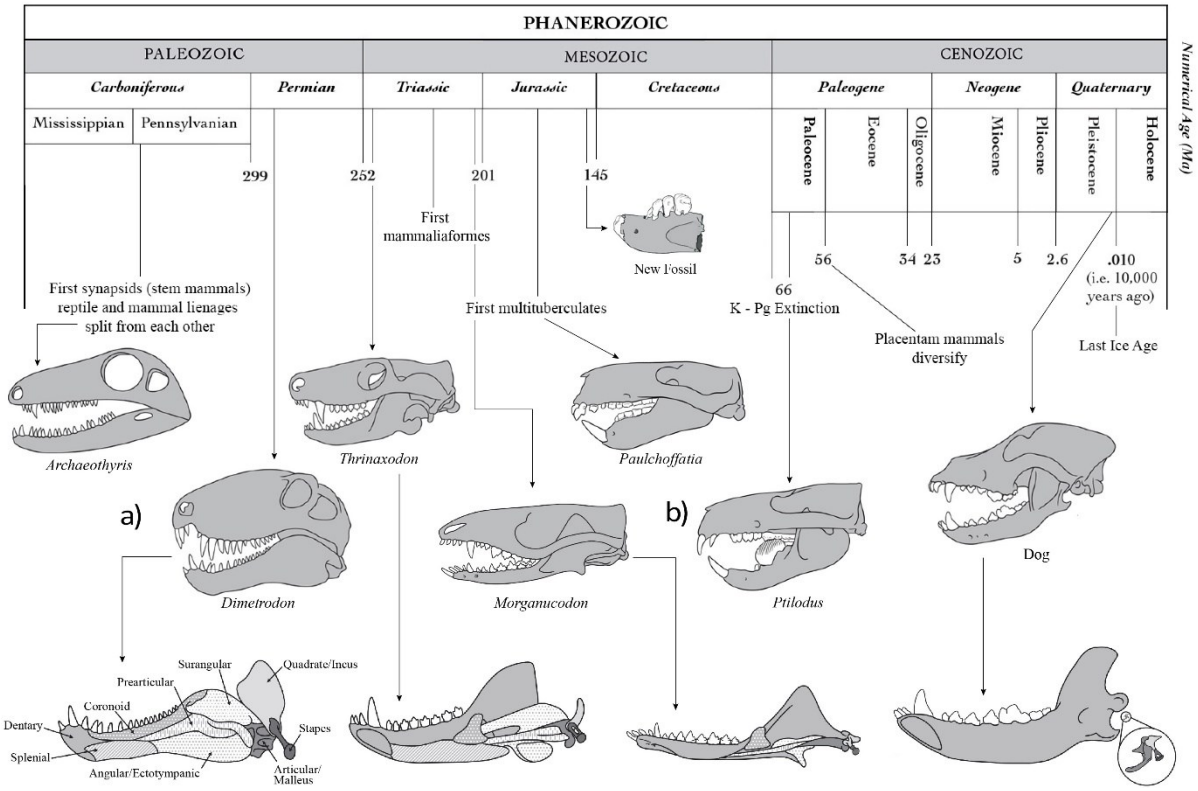

Figure 1.7 — This timeline showcases the evolutionary trajectory of synapsid skulls and teeth, highlighting their progression towards greater complexity and specialisation. Parallel to that, it depicts the simplification of the mandible through the reduction of its bones, ultimately resulting in a single lower jaw bone, the dentary. This transformation resulted in the emergence of the distinctive mammalian lower jaw and the associated ear ossicles. The "new fossil" featured in the image is the primary focus of this study (modified from Brusatte, (2022) (a); Kielan-Jaworowska and Nessov, (1992); Carvalho, in this work).

1.4.1 The Mezosoic Radiation

The Mesozoic era was a period of major evolutionary innovation and ecomorphological variation among mammaliaforms, substantially increasing their taxonomic diversity, especially during the Middle to Late Jurassic. Nevertheless, the majority of Mesozoic mammaliaform clades had a brief evolutionary history, grouping into short branches, most of which are phylogenetic dead ends with no ancestor-descendant connection to analogous dead-end branches in previous or subsequent episodes (Luo, 2007). This pattern was not exclusive to the Middle to Late Jurassic. The same was true for most orders and families from the Late Triassic and Early Jurassic, including the sinoconodontids and morganucodontans. Generally, these orders and families are remotely connected to extant mammals and did not directly contribute to the evolution of the Middle and Late Jurassic mammaliaforms (Kielan-Jaworowska *et al.*, 2004).

The Jurassic radiation led to the rapid emergence of several morphologically distinct lineages, such as eutriconodontans, docodontans, multituberculates, dryolestids, metatherians or eutherians. This period of diversification was not characterised only by a significant increase in morphological diversity but also by the development of key mammalian traits in teeth, middle ear and endothermic physiology. The burst pattern of Mesozoic mammaliaform evolution closely resembles trends linked to the origin of other main vertebrate groups, for instance, lungfishes, tetrapods, amniotes, archosaurs and birds (Close *et al.*, 2015). These trends are compatible with the occurrence of large-scale adaptive radiation, normally propelled by ecological opportunity, which impacts lineage diversification, once different environmental conditions can drive or hinder the evolutionary processes leading to diversity. Ecological opportunity arises from fundamental elements, such as when a species enters new environments, the extinction of existing populations, or the development of significant new traits (Wellborn & Langerhans, 2014).

A few decades ago, the prevailing scientific consensus was that the major Mesozoic mammaliaform groups were characterised by a lack of ecological specialisation, exhibiting instead generalised habits. However, new findings and new analysis technologies have proved

these assumptions wrong. Although most of the mammaliaforms were probably generalists, strong evidence for ecological specialisations (Fig. 1.8) in different clades is now available, featuring anatomical adaptations for swimming, feeding on colonial insects, climbing, scavenging and scratch digging (fossorial behaviour), this one is the predominant specialisation among multituberculates (Luo, 2007). Even though some mammalian species could reach a considerably large size, i.e., *Repenomamus giganticus*, whose estimated body mass could reach 12–14 kg (Hu *et al.*, 2005), from the Triassic until the mass extinction at the end of the Cretaceous, the synapsids, outnumbered by the ancestors of the dinosaurs, remained a diverse group in *taxa* but conservative in small body size and form. Generally, these mammaliaforms did not exceed the size of shrews (Kemp, 2005; Milsom & Rigby, 2009).

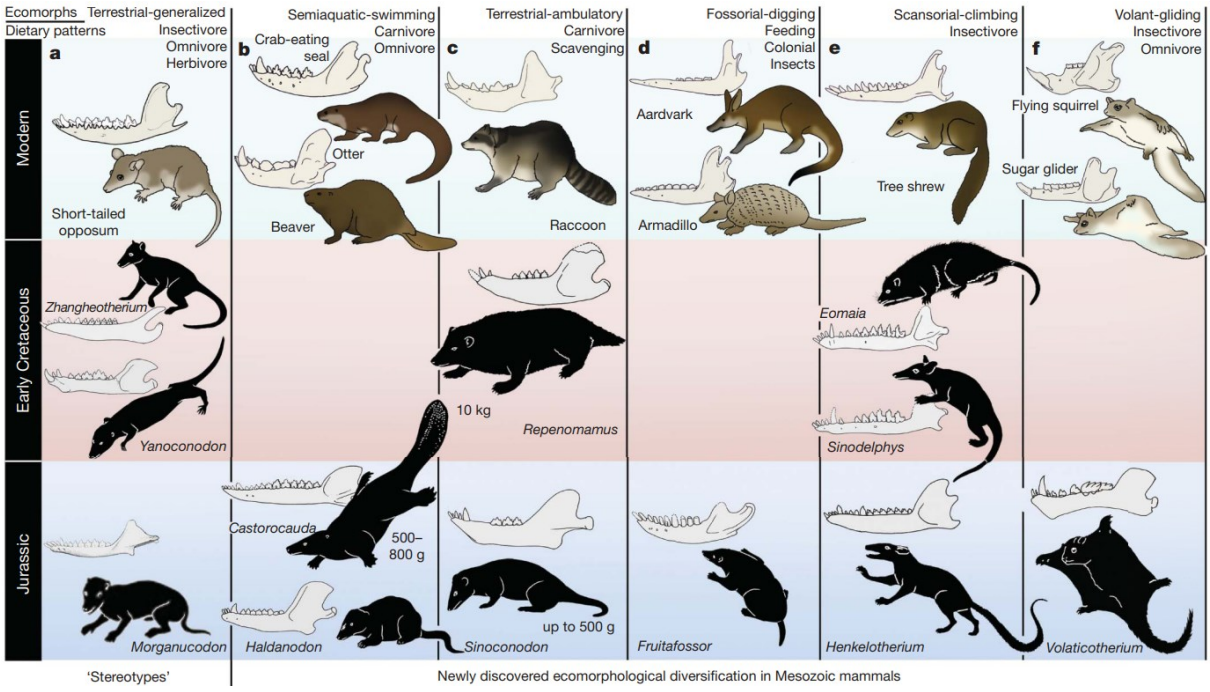

Figure 1.8 — The diversity of ecological adaptations among Mesozoic mammaliaforms and mammals, and their environmental convergence with modern mammals (Luo, 2007).

1.4.2 Multituberculata

Multituberculata Cope, 1884, is classified under the subclass Allotheria, established by Marsh in 1880 (Kielan-Jaworowska *et al.*, 2004). This order of extinct, usually holartic mammals, belongs to the Theriimorpha, i.e., the clade of mammals more closely related to therians than monotremes (Rowe, 1993). In geological terms, their presence in the fossil record is one of the most extensive among mammals, spanning around 130 Ma from the Middle Jurassic to the Late Eocene, this longevity surpasses that of any other mammalian order, including placental mammals (Zachos & Asher, 2018). Besides this impressive span range, multituberculates form the largest and the most well-known group of Mesozoic mammals despite having significant gaps in their fossil record (Kielan-Jaworowska *et al.,* 2004; Benton, 2014). In the context of ancient biotas, they typically comprised the predominant mammalian group, particularly during the Cretaceous and Palaeocene, where they represented around 75% of species found in those mammalian communities (Kemp, 2005). Situated in Leiria, Portugal, the Guimarota coal mine, the most significant Late Jurassic mammal site in Western Europe, also displays the same trend. Dated to the Kimmeridgian stage (Martin & Krebs, 2000), the Guimarota Beds display a higher diversity of multituberculates, composed of 21 *taxa* and another 12 left in open nomenclature, that exceeds the variety of other mammalian species found there. However, although this number of *taxa* is inflated due to unidentified *taxa*, which likely correspond to known species, and upper and lower dentitions belonging to the same *taxon* but categorised under separate names, the Guimarota Beds bears a remarkably diverse assemblage of multituberculates (Kielan-Jaworowska *et al.*, 2004). A notable aspect of the *taxa* discovered in the Guimarota Beds is that the specimens predominantly consist of older individuals, identifiable by their significantly worn teeth. Hahn (1978a) suggests that carnivorous mammals were either absent or scarce in the Guimarota biota, whilst the contemporary reptiles likely struggled to prey on these agile mammals, which possessed large eyes, better hearing, and a highly developed sense of smell.

Multituberculates were first documented in the European fossil record during the Middle Jurassic period, specifically in the late Bathonian (ca. 165-168 Ma), a time marked by the flourishing of docodonts and haramiyidans. The earliest and known multituberculates specimens were found in the Forest Marble of Oxfordshire and Dorset, England, and in the Berezovsk coal mine, in Western Siberia, Russia (Butler & Hooker, 2005; Averianov *et al.*, 2020).

Subsequently, from the Middle Jurassic, multituberculates radiated to different parts of Laurasia, being reported in various parts of Europe, North America, and Asia (Zachos & Asher, 2018), undergoing a significant diversification 20 Ma before the K-Pg mass extinction (Benton, 2014). However, no fossils definitively attributed to multituberculates have been discovered in the southern regions of Pangea. This lack of fossils is probably due to the separation of the northern and southern sectors of the supercontinent by the Tethys Sea during the multituberculate taxonomic diversification in the Cretaceous (Brusatte, 2022).

In their revision of Multituberculata systematics, Kielan-Jaworowska and Hurum (2001) categorised the order into two main suborders: the paraphyletic unit "Plagiaulacida" Ameghino, 1889, (Plagiaulacoidea, refined by McKenna in 1971) and the monophyletic suborder Cimolodonta, McKenna, 1975. Additionally, they identified the family Arginbaataridae, which they placed in a suborder of uncertain placement (*incertae sedis*). Plagiaulacida (or "plagiaulacoidans") is distinguished by several plesiomorphic dental traits, spanning from the earliest known multituberculates (Bathonian stage) to the late Cretaceous *taxa*. This group includes three informal, and partially paraphyletic, lineages: the alodontid, paulchoffatiid, and the "plagiaulacid" lineages (Zachos & Asher, 2018).

The origins of multituberculates remain a subject of ongoing debate. Haramiyida may have given origin to multituberculates (Zheng *et al.*, 2013; Brusatte, 2022), but even the placement of haramiyidans on the mammal family tree is also under debate. Due to the similarity of dental and mandibular characteristics, some authors place Multituberculata together with the haramiyidans in Allotheria, within the crown group of mammals (Bi *et al.*, 2014; Krause *et al.*, 2014; Meng *et al.*, 2014). On the other hand, other authors suggested that Haramiyida, considered stem-mammals, are not closely related to multituberculates, which are part of the crown Mammalia group (Zhou *et al.*, 2013; Luo *et al.*, 2015; Puttick *et al.*, 2017).

When considering some anatomical aspects of multituberculates, it is possible to draw parallels with more modern rodents. Their incisors were large and protruding, enabling them to gnaw effectively, their movements mirrored those of contemporary mice and rats, being able to run quickly across the ground, dig, jump and hop, and climb up and down trees. Despite the similarities, such rodent-like specialisations resulted from convergent evolution, once they likely occupied the same niches (Brusatte, 2022).

The most notable trait of multituberculates is their distinctive dentition, which represents a unique dental adaptation among mammals of the Mesozoic (Zachos & Asher, 2018).

The dental formula of the early multituberculates consists of, in the lower dentition, a single, prominent incisor, three or four premolars and two molars. The upper dentition formula comprises three pairs of incisors, five or four premolars and two molars (Kielan-Jaworowska *et al.*, 2004). Among the upper incisors, the second is noticeably pronounced and primarily engages with the lower incisor, during mastication. Advanced multituberculates lack the presence of a canine, whereas it is commonly found in the majority of Late Jurassic *taxa*. The lower premolars, equipped with a serrated crest formed by the lingual cups (Fig. 1.9), align to form a blade-like structure, while the buccal cusps (basal cusps) are reduced or lost (Kemp, 2005). These distinctive, sharp lower premolars occlude against the multicusped upper premolars, another unique specialisation of these primitive mammals (Benton, 2014).

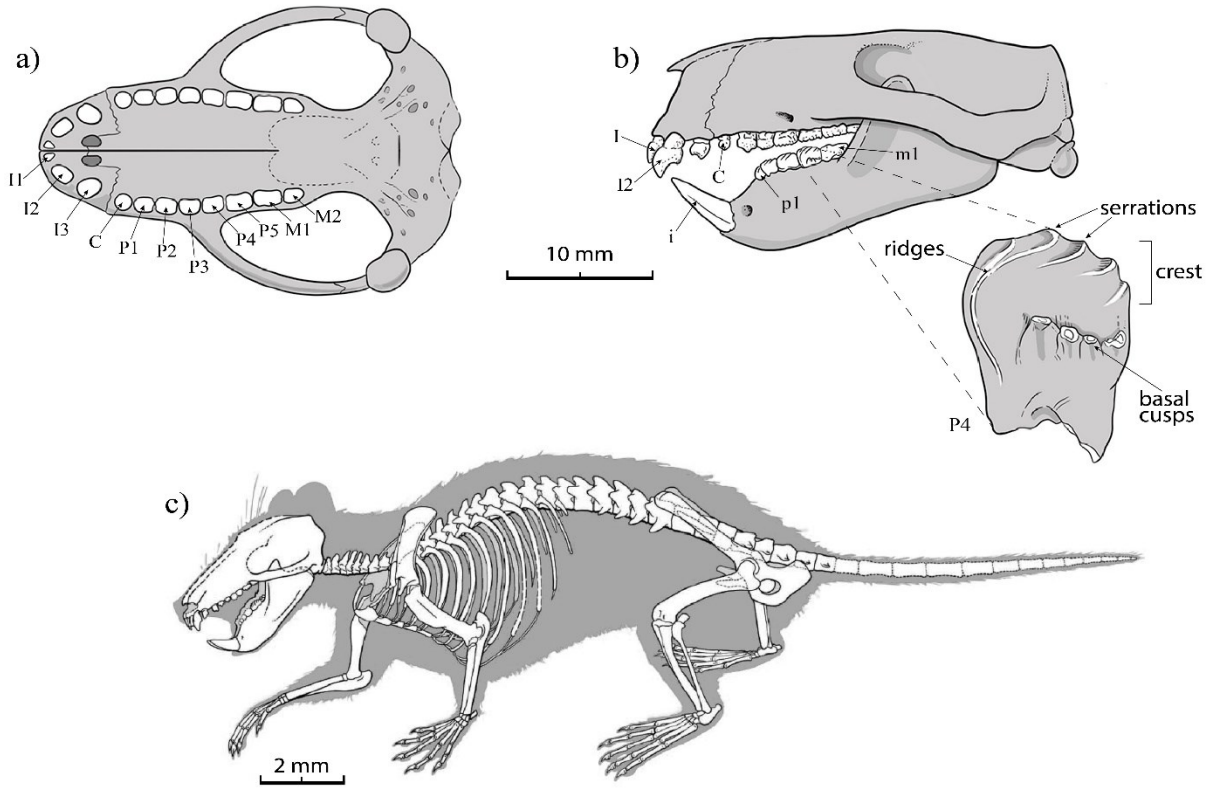

Figure 1.9 — The anatomy of multituberculates: a) The skull of the Portuguese *taxon Paulchoffatia delgadoi*, shown in ventral view, highlights the least derived dental arrangement of this group. b) The same skull in lateral view alongside a detailed close-up of the morphology of the fourth premolar (p4). c) Postcranial reconstruction of the Chinese paulchoffatiid *Rugosodon eurasiaticus*, providing the sole skeletal character information available for the Paulchoffatiidae family (Yuan *et al.*, (2013); Carvalho, in this work, adapted from Hahn, (1969); Kielan-Jaworowska and Nessov, (1992)).

The numerous cusps on their premolars and molars are so characteristic that they inspired the name of the group; in Latin, "*multi*" means many and "tuberculum" refers to a small cusp. On the molars, these cusps are arranged in longitudinal rows, whose numbers may vary between the less derived and more advanced multituberculate *taxa*. (Zachos & Asher, 2018). Their specialised jaw joint permits these mammals to have a fully propalinal (back-to-front) occlusal movement (Butler, 2000). The cusps arrangement of the lower premolars combined with their nearly horizontal chewing strokes were very effective for shearing or chopping the food against the multicusped upper premolars. Multituberculates exhibited ear ossicles completely detached from the mandible (Kemp, 2005). This anatomical trait, along with the absence of both the postdentary trough and Meckel's groove, aligns them more closely with crown Mammalia (Zachos & Asher, 2018). Notably, the articular process is not present in Multituberculata (Kielan-Jaworowska *et al.*, 2004), and the only postdentary jawbone identified within this group is the coronoid, found in the paulchoffatiid species *Kuehneodon* from the Late Jurassic of Portugal (Hahn, 1969).

As stated by Hahn (1978b), in "Plagiaulacida", the less-derived Kimmeridgian multituberculates (paulchoffatiids), the dentition is preadaptive, in the sense that it is not yet used for cutting, which is why many specimens present chewed-off teeth. Posteriorly, in the Early Cretaceous, the dentition of the Purbeckian Plagiaulacidae is fully developed, with the incisors surrounded by enamel and the premolars being used for cutting purposes. As the multituberculates evolved, the cutting function was maintained, but there was a reduction in the number of premolars, while the lower jaw diastema became longer. During the Late Cretaceous to Early Paleogene period, the 'advanced' multituberculates known as Cimolodonta developed highly derived teeth, marking a significant phase in the evolution of this group (Kielan-Jaworowska & Hurum, 2001). This swift expansion in taxonomic diversity and the evolution of complex dental specialisations occurred alongside the ecological rise of angiosperms since many of these changes in dentition were probably adaptations to a diet based on these generally more nutritious new plants (Williamson *et al.*, 2015; Brusatte, 2022). The defining dental characteristics of Cimolodonta include the absence of the first upper incisor and a reduction in the number of premolars to four in the upper jaw and two in the lower (Fig. 1.10). Additionally, the shearing action was focused only on the most posterior premolars (Kemp, 2005).

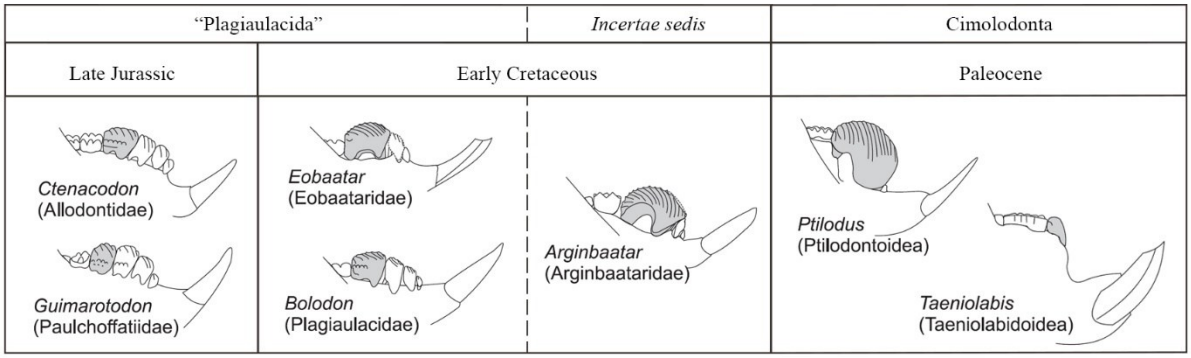

Figure 1.10 — The two main suborders of Multituberculata, the paraphyletic unit "Plagiaulacida", and the monophyletic suborder Cimolodonta, along with the family Arginbaataridae, display an evolutionary dental trend such as the reduction in the number of premolars and teeth specialisation from Late Jurassic to Paleocene (modified from Kielan-Jaworowska *et al.*, (2004)).

At the end of the Eocene, around 34 Ma, the multituberculates disappeared from the fossil record. Over the past few decades, several suggestions have been proposed regarding the causes of the extinction of multituberculates. However, the most widely accepted theory attributes their extinction to the competition with more advanced therian mammals, particularly rodents, once both shared similar overall biology and occupied equivalent niches (Kemp, 2005). According to Brusatte (2022), the superior eating adaptations of rodents, particularly their ever-growing massive incisors, which enable them to exploit resources more efficiently, may have given them an advantage over the once-diverse multituberculates.

Until this study, within the Multituberculata, the Pinheirodontidae was known only by isolated teeth and their dental formula was unknown. This family was established based on 250 isolated teeth found in Portugal (Kielan-Jaworowska & Hurum, 2001). Hahn and Hahn (1999) affirmed that this material was recovered in the Cretaceous layers of Porto Dinheiro. However, in Porto Dinheiro crops out the Amoreira – Porto Novo Members (Upper Kimmeridgian) and the Praia Azul Member (Upper Kimmeridgian to Lower Tithonian), which belong to the Lourinhã Formation (*sensu* Hill, 1988). More recent biostratigraphical evidence supports the indications that the Lourinhã Formation is Upper Kimmeridgian to Lower Tithonian in age (Taylor *et al.*, 2013). Additionally, these authors misspelled the name of the locality as Porto Pinheiro, leading to the designation of the Pinheirodontidae family and the genus *Pinheirodon*. Despite the error, this nomenclature persisted following the publication.

Pinheirodontidae was initially published based on four Portuguese species: *Pinheirodon pygmaeus*, *P. vastus*, *Bernardodon atlanticus* and *Iberodon quadrituberculatus* (Hahn &

Hahn, 1999). Outside of Portugal, another poorly known species is *Gerhardodon purbeckensis*, initially assigned to the Paulchoffatiidae (Kielan-Jaworowska & Ensom, 1992). This pinheirodontids is documented through isolated premolars discovered in Dorset, Southern England. These remains date back to the Early Cretaceous (Berriasian). Three more species of pinheirodontid are also known from isolated teeth recovered from Early Cretaceous strata: *Bructerodon alatus* (Martin *et al.*, 2021), found in Balve-Beckum, North Rhine-Westphalia, Germany (Aptian–Albian), *Lavocatia alfambrensis,* initially assigned as a paulchoffatiid (Canudo & Cuenca-Bescós, 1996), found in Teruel Province, Galve, Spain, dating from the Early Barremian (Kielan-Jaworowska *et al.*, 2004), and *Cantalera abadi*, also from Teruel, Spain, dating from the Hauterivian-Barremian transition (Badiola *et al.*, 2008).

2

Palaeogeographical Context

The Jurassic period of Portugal is represented onshore by three basins, resulting from the fragmentation of Pangea and the formation of the North Atlantic, namely: the Lusitanian Basin, located in the central west, the Alentejo/Santiago do Cacém Basin in the southwest and the Algarve Basin found in the south of the Portuguese territory (Brilha *et al.*, 2005; Vergés *et al.*, 2019). The Lusitanian Basin was named after the Swiss geologist Paul Choffat in 1885, who pioneered its stratigraphy (Rocha & Kullberg, 2017). The basin that emerges west of the Iberian plate measures up to 100 km in width and 200 km in length (north to south) (Kullberg *et al.*, 2013). Its depositional layers compose a 6 km thick sedimentary pile that extends over approximately 22,000 km^2 (Fig. 2.1.a), covering both the offshore and onshore of Portugal (Taylor *et al.*, 2013). The onshore portion is the largest part of the basin (Kullberg *et al.*, 2013). The tectonic development of the Lusitanian Basin followed the existing faults formed during the Paleozoic Variscan orogeny (ca. 300-280 Ma). These lineaments defined and controlled the structural boundaries of the basin together with diapiric activities, during the nonvolcanic rifting episodes triggered by the North Atlantic opening in the Mesozoic (Pinheiro *et al.*, 1996; Kullberg *et al.*, 2013). According to many authors, since the start of its formation, from the Late Triassic to the Early Cretaceous, there were four rifting phases in the Lusitanian Basin (e.g., Rasmussen *et al.*, 1998; Kullberg, 2000; Alves *et al.*, 2002, 2006; Kullberg *et al.*, 2013, Taylor *et al.*, 2013). However, other authors consider three rifting episodes (e.g., Jolivet *et al.*, 1984; Montenat *et al.*, 1988; Wilson, 1988; Stapel *et al.*, 1996; Pinheiro *et al.*, 1996; Pena dos Reis *et al.*, 2000). Re-

cently, Barbarand *et al.* (2021) proposed that two rifting stages started and ended in the Mesozoic, while a third one started in the Albian (ca. 110 Ma) and is still undergoing in the present day.

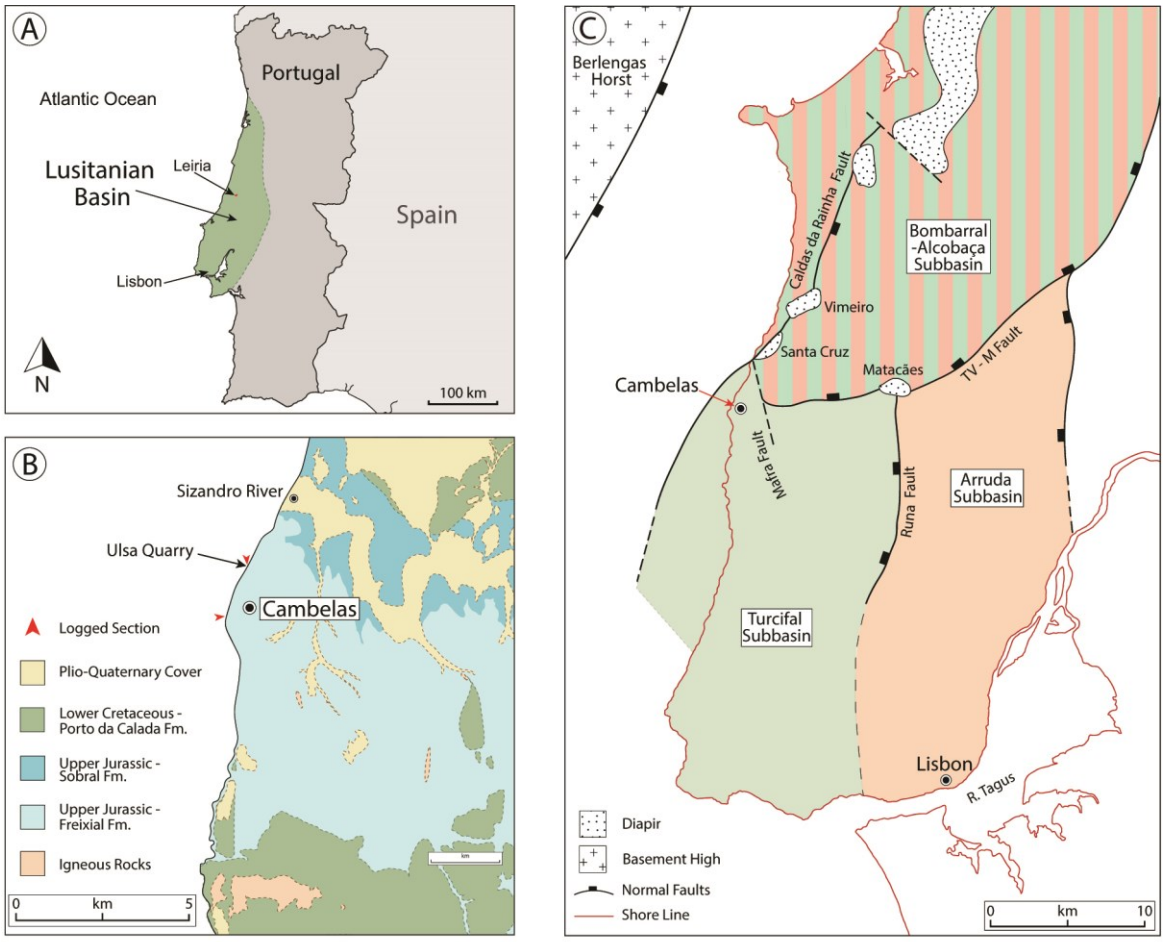

Figure 2.1 — a) Overview of the map of Portugal showing the perimeter of the Lusitanian Basin and the study area located in the southernmost portion of the central sector of the basin; b) Simplified geological map of the Cambelas region, where the studied quarry is located; c) Map depicting the location of the three Subbasins of the Lusitanian Basin and the faults that delimit them. Note that Cambelas is located in the northmost part of the Turcifal Subbasin (Carvalho, in this work, modified from Manuppella *et al.* (1999); Martinius and Gowland (2011); Fürsich *et al.* (2021)).

Considering the four rifting episodes scenario, the third rift phase that happened in the Kimmeridgian–Berriasian is linked to the Central Lusitanian Basin's development. It also caused the main subsidence of the basin that progressed between the Late Oxfordian and Tithonian, and the subsequent formation of its three depocentres (the Arruda, Bombarral-Alcobaça, and Turcifal Subbasins) (Leinfelder, 1993). In agreement with Mocho *et al.* (2017), the Upper Jurassic strata are marked by their extensive lateral variation that contributes to their

complexity. This fact resulted in several stratigraphic interpretations of these depositional sequences (e.g., Hill, 1988; Leinfelder, 1993; Manuppella *et al.*, 1999; Kullberg *et al.*, 2006; Schneider *et al.*, 2009; Martinius and Gowland, 2011; Taylor *et al.*, 2013). In this transitional rifting context, different basin regions started to be infilled with mixed siliciclastic (due to an uplift episode) and carbonate deposits. More than 2 km of this new influx accumulated in the depocentres of the basin (Pena dos Reis *et al.*, 2000). This sedimentation demonstrates an alteration in the depositional environment, from the calcareous shelf marine deposition to the predominant terrigenous clasts formed by fluvial and deltaic habitats or transitional environments (Leinfelder & Wilson, 1999).

The Freixial Formation is the youngest Jurassic lithostratigraphic unit in the region. Based on foraminifera and dasycladaceae green algae, it is believed that these strata date from the Upper Tithonian (Schneider *et al.*, 2009). The Freixial Formation extends from south of the Sizandro River overlapping the Arranhó Formation limestone and marl sequences to the south (Fig. 2.2). Subsequently, its dominant red mudstone layers are replaced by the fluvial sandstone levels of the Upper Jurassic–Lower Cretaceous Porto da Calada Formation, marking the upper border of the Freixial Formation (*sensu* Hill, 1988; Kullberg *et al.*, 2013).

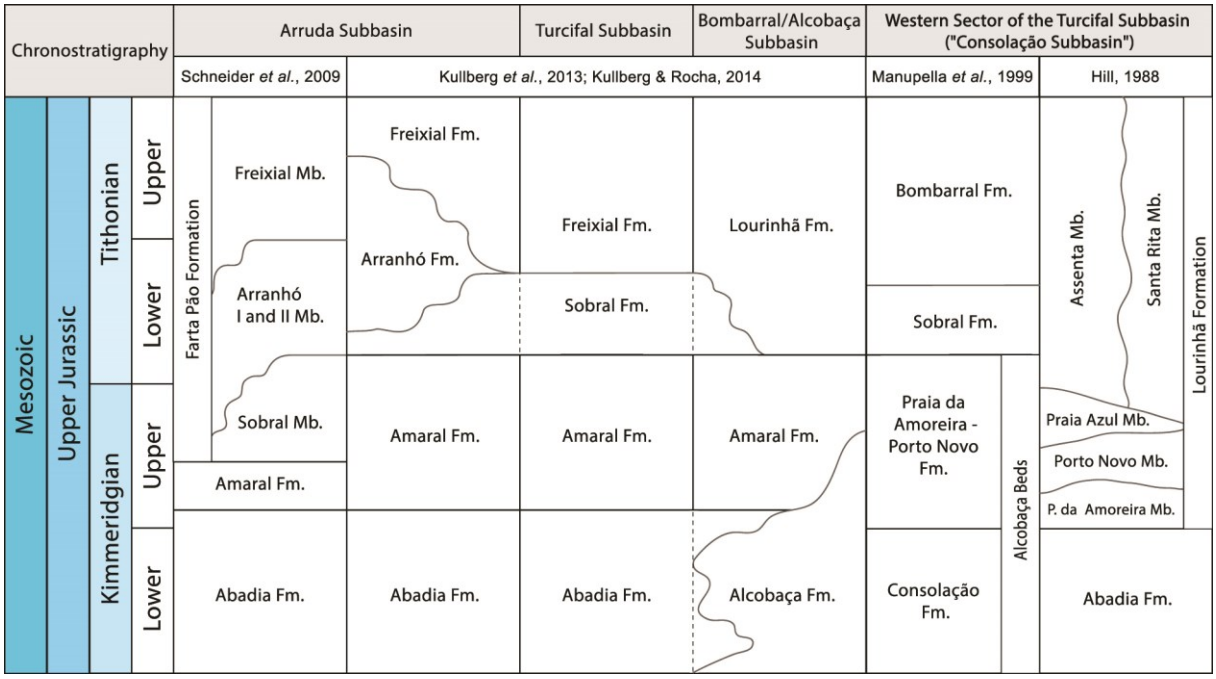

Figure 2.2 — Lithostratigraphic summary of the Upper Jurassic units of the central sector of the Lusitanian Basin (Carvalho, in this work, modified from Hill (1988); Manuppella *et al.* (1999); Schneider *et al.* (2009); Kullberg *et al.*, (2013)).

The studied area of the Freixial Formation is the Ulsa quarry located in Cambelas, a small village of São Pedro da Cadeira, municipality of Torres Vedras. The quarry is named after a regional designation given to a small projection on the cliffs which protrude towards the sea, separating two beaches. The strata of the Freixial Formation that emerge at the top of the cliffs of Cambelas are mainly composed of reddish mudstone/siltstone layers with a significant amount of carbonate concretions (caliche). Eventually, sandstone interbedding gets more regular and uniform within these strata as the layers go toward the underlying levels. On the top layers of the quarry, this reddish structureless silty mudstone level gradually changes into a dark brown mudstone. Both layers are rich in fossiliferous material and mica. In the first unit, from top to bottom, there are fossil assemblages of macrovertebrates (i.e., non-dryosaurid dryomorphans dinosaurs) followed by a progressive microvertebrate deposition. Although these macrofossils are not as well-preserved as the ones in the following layer, some show a certain level of articulation, as, the microfossils are more fragmentary and scarcer. In the subsequent unit, there is a reversal in the fossilisation process. While the microfossils are more abundant and better preserved, presenting even some articulated bones, the macrovertebrate fossils are fewer and all disarticulated or dissociated (Fig. 2.3). It is thought that the deposits of the Freixial Formation in the Cambelas region correspond to mostly continental fluviatile sediments with sporadic marine intrusions, displaying an alternation of carbonate and siliciclastic material (Hill, 1988; Kullberg *et al.*, 2013). In the Ulsa quarry, below these fossiliferous levels, there are a few lenticular palaeochannel bodies of sandstone, which tend to fine-upward into reddish silty mudstones where profiles of caliche soil are formed. According to Hill (1988), this lithology characterises the upper layers of this region's geology. Furthermore, a progressive change occurs towards the bottom of the Freixial Formation with the outcropping of finely laminated silts and thin sands, interpreted as lacustrine deposition.

The Ulsa quarry was discovered in 2021 during the summer excavation by Graça Ramalheiro, one of the members of the Sociedade de História Natural (SHN) organisation. That same year, a block measuring ≈ 120 x 100 x 50 cm was removed from the quarry with the help of a tractor and taken to the laboratory (Fig. 2.4). In this way, the fossils could be extracted more carefully, since their fragmentary nature made the process more challenging. Since then, the digging has taken place every summer in the quarry in search of new, unique palaeontological findings along with laboratory work.

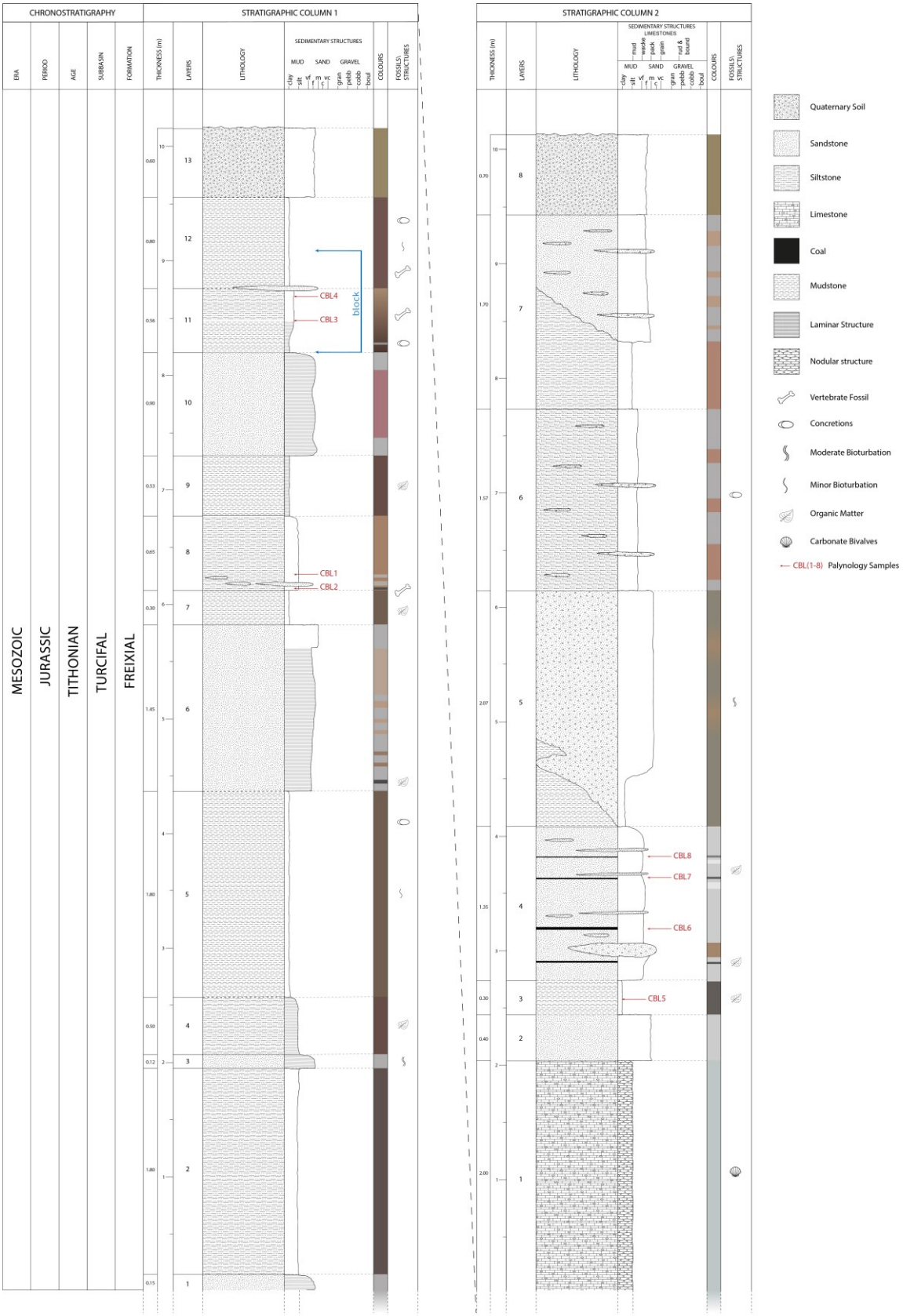

Figure 2.3 — Stratigraphic logs of the Ulsa quarry and a second section done for correlation and palynology purposes. Both locations are 1, 58 km apart. The blue lines mark out the position of the block in the stratigraphic column.

Figure 2.4 — Preserving history: A plaster jacket encases a block loaded with micro and macrofossils from the Ulsa quarry for safe removal, in summer 2021 (Picture: Verena Fuchs).

3

MATERIALS AND METHODS

3.1 Microvertebrates

3.1.1 Samples Collection

Following 2021, after the block extraction, it was possible to access the underlying compact, laminated mudstone layers after reopening the quarry in 2022 (Fig. 3.1). After every summer excavation, the quarry is always carefully sealed with geotextile fabric to prevent erosion of materials down the cliffs during the rainfall season. Remarkably, during the same year, the palaeontological analysis of the samples taken from the laminated mudstone layers, initially collected for testing, revealed a rich presence of microfossils. Such a finding led to a more systematic search for microfossils, which began in 2022. (Fig. 3.2).

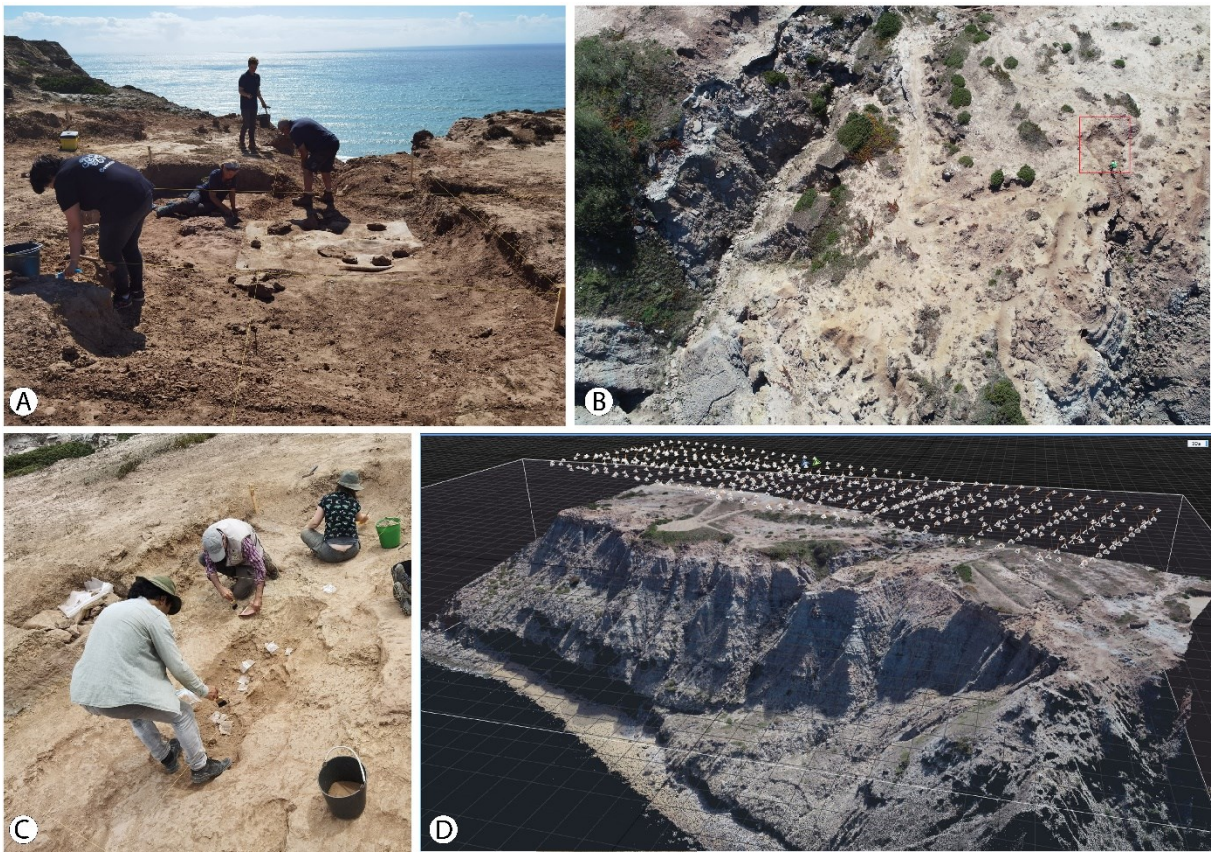

Figure 3.1 — Fieldwork and the geological information surveys of the quarry carried out in 2022: a) SHN members working around the quarry looking for its limits; b) Aerial drone photograph captures the quarry location near the border of the cliff; c) Members of SHN working in the quarry following its reopening, in front of them, lays the microfossil-rich layer where the samples were collected; d) 3D model captured by drone of the Ulsa quarry, utilised for geological studies of the area and to identify the optimal layers for palynological sampling (Pictures: Darja Dankina).

The new samples from the digging site were collected during the summer campaigns of 2022 and 2023. Generally, the fieldwork in the Ulsa quarry lasted around seven to ten days every year with the help of several members of SHN and volunteers. Alongside the fieldwork material, additional samples were obtained from the sediment discarded during the laboratory preparation of the extracted block. Once collected, the samples from both sources were transported to the palaeontological laboratory at SHN for further work. There, all samples were labelled with a number, a brief description, the location, and the weight. The total weight of the samples collected from the Cambelas outcrop reached approximately 350 kg before undergoing chemical treatment and screen washing.

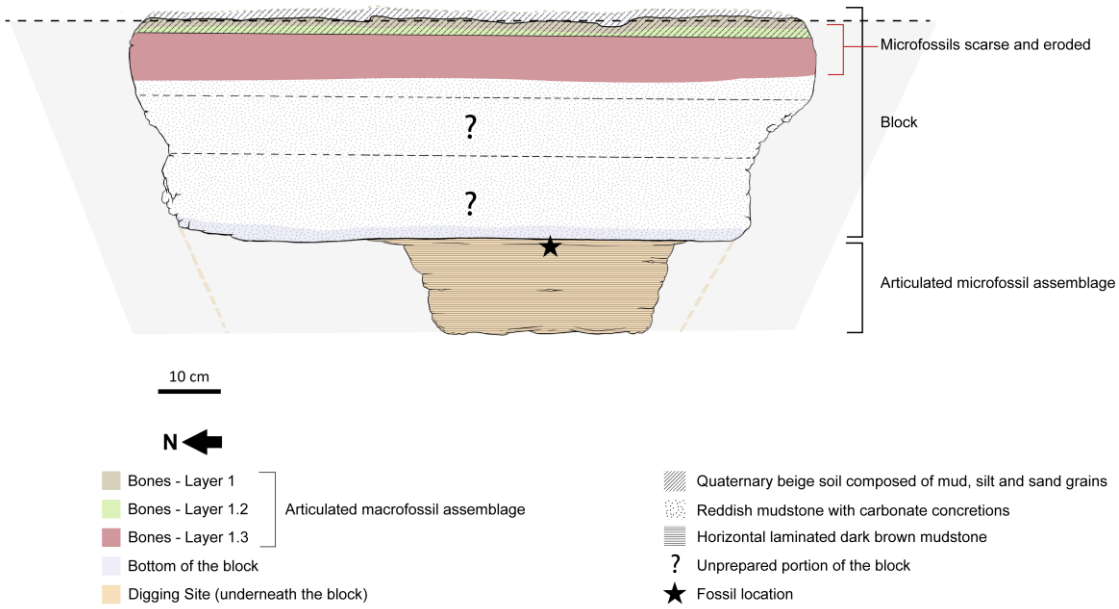

Figure 3.2 — Lateral view of Ulsa quarry highlighting the lithological profile of the block extracted in 2021, which revealed the layers rich in microfossils excavated in 2022 and 2023. The black star marks the location of the studied material of this work.

3.1.2 Samples Chemical Preparation

Since the sediment from the Ulsa quarry contains significant amounts of caliche and carbonate concretions, hydrogen peroxide (H_20_2) 30% was necessary to help disintegrate the carbonated muddy sediment before the screen washing (Green, 2001). Therefore, the samples were soaked for ≈ 24 hours in a mixed solution of water and H_20_2. Once the chemical reaction stopped and the muddy cement had dissolved, the contents of the buckets were carefully decanted into a large sieve. Bulkier, undissolved fragments were cautiously crumbled between fingers. Subsequently, the materials were gently screen-washed under a stream of low-pressure water to ensure the cleaning processes did not damage any paleontological materials. The residues were dried at room temperature and sifted through sieves ranging from 0.075 to 2 mm. In total, the dried unsolved residue weight reached around 87 kg. Finally, the picked microremains were meticulously separated from the residues, placed into specially labelled microslides, and stored in sample containers for further examination under a binocular microscope. This part of the process was also divided according to the reopening of the quarry and access to the fossiliferous layers. Thus, the microfossil-picking process took approximately five months to complete, spanning two months in 2022 and three months in 2023. This effort

yielded a diverse array of microfossils, ranging from macrofossil fragments to articulated microvertebrate bones (Fig. 3.3).

Figure 3.3 — Microfossil collection techniques: a) Samples soaked in water with hydrogen peroxide (H_20_2); b) Picked micro remains separated from the residues, placed into specially labelled micro slides and stored in sample containers; c) Picking the microfossils under a binocular microscope in the SHN laboratory (Pictures a and c: Darja Dankina).

3.1.3 Samples Visual Processing

After isolating the most diagnostic microfossils from the sediment, it was necessary to classify them by their morphological characteristics. Several visits were made to the Guimarota microfossil collection housed at the Geological Museum in Lisbon to assist in this process. Furthermore, the selected specimens were photographed twice using a scanning electron microscope (SEM). At the HERCULES Laboratory of the University of Évora, the model used was an EDS Hitachi S3700N, while additional images were captured with a Hirox microscope model HXR-01. The second set of SEM images was taken at the NOVA School of Science and Technology/NOVA FCT using a Hitachi SU3800 to clarify uncertainties regarding the morphology of the fossil subject of this study. Due to the size and complexity of the specimens

studied, nano-computed tomography (nano-CT) was performed for further systematic analysis at Instituto Superior Técnico in Lisbon with a Multiscale Skyscan 2214 X-ray nanotomograph (Fig. 3.4). In total, seven unique fossils were segmented for detailed analyses of their outer and inner morphological features. As a result of the segmentation process, 3D models were reconstructed using DragonFly software, Version 2022.2 Build 1409, based on the methodology described by Piché *et al.* (2017) at the SHN laboratory. Subsequently, the model was rendered utilising Zbrush Version 2020.1 and Adobe Photoshop Version 21.0.2. Meanwhile, the 2D figures representing the fossil models were created using Adobe Photoshop Version 21.0.2, Adobe Illustrator Version 24.1.2 and Procreate Version 5.3.9 software.

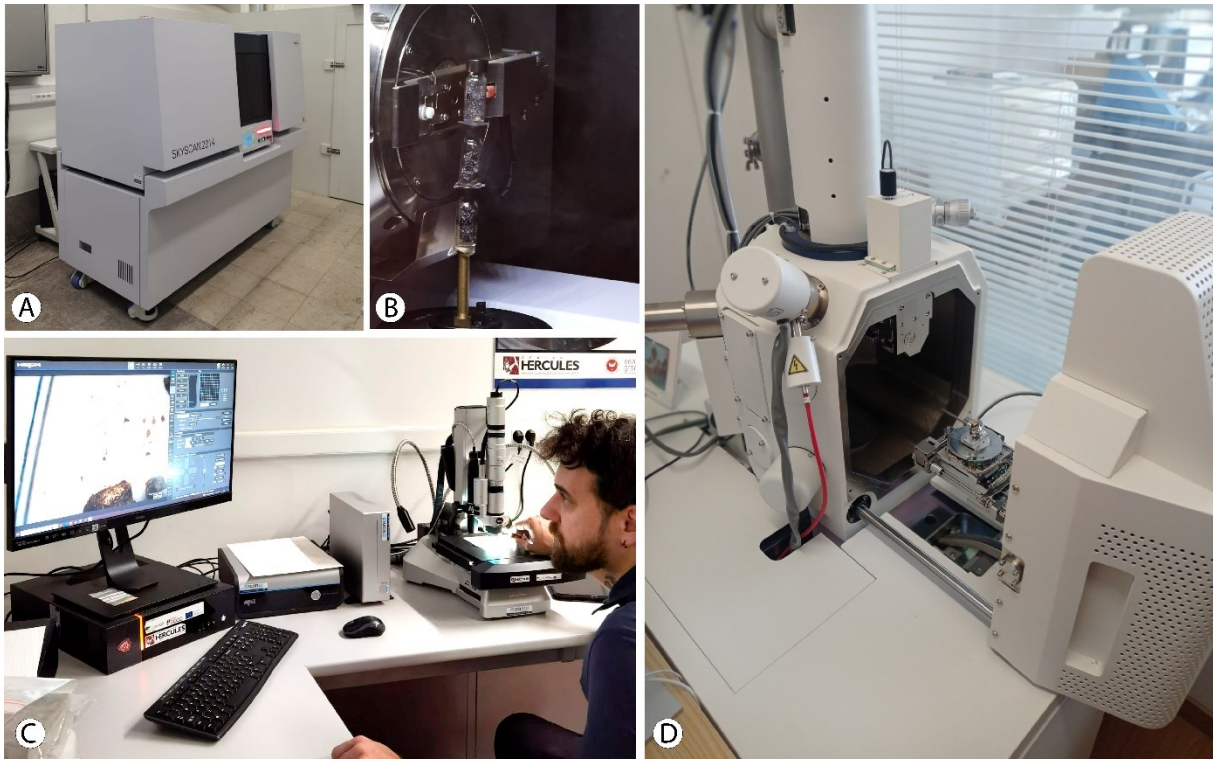

Figure 3.4 — Visual Processing: a) The Multiscale Skyscan 2214 X-ray nanotomography at Instituto Superior Técnico in Lisbon; b) Detail of three samples positioned inside the nanotomography; c) Capturing images with the Hirox microscope at the HERCULES Laboratory of the University of Évora; d) A sample positioned inside the Hitachi SU3800 is ready to be photographed at the laboratory of NOVA School of Science and Technology/NOVA FCT (Picture c: Darja Dankina).

3.1.4 Vertebrate Fossils Findings in the Collected Samples

While the samples from the block preparation yielded fragments, as previously mentioned, the laminated mudstone layers beneath the block proved to be extremely rich in vertebrate microfossils. However, no invertebrate microfossils were detected in either the lower or upper sediment samples. Notably, the presence of microbioturbations resembling small burrows or galleries was observed in the laminated mudstone. All samples extracted from the digging site layers revealed the presence of microvertebrates, predominantly comprising post-cranial bones and teeth fragments from different taxonomical groups.

Through detailed anatomical analyses and comparative studies conducted both at the Geological Museum and within the collections of the SHN, it was possible to confirm the presence of at least three distinctive groups: crocodylomorphs, lepidosauromorphs, and mammals (Table 3.1; Fig. 3.5). Among these, mammals were the most abundant, displaying identified specimens from Dryolestidae and Multituberculata. The preliminary studies suggest the presence of at least two different species of multituberculates, including one that is presented in detail in this study. The taxonomic classification of dozens of specimens remains the subject of active research, as many are still partially covered by the matrix and require further analysis through nanotomography. Likely, after these future analyses, it will be possible to confirm the existence of additional vertebrate groups in the Ulsa quarry.

Table 3.1 — Palaeontological Findings from the Ulsa quarry: Comparative weights of samples before and after chemical treatment and collection dates.

Sample (nº)	Year	Original weight (kg)	After chemical preparation (kg)	Palaeontological findings
CAMB4	2022	17	4.2	Multituberculate Maxilla Fragment
CAMB6	2022	15	3.7	Right Multituberculate Dentary Ornithopod Small Tooth Multituberculate Premolar Left Multituberculate Maxilla
CAMB9	2023	15.7	3.9	Mammalian Isolated (?) Caudal Vertebra
CAMB10	2023	18	4.5	Mammalian Articulated Vertebrae Mammalian Articulated Vertebrae Mammalian Articulated Vertebrae

				Mammalian Articulated Vertebrae Mammalian Articulated Vertebrae
CAMB11	2023	17.1	4.2	Mammalian Articulated Vertebrae Mammalian Articulated Vertebrae Mammalian Isolated Vertebra
CAMB12	2023	17.3	4.3	Mammalian Isolated Vertebra Mammalian Isolated Vertebra Mammalian Isolated Vertebra
CAMB13	2023	15.7	3.9	Multituberculate Incisive Dryolestid Isolated Tooth Dorsetisaurid Articulated Maxilla and Dentary Dryolestid Jaw Fragment
CAMB15	2023	16.5	4,1	Mammalian Femoral Head (?) Mammalian Axis (?) Mammalian Occipital Bone
CAMB16	2023	17.3	4.3	Atoposauridae Femoral Head Atoposauridae Femoral Head Atoposauridae Femoral Head
CAMB17	2023	17.4	4.3	(?) Atoposauridae Pubis Fragment Atoposauridae Tibia Distal Fragment Atoposauridae Tibia Distal Fragment
CAMB20	2023	16.7	4.7	(?) Procoelous Vertebra
CAMB21	2023	15.8	3.9	(?) Avialan Tooth

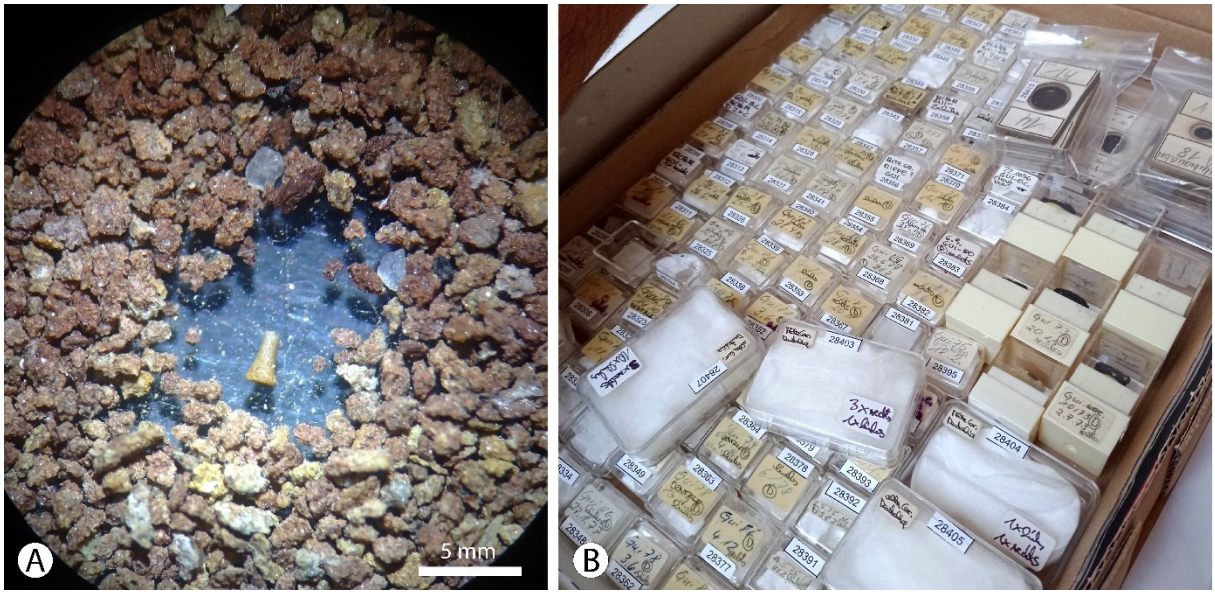

Figure 3.5 — Microfossil collection techniques: a) Samples soaked in water with hydrogen peroxide (H_20_2); b) Picked microremains separated from the residues, placed into specially labelled microslides and stored in sample containers; c) Picking the microfossils under a binocular microscope in the SHN laboratory (Pictures a and c: Darja Dankina).

3.2 Palynology

3.2.1 Samples Collection

Eight samples (CBL1-8) were collected from two distinct outcrops. Half of it (CBL1-4) was gathered in the Ulsa quarry, while the other half (CBL 5-8) was in the following upper corresponding deposits to the quarry. The sampled layers were selected based on their lithological characteristics favourable to palynological preservation since palynomorphs are generally preserved in unoxidised, finely-grained, usually dark-coloured (grey to black) silty or fine-grained mudstone, suggesting deposition in a tranquil aqueous environment (Askin & Jacobson, 2003) (Fig. 3.6).

Figure 3.6 — Sampling for palynological analysis in the greyish layers of the Ulsa quarry.

Before gathering the sediment, the exposed surface was removed, thus eliminating the altered or weathered outer layer. Cross-contamination from dirty instruments or the surrounding matrix was avoided at all costs. Modern soil, rock fissures, surface weathering and recent erosion are all common sources of contamination in outcrops (Bercovici & Vellekoop, 2017). Subsequently, around 300 to 400g of sediment was collected using a geologist pick rock hammer, appropriately packaged, sealed, and labelled in individual plastic bags. The code used to label the sample bags is composed of the abbreviation of the geographical location of the quarry followed by a numerical sequence (Fig. 3.7).

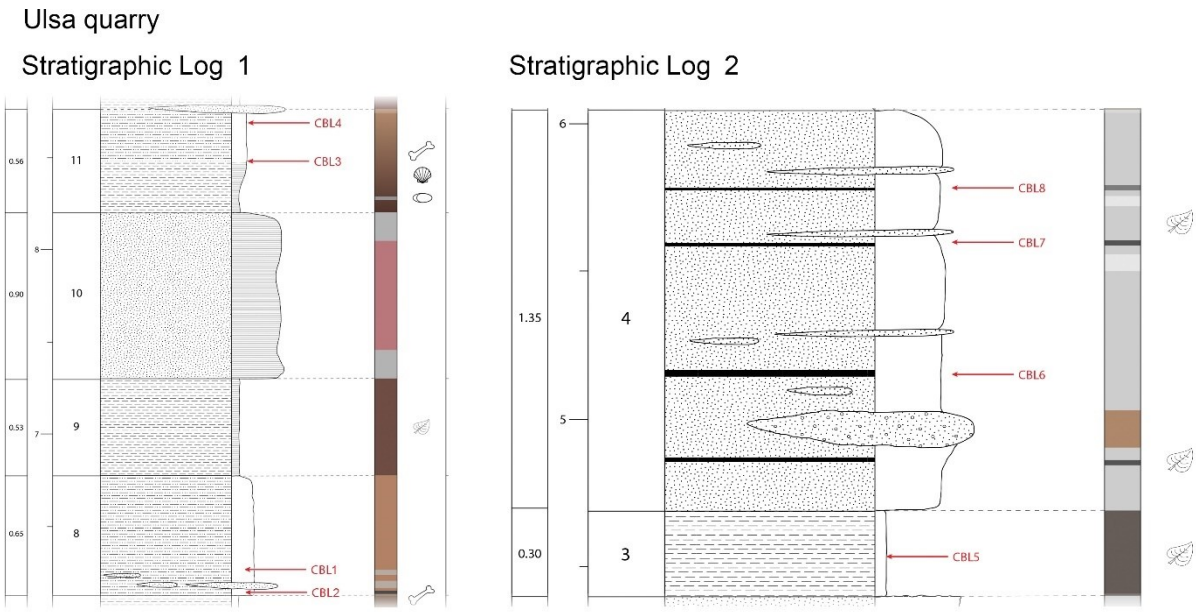

Figure 3.7 — Sampling for palynological analysis in the greyish layers of the Ulsa quarry.

3.2.2 Laboratory Treatment

The sampling was followed by the palynological treatment processes conducted at the Laboratory of Palaeontology of the Department of Earth Sciences at the NOVA School of Science and Technology/NOVA FCT. According to Castro (2006), these processes have as their objective the disaggregation of the sample and elimination of inorganic substances, thus concentrating only the organic components, including palynomorphs and undifferentiated organic matter, which, after being cleaned, are examined under a microscope. The concentration of palynomorphs resulting from these processes may exhibit considerable variation from the original content to losses incurred throughout the sample preparation processes.

In the lab, the first step in the preparation was the elimination of mineral fractions through chemical treatments. From each sample collected in the outcrop, one portion of 30g of sediment was separated, resulting in eight samples. Next, hydrochloric acid (HCl 37%) was added to remove carbonates. After one hour of HCl action, the samples were diluted with distilled water to eliminate formed chlorides. All washing carried out through the laboratory procedure was done with distilled water to avoid contamination since modern pollen tends to be carried in the surrounding air and tap water (Bercovici & Vellekoop, 2017). Following that, the samples were left to decant in distilled water, which was replaced after four hours and placed to decant again, allowing the palynomorphs to settle in the bottom of the receptacle.

The residue was then transferred to a Teflon container to begin the second acid treatment, which was done with hydrofluoric acid (HF 48%) to remove silicates. Subsequently, the containers were placed in an orbital shaker at 50°C and 90 rpm for approximately four hours, followed by almost twenty-four hours of HF decantation (Fig. 3.8). At the end of the reaction, the organic residue was cleaned of the acid by a series of washings until its neutralisation and subsequent elimination of fluorides and sulfides through HCl. Once more, several washes were carried out alternating with decantations every four hours until the elimination of HF and the water became clear. Thereupon, the samples were placed back into the regular plastic receptacles. To complete the cleaning process, a non-acidic preparation technique using sodium hexametaphosphate [$(NaPO_3)_6$], the active ingredient in the dispersant Calgon® (Hodgkinson, 1991) was applied as a clay deflocculant. This substance is adsorbed by the clay particles, which start repelling each other and causing them to break apart or disperse (Riding, 2021). After four hours, distilled water was added to Calgon® for decantation, followed by a few washes until it became transparent.

Figure 3.8 — Palynological treatment processes: a-b) The fractioned outcrop samples, 30 g per container, before the hydrochloric acid (HCl 37%) treatment; c) Samples in Teflon containers following the second acid treatment with hydrofluoric acid (HF 48%) to dissolve silicates, agitating on an orbital shaker.

3.2.3 Microscopic Slides Assemblage and Examination

Once the organic palynological residue was completely clean, it was sieved to remove the largest fragments (i.e., megaspores) and the smallest amorphous organic particles, leaving only the components retained between the 15 and 125 μm sieves. From this point on, slides for microscopic observation could be prepared from the obtained palynological residue. Coverslips and thin sections were cleaned with alcohol-moistened toilet paper and placed on a heating plate (≈ 50˚C) (Fig. 3.9). From the mixed and dispersed palynological sample, a few drops were placed in the centre of the slide, carefully spread, and left to dry. After the palynological residue was dry, melted glycerinated gelatine was used to seal the coverslip, providing a defence against fungi due to the antibiotic in its composition. To conclude, two slides per sample were produced and labelled, thus making them ready for observation under the microscope. Nevertheless, of the 8 samples collected in the field, only samples CBL5, CBL6 and CBL7 produced palynomorphs. A Nikon Eclipse E-600 optical microscope was used to analyse the slides from top to bottom in horizontal lines with a 40x objective lens. All the specimens found were photographed, and their coordinates in the slides were documented.

Figure 3.9 — The slides preparation for microscopic observation: a) Coverslips and thin sections placed on the heating plate along with melted glycerinated gelatine suppositories used to seal them; b) Slides drying post-placement of palynological residues and coverslips; c) Photographic documentation of an analysed slide revealing palynomorphs.

3.2.4 Palynomorphs Findings in the Collected Samples

After photographing all specimens present on each of the slides containing palynological material, morphological analysis facilitated the identification of various palynomorphs *taxa* of continental origin. However, before any identification could be made, it was necessary to survey all the palynomorphs already found and identified from the outcrops of the Lusitanian Basin. When characterising the spores and pollens, the palynomorphs present were identified only at the genus level, as this is not the main objective of this work. Their systematic classification followed the taxonomy outlined by Ash (1978), Santos *et al.* (2022) and Santos *et al.* (2024).

Posteriorly, the identification process yielded a total of three pollen genera and eight spore genera, resulting in eleven distinct genera (Table 3.2). Additionally, five other palynomorphs displaying distinct morphologies were observed, including bissacate pollen grains, although their precise taxonomic identification remains unresolved.

Although the number of spore genera identified in the samples is higher than the number of pollen genera, the number of pollen and spore specimens, present in the samples does not follow the same proportion. On the contrary, pollen is the dominant palynomorph in all samples, representing almost three-quarters of the total palynomorphs. It is possible to verify that even among pollen, some genera are more abundant than others (Fig. 3.10).

Table 3.2 — List of palynomorphs identified in samples CBL5, CBL6 and CBL7.

Sample (nº)	Identified Genus	Palynomorphs
CBL5, CBL6, CBL7	*Classopollis* sp.	pollen
CBL5, CBL6, CBL7	*Spheripollenites* sp.	pollen
CBL5, CBL6, CBL7	*Exesipollenites* sp.	pollen
CBL5	*Cicatricosisporites* sp	spore
CBL6	*Matonisporites* sp	spore
CBL5, CBL6	*Ischyosporites* sp.	spore
CBL5, CBL6, CBL7	*Deltoidospora* sp.	spore
CBL5	*Staplinisporites* sp.	spore
CBL6, CBL7	*Striatella* sp.	spore
CBL5	*Verrucosisporites* sp.	spore
CBL5	*Trilobosporites* sp.	spore

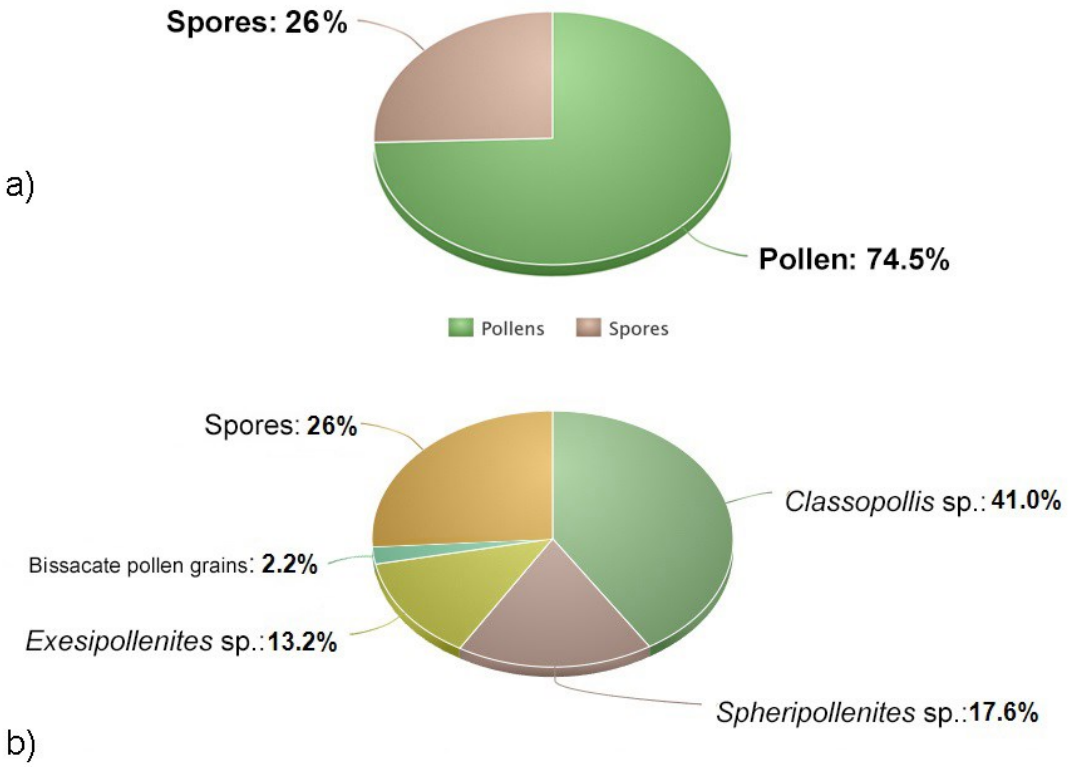

Figure 3.10 — Distribution of the number of specimens by genera considering all the collected samples. a) Distribution between pollen and spores considering all the samples that produced palynological material; b) The different percentages of pollen show the dominance of the genus *Classopollis* sp.

4

SYSTEMATIC PALAEONTOLOGY

4.1 Mammalian Mandible

Class Mammalia Linnaeus, 1758

Infraclass Allotheria Marsh, 1880

Order Multituberculata Cope, 1884

Suborder "Plagiaulacida" Ameghino, 1889

Family Pinheirodontidae Hahn and Hahn, 1999

Genus *New genus whose name will be determined upon publications*

Material: Right hemimandible with i-p_4.

Distribution: Ulsa quarry, Cambelas, São Pedro da Cadeira, Torres Vedras, Portugal.

Description: The right hemimandible is a small non-compressed specimen of an odontologically immature (juvenile/paedomorphic) individual (Fig. 4.1). Except for the base of the premolars and some concavities, the specimen is almost clear from the matrix. The posterior portion of the dentary bone is fragmentary, with both the coronoid and condylar processes missing. The tooth row forms an angle of ≈ 16˚ to the axis of the dentary.

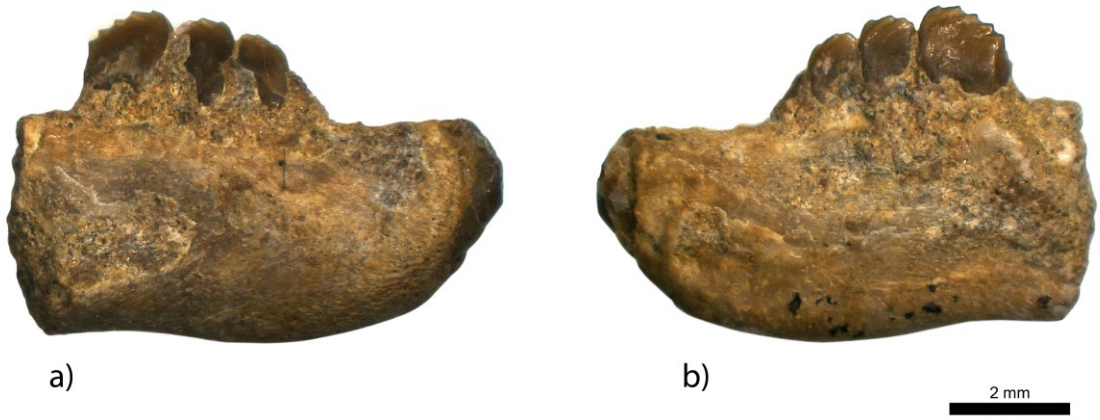

Figure 4.1 — This image, captured using the Hirox HXR-01 microscope at the HERCULES Laboratory of the University of Évora, presents a detailed view of the studied fossil. Although some mechanical cleaning has been carried out, sediment can still be seen at the base of the teeth. This is due to the fragile nature of the fossil, which has prevented further cleaning. a) labial view; b) medial view.

The deciduous incisor of the specimen is broken, leaving only a small portion of its crown to be exposed out of its alveolus. Despite the fracture, its root is present in situ. It is inserted steeply inside the mandible at an angle of ≈ 45˚, curving to a nearly horizontal position within. The root of the deciduous incisor is long, passing ventrally along the incisor and the apical portion of p_1, dp_2, and p_2, ending orthogonally at the level of the distal root of dp_2 (Fig. 4.2). The incisor is positioned immediately distal and dorsal to the primary incisor inside the dentary. It is a long conical tooth with only one cusp curved towards the apex. The mesial surface of its crown is convex whereas its root has not yet evolved. The anterior portion of the diastema is slightly damaged, revealing the tip of the erupting incisor. The posterior portion of the incisor is horizontally oriented to the jawline, ending orthogonally at the level of the distal root of p_4. A small portion of the mandibular symphysis is preserved on the anterior portion of the lingual side of the dentary bone, marked posteriorly by a semi-circular shallow depression. The diastema between the deciduous incisor and p_1 is long and straight in medial/lateral view, and its level is subequal to the alveolar margin of the premolars. From the incisive alveolus until the alveolar socket of m_1, the upper edge of the jaw follows a straight line. The small mental foramen is located ventral to the diastema, orthogonal to its mid-section, on the labial side dorsal to about mid-height of the mandibular body.

Gradually, a perfectly preserved row of four premolars grows mesiodistally in size. Except for the unicuspid p_1, which is nearly peg-like shaped, all the other premolars (dp_2, p_3, and

p_4) are blade-like. In labial view, p_{2-3} are subtriangular and tall, whereas p_1 is rhomboidal and p_4 quadrangular. The crowns of all four premolars are labiolingually compressed into flat oblique surfaces, with the posterior three forming a shearing edge. Nonetheless, it is imperative to emphasise that the crowns of the premolars are not compressed as a whole. Coronally to the cervical margin, they are swollen and broader than their corresponding roots. Compared to the other premolars, p_1 is smaller and shorter, not reaching the mesiodistal cutting edge formed by the distal premolars. It attaches to the mandible at an oblique angle in lateral view, using two straight roots of subequal length, while the other premolars are inserted more orthogonally. However, the mesial root of p_1 is almost twice as thick as the distal one. The subtriangular lobe advances far apically, making its crown higher than wide, although it is not as contrasting as in the distal premolars. Above the cervical margin, the lobe bulges on both sides of the crow, but it is significantly longer on the labial side. In occlusal view, p_1 shows a sub-quadrangular shape while its tip touches the anterior surface of dp_2. It is possible to observe a unique subtle ridge which runs basally obliquely on the labial side, corresponding to the single projection of p_1.

Except for the occlusal crest, dp_2 and p_3 are similar in size and shape, although p_3 is still larger. Both have a bulky and deeply extended subtriangular lobe rounded near their cervix that reaches next to the basal part of the mesial roots, with p_3 having the bulkiest lobe of all four premolars. The shape of the lobes is distinct on each side of the crowns, being more elongated on the labial side. This rule applies to all premolars in the fossil, including the bilobed p_4, making the labial surface of the crown always longer than the lingual surface. The second deciduous premolar is biradiculate. The two roots project almost to the same depth, with the mesial root being longer and substantially thicker than the distal root. The mesial root grows straight to the ventral portion of the jaw, while the distal one grows quite distally convex in lateral view. It is noticeable that the roots of dp_2 have the starkest size contrast among all premolars. Approximately in the middle of the mesial root of dp_2 on the lingual side, there is a concavity where the developing p_2 attaches. The occlusal crest of dp_2 has the exact contour expected for a primary tooth of a Kimmeridgian multituberculate: its serrated crest goes downward and forward, bearing three angular projections and two notches, the first of which is noticeably lower than the rear two. On both lingual and labial sides, two low ridges extend obliquely downward and forward, corresponding to the second and third crest projections. Although both distal projections are almost equal in height (the third one is slightly higher), the second crest elevation has the longest leading flank and a subtly lengthier ridge. As it is the last deciduous premolar in

situ, dp_2 has more rounded projections due to its use when compared to other premolars, which have sharper cutting edges.

The p_2 is inclined at an angle of 21° upward from the concavity of the mesial root of dp_2, touching gently the dp_2 distal root. It is also tilted 38° to the lingual side, causing its curved edge to point in the same direction. No serration is visible on the crown of p_2, nor are traces of radial structures in its apical portion. However, despite its sub-rounded morphology, a milder compression on both oblique sides of the crown is conspicuous.

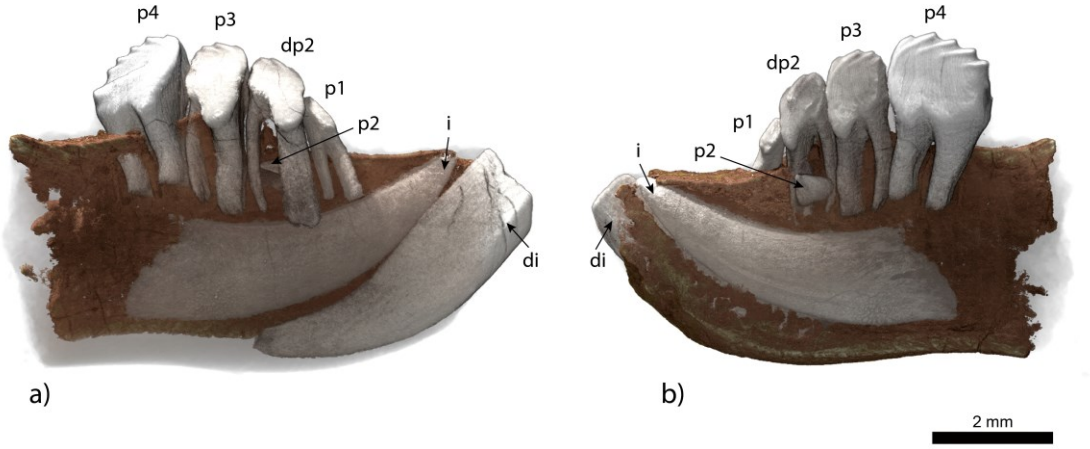

Figure 4.2 — The nano-computed tomography (nano-CT) conducted at Instituto Superior Técnico revealed the ontogenetic state of the specimen, with its deciduous teeth yet to erupt: a) labial view; b) lingual view; di) deciduous incisor; i) incisor; p1) first premolar; p2) second premolar; dp2) deciduous second premolar; p3) third premolar; p4) fourth premolar.

The p_3 has four notches and five angular projections, the second being the most prominent, followed by the third. These two more pronounced projections have low ridges that extend obliquely downward and forward on both sides of the crown. The most mesial ridge of p_3 is longer, curving mesially and downwards at the level of the first projection toward the mesial root on both the labial and lingual surfaces of the crown. The most distal portion of the p_3 crest is characterised by a short, rounded slope, which points distally and basally toward the most mesial wall of p_4. The fourth and the fifth projections grow over this inclined portion, with the fifth being the smallest and also pointing backwards to p_4. Despite that, the overall outline of the crest is nearly horizontal, forming a chisel-like edge, being taller than long. On the labial surface of the crown of p_3, in the basal cusp area, there is a shallow oval cavity bordered by an enamel ring that fades towards the distal root direction (Soc, Fig. 4.3 a, c). Hence, the enamel ring does not encompass the entire fossa. The enamel ring is positioned almost in the centre of

the labial surface, only slightly mesially displaced. SEM images revealed that the depression was caused by abrasion, as the wear marks on the inside contrast with the smooth enamel outside the concavity (Fig. 4.3). A similar pattern is found in the basal cusps of some specimens of *Ctenacodon serratus* (USNM V 2688; YPM 11832) and *Paulchoffatia delgadoi*, which would indicate that the specimen must have had, at least one large basal cusp on its p_3. Two slightly inward curved roots attach p_3 to the dentary bone. The distal root is flat mesiodistally, making it as wide as the mesial root in apical view, although this is the most voluminous. Because of the aforementioned flattening, the distal root is half the width of the mesial root in the lateral view.

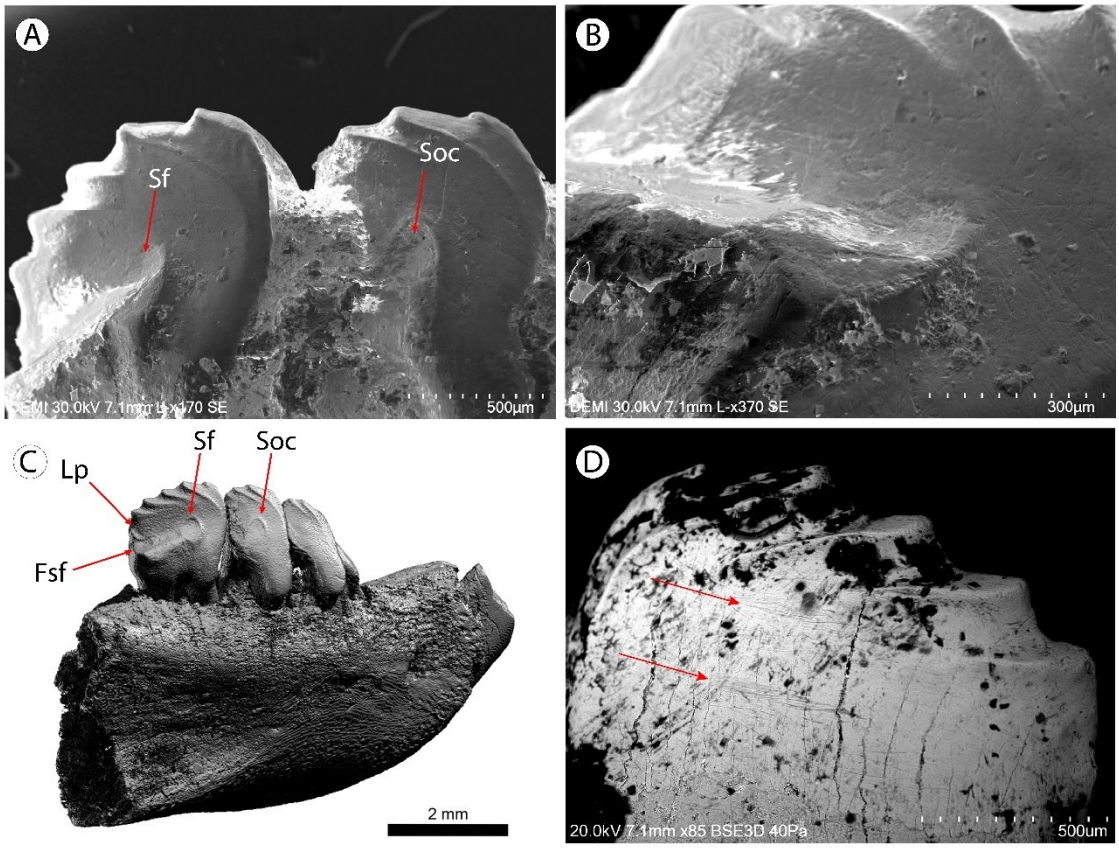

Figure 4.3 — Abrasion and microwear mark: a) SEM image taken with the model Hitachi SU3800 at the NOVA School of Science and Technology Laboratory, displaying shallow oval cavities caused by abrasion on the labial view of p_3 and p_4; b) Detail of the wear marks contrasting with the smooth enamel outside the concavity on the labial surface of the crown of p_4; c) Render of the nano-computed tomography (nano-CT) created with Zbrush Version 2020.1 and Adobe Photoshop Version 21.0.2 software, showing clearly the abrasion marks on p_3 and p_4; d) Abrasion marks on the lingual surface of p_4. SEM image taken with the model EDS Hitachi S3700N at the HERCULES Laboratory of the University of Évora. Ffs, faint shallow fossae; Lp, lump; Sf, shallow fossa; Soc, shallow oval cavity.

The p_4 is the only tooth that indicates the presence of a second lobe above the distal root, which is easier to distinguish on the lingual side. Although it is 1.6 times longer in labial view than p_3, making it the largest tooth of the specimen, compared to dp_2 and p_3, it has the shortest subtriangular lobe. Compared to the anterior lobe, its posterior lobe is distinctly less prominent, both being separated by a thin, deep slot. The p_4 has four notches and five angular projections forming a shearing edge. The first and second projections are the highest and have nearly the same height, whereas the second is the tallest and has the longest leading flank. In lateral view, the cutting line of the p_4 slopes distally and basally to the distal most portion of the tooth. The low ridges on both lateral surfaces of the crown appear under the second projection, becoming shorter and fading distally until disappearing entirely in the fifth projection. These ridges correspond to the second, third and fourth projections. As for the p_3, the mesial most ridge is the longest, curving mesially and basally toward the mesial root. Distally to the fifth projection of the crest, a small additional protuberance is conspicuous on the lingual side. This lump (Lp, Fig. 4.3 c) is part of a low ridge that grows around a superficial concavity on the labial side, which fades mesially under the fifth projection. On the same side, approximately in the mid-body height of the p_4 grows, a step-shaped facet that slopes basally, bearing three abrasion concavities. In the posterior view, the contact point between this facet and the labial surface of the crown creates an obtuse angle. As found on p_3, a shallow (Sf, Fig. 4.3 a-c) fossa bordered by an enamel ring is the most mesial among other abrasion marks. However, this depression, rather than being oval, is more circular, and its ridge is less distally faded, making its shape more evident. This discrete concavity has an angle of 69° tilted apically and towards the mesial portion, being succeeded distally by two faint shallow abrasion fossae, almost indistinguishable (Fsf, Fig. 4.3, c). The most distal abrasion depression, which is best preserved, would indicate the presence of at least one worn basal cusp. Both roots of p_4 are subequal in height and thickness. They also have the same shape, being flattened mesiodistally, which makes them mediolaterally wider.

The m_1 is missing, but in occlusal view, distal to p_4 and mesial to the broken portion of the dentary bone, its alveolar socket is partially preserved (M1as, Fig. 4.4 a). The preserved portion of the alveolar socket does not allow to deduce whether m_1 is two-rooted. Its concavity is slightly smaller than the alveolus of p_4. Situated in the posterior portion of the labial side of the mandible, a large masseteric fossa extends anteriorly to the level of the mesial root of p_3, merging gradually with the lateral side of the jaw (Fig. 4.4).

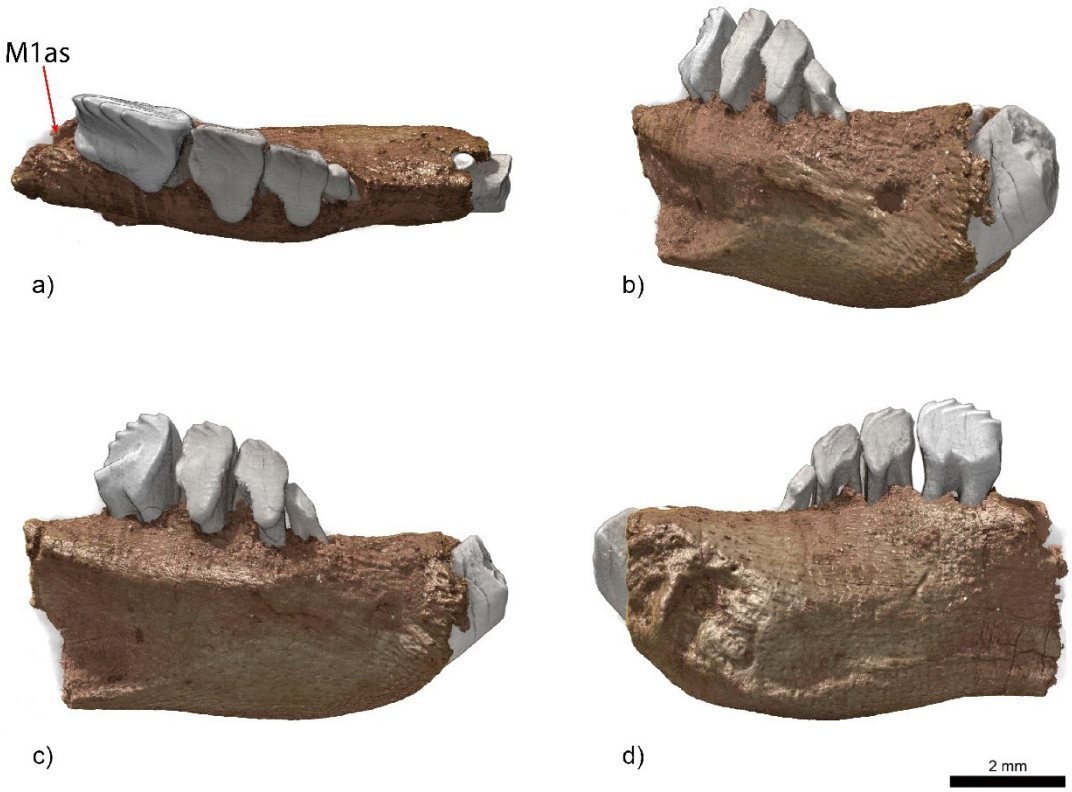

Figure 4.4 — Render of the studied fossil created with DragonFly software, Version 2022.2 Build 1409. a) dorsal view; b) anteroposteior virew; c) labial view; d) lingual view. M1as, alveolar socket of the missing, first lower molar.

(Comparative morphology with Portuguese Multituberculates). Given that the most diverse multituberculate fossil record in Europe comes from the prolific Portuguese coal mine of Guimarota, such a collection is the best starting point for comparing materials (Codrea *et al.*, 2017). There are ten species of multituberculates known through their lower dentition, among other parts, from the Guimarota lignites. However, some are based only on the lower molars (Hahn & Hahn, 1998b). Because the specimen here presented has no molars preserved, the species that can be used for comparison is restricted to six: *Paulchoffatia delgadoi*, *Kuehneodon dietrichi*, *Kuehneodon guimarotensis*, *Guimarotodon leiriensis* (Hahn, 1969), *Kuehneodon uniradiculatus* and *Meketibolodon robustus* (Hahn, 1978a). Although all these species belong to Paulchoffatiidae (Hahn, 1969), a more detailed examination is necessary due to its high dental morphological variability. Regardless of not coming from the Guimarota strata, two more paulchoffatiids from Kuehneodontinae are known from their lower dentition: *Kuehneodon hahni* and *Kuehneodon barcasensis* (Antunes, 1998; Hahn & Hahn, 2001).

According to Hahn (1978a), among the different genera of Kimmeridgian multituberculates, the incisor of the lower jaw presents notable variations, especially its overall structure and the size of its root, which are relevant for diagnostic purposes. Although the deciduous incisor of the specimen is broken, it is possible to conclude that it is steeply inserted in the mandible at the same plesiomorphic angle of 45° as *Paulchoffatia*. This trait resembles the angle of the incisor of *Guimarotodon*, which is also steeply implanted and short-rooted but differs from Kuehneodontinae and *Meketibolodon*, whose incisors are longer and more horizontally inserted in the jaw (Hahn, 1969; 1978a). Comparing the completely preserved deciduous incisor of the paulchoffatiid (V.J. 466-155) with the deciduous incisor of the studied fossil, it is possible to verify that their roots differ in size and shape, being the latter slender, longer, and more curved (Hahn, 1987: Table 2, Fig 1). The diastema of the new fossil is proportionally longer than any diastema found in the Guimarota species. Even so, the root of the deciduous incisor extends posteriorly to below the distal root of dp_2, demonstrating that it is a long tooth despite not reaching the most posterior premolars like in Kuehneodontinae. Although there are some deciduous incisors from Guimarota (Hahn, 1978c: Figs. 1 a-c, 2 a-b, 3 a-b, 5), it is not feasible to use the length of the di from the specimen for comparative purposes. This impossibility happens because most of the complete jaws found were attributed to adult individuals. The same problem occurs with the incisor, which is still inside the jaw and does not yet have a developed root. However, it can be observed that, regardless of its ontogenetic stage, the incisor has a more advanced upturned crown, which structurally reminds more of the species from the Kuehneodontinae than Paulchoffatiinae.

The angle of ≈16° between the premolar row and the dentary axis of the specimen is the same as the one found in *Meketibolodon* (diverging between 12°-16°) and *Guimarotodon* (15°) (Hahn, 1978a; 1987). It also differs from Kuehneodontinae, which has an angle of 20°, and from *Paulchoffatia*, whose premolars run almost parallel to the longitudinal axis of the jaw, having the lowest angle, ranging between 7°-10° (Hahn, 1969; 1978a).

According to Lazzari *et al*. (2010), among multituberculates, Kimmeridgian paulchoffatiids are believed to have unique morphology of the lower premolars, in which the p_3 and p_4 are subequal in length. In this regard, the p_4 of the specimen is longer (1.6 times) than its p_3, differing it from the usual paulchoffatiid proportion and bringing it closer to more derived *taxa* (Kielan-

Jaworowska & Ensom, 1992). The p_{1-3} of the new fossil differs from the premolars of Paulchoffatiidae for having elongated subtriangular lobes, conferring them a triangular outline instead of sub-rectangular premolars (Fig. 4.5).

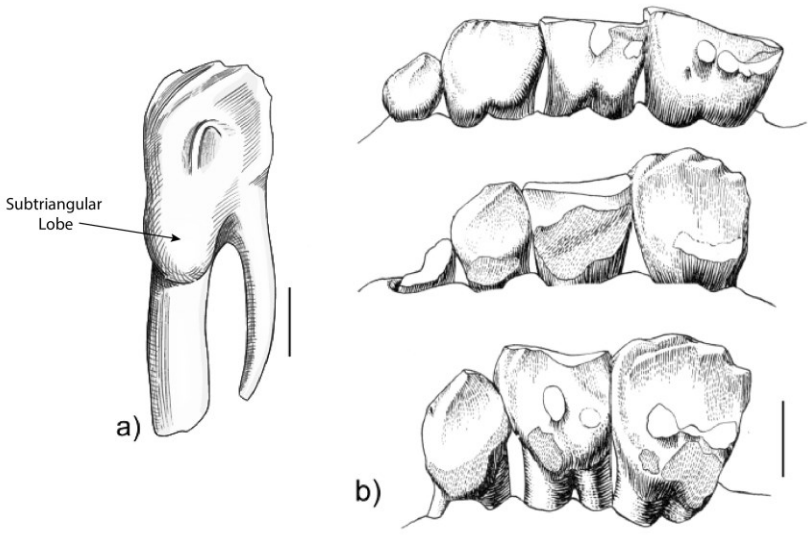

Figure 4.5 — Comparison between the a) elongated subtriangular lobe of the p_3 of the specimen and b) the sub-rectangular premolars of the paulchoffatiids (top to bottom) *Paulshoffatia delgadoi*, *Kuehneodon dietrichi* and *Kuehneodon guimarotensis* (Carvalho, in this work, modified from Hahn, (1969)). Scale bar: a) 0,5 mm; b) 1 mm.

Among the Kimmeridgian multituberculates, the p_1 is the tooth with the greatest morphological variability within the lower premolars. Based on Hahn (1978a), this wide variance in p_1 suggests that the tooth was becoming evolutionarily atrophied and had a reduced masticatory purpose. Its shape can vary even within the same genus, depending on which specimen is being analysed. This fact makes the use of p_1 crown morphology for diagnostic purposes impractical. However, the roots of p_1 are more informative. The bi-rooted p_1 of the specimen is a more plesiomorphic trait, which again brings it closer to Paulchoffatiinae. Although some kuehneodontines share this same characteristic (e.g., *Kuehneodon hahni and K. dietrichi*), the trend in Kuehneodontinae was already the reduction in the number of roots, from two to one, or the total loss of the p_1, *K. uniradiculatus* and *K. guimarotensis*, respectively. Bi-rooted p_1s can also be found in other *taxa* (e.g., Pinheirodontidae) (Hahn & Hahn, 1999).

Both p_3 and p_4 of the studied fossil have five angular projections that differ from the Paulchoffatiidae p_3, which has three or four points on the cutting edge, and p_4, whose average number of projections is four (Hahn, 1978a). Some paulchoffatiids can develop a fifth projection on

p_4. However, this trend is not substantially represented in this family. Whenever this fifth elevation is conspicuous, it tends to be the smallest. Sometimes, it is so tiny that it is difficult to distinguish it from a small protrusion (Hahn, 1971). Another visible characteristic is that in Paulchoffatiidae, the second elevation tends to be the highest point of the crown, contrasting with the smaller first one (Hahn, 1969: Fig. 29 a; Hahn & Hahn, 1998a: Figs. 14 - 23). Both these traits are not present in the p_4 of the specimen. All its five projections on the shearing edge are distinctly developed, being the fifth strongly defined and having the same size as the previous two, while the first and the second projections have almost the same height.

In Paulchoffatiidae, the number, arrangement, and distribution of basal cusps on the lower premolars may vary considerably. The most common morphology is the p_3 having one row of basal cusps consisting of two to three humps, whereas the p_4 has one row of four to five cusps (Hahn, 1978a). Nonetheless, some species developed a second row of ornamental cuspules below the main row of cusps (Hahn & Hahn, 1998a), whereas others can grow them on their dp_2 (Hahn, 1978b: Fig. 12 a-c). Due to the wear found in the basal cusps area of the studied fossil, it is difficult to compare the basal cusps distribution with Paulchoffatiidae precisely.

Outside the context of the Guimarota *taxa* but still within the Paulchoffatioidea of the Portuguese Late Jurassic, the Pinheirodontidae family is better represented by the isolated teeth found in Porto Dinheiro, Portugal. Although the author claims that 250 teeth have been found, only a few specimens have been published. Furthermore, some tooth correlations have been made arbitrarily, basing them on the state of preservation as if they were relevant morphological characters. The known lower dentition of pinheirodontids supposedly belongs to four species*:* *Pinheirodon pygmaeus*, *P. vastus*, *Bernardodon atlanticus* and *Iberodon quadrituberculatus* (Hahn & Hahn, 1999). Despite this, only three morphological types can be distinguished in Pinheirodontidae instead of four.

Typically, the Portuguese, pinheirodontid genera have four projections on their p_3 and six on their p_4, differing from both the p_3 and p_4 of the specimen. As in the studied material, the ridge that descends from the second projection of the premolars of pinheirodontids is always the longest.

It is important to note that *Pinheirodon pygmaeus* and *P. vastus* are identical in every aspect except size. Some specimens of *P. vastus* can be twice the size of *P. pygmaeus*. Because no p_4 found was assigned to *P. vastus*, only its p_3 can be used for comparison. The premolars

belonging to *Pinheirodon* have bulges above the cervical margin that may indicate traces of basal cusps (Kielan-Jaworowska *et al.*, 2004). However, due to its state of preservation, it is not possible to make any comparisons with the new fossil. In distal view, the p_4 of *P. pygmaeus* is similarly structured, having both lingual and labial sides of its crown sloping almost symmetrically, forming a triangle. Still, in distal view, the p_4 of the new fossil has a different outline due to its distinctive sides. The occlusal facet of the labial surface makes the crown bulkier. The p_{2-3} of *P. vastus* is bilobed, a trait that differs from the studied material that has only one subtriangular lobe above the mesial root (Fig. 4.6). Although the mesial lobe of *P. vastus* is large and prominent, reaching the proximal portion of the mesial root, the single subtriangular lobe of the specimen is bulkier and longer (Hahn & Hahn, 1999).

As in *Pinheirodon vastus*, the p_{2-3} of *Bernardodon* is bilobed, thus also differing from the new fossil. In posterior view, both lingual and labial sides of p_{2-3} of *Bernardodon* bulge out convexly, giving it a rounded shape, which contrasts with the triangular shape of the p_{2-3} of the new fossil. Another noticeable difference is that on the labial surface, the p_{2-3} of Bernardodon develops a prominent facet where its basal cusps project (Hahn & Hahn, 1999). In the specimen, the crown also widens basally until the proximal portion of the roots, but they are flat. The surface of the lingual side is completely straight, while the labial surface is also straight with an almost imperceptible bulge. Although the basal cusps of the sample p_{2-3} are worn, it is possible to infer that *Bernardodon* had a superior number of basal cusps.

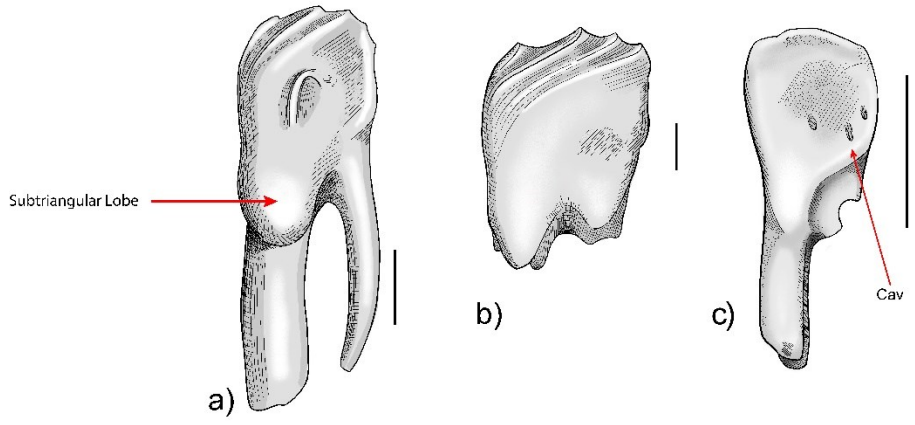

Figure 4.6 — Comparison between the p3 of the a) specimen and the b) p3 of the pinheirodontid *Pinheirodon vastus* (mirrored). Although the premolar of *P. vastus* has a more developed subtriangular lobe than the paulchoffatiids, it is still smaller than that of the specimen, a pattern that occurs in all species of pinheirodontids, and it also displays a second lobe over the distal root; c) the cavities (Cav) on the labial side of the p_3 in *Iberodon*, mirrored illustration (Carvalho, in this work, modified from Hahn and Hahn, (1999)). Scale bar: 0, 5 mm.

According to Kielan-Jaworowska and Ensom (1992), Hahn and Hahn (1999), and Kielan-Jaworowska *et al.* (2004), *Iberodon quadrituberculatus* is the only species which developed an autapomorphy among pinheirodontids: the replacement of the cusps of both p_3 and p_4 with pits. Nevertheless, in agreement with Martin *et al.* (2019), these pits are merely preservation artefacts caused by intense wear. Since enamel is generally significantly harder, these cavities are left after the dentine of the basal cusps is worn away (Cav, Fig. 4.6 c). In addition, *Iberodon* presents the most intense worn among the pinheirodontid species. This thesis also agrees with Martin *et al.* (2019) in that this phenomenon is also present in some paulchoffatiids housed at the Geological Museum in Lisbon. Thus, the premolars in *Iberodon* seem to have originally had five small basal cusps. Although, in both specimens, the basal cusps are worn, it can be inferred that the studied fossil had a much larger first basal cusp than *Iberodon* (Fig. 4.6 a-c). The p_{2-3} of *Iberodon* shares with the new fossil no development of a posterior lobe on the crown. However, its subtriangular lobe is smaller and less robust when compared to the new fossil (Hahn & Hahn, 1999). Aside from this difference, the lower crown border distal to the subtriangular lobe goes up in a steep ascending line towards the posterior edge of the crown in a very similar curvature to the specimen. Apart from the basal cusps, the p_4 of *Iberodon* differs from the new fossil due to a less pronounced anterior lobe compared to the posterior lobe. In posterior view, the p_4 of *Iberodon* shows a less marked and more rounded facet, probably caused by wear (Fig. 4.7). This feature, together with a slightly concave labial surface, makes its posterior portion almost symmetrical, in what Hahn and Hahn (1999) called "bottleneck shape". Due to the state of preservation of p_4, it is not possible to make a more accurate comparison from this point of view. Within pinheirodontids, *Iberodon* and *P. pygmaeus* have the closest p4:p3 ratio to the studied sample, where p_4 is 1.7 and 1.5 times greater than p_3, respectively.

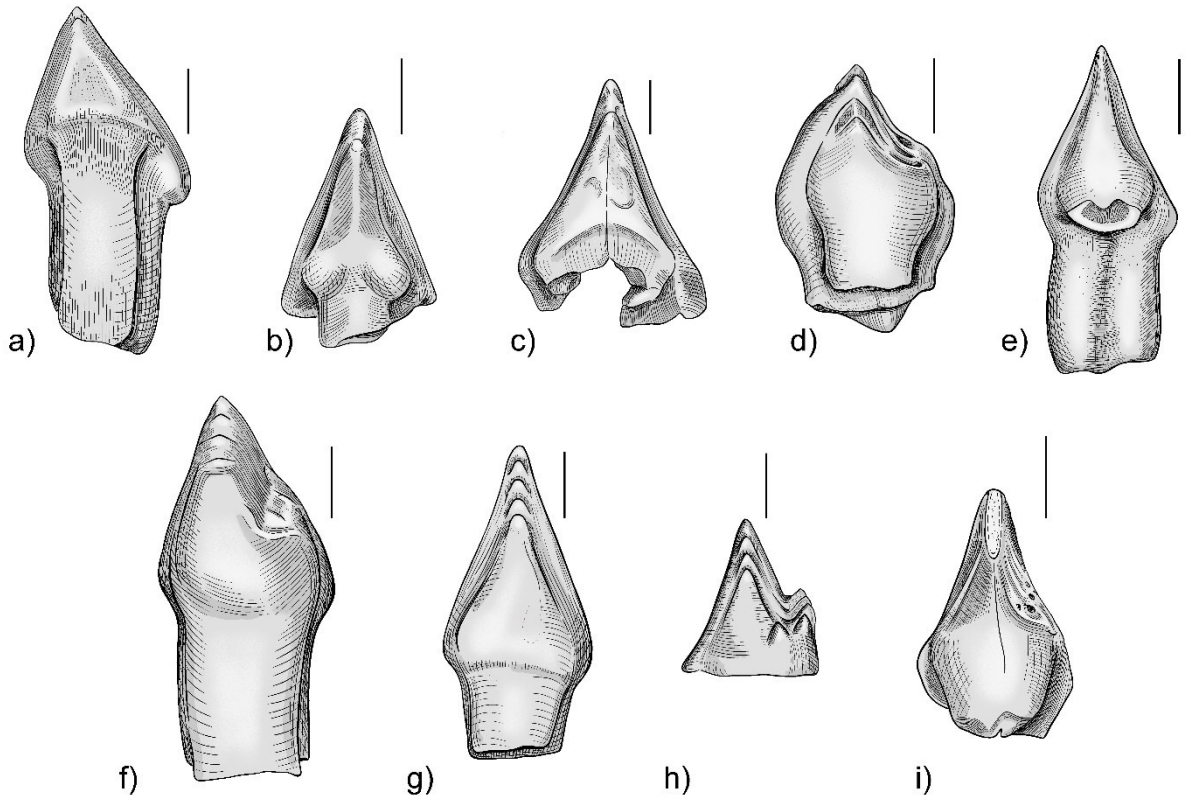

Figure 4.7 — Comparison between p_3 and p_4 of the specimen with the p3 and p4 of pinheirodontids in posterior view: a) p_3 of the specimen; b) p_3 of *Pinheirodon pygmaeus*; c) p_3 of *P. vastus*; d) p_3 of *Bernardodon atlanticus*; e) p_3 of *Iberodon quadrituberculatus*; f) p_4 of the specimen; g) p_4 of *P. pygmaeus* (mirrored); h) p_4 of *B. atlanticus* (mirrored); i) p_4 of *I. quadrituberculatus* (modified from Hahn and Hahn, (1999)). Scale bar: 0, 5 mm.

(Comparative anatomy with Plagiaulacidae and Allodontidae). For many decades, the only uncontested plagiaulacids were found in England, *Bolodon* and *Plagiaulax* (Falconer, 1857; Owen, 1871; Kielan-Jaworowska *et al.*, 2004). In recent years, a new species from North America was described as belonging to *Bolodon* (Cifelli *et al.*, 2012), which now has six species (four with known lower dentition), despite the still present uncertainty that *"B." elongatus* to belong to this genus (Hahn & Hahn, 1983; Kielan-Jaworowska & Hurum, 2001). These multituberculates show characteristics present in Early Cretaceous specimens. In the lower dentition, they have a reduction they have a reduction in the number of premolars, whereas their size, number of projections and level of morphological complexity increased (Kielan-Jaworowska & Ensom, 1992). Although *Plagiaulax* loses p_1, consequently remaining with only three premolars, *Bolodon* has four lower premolars. In that sense, the new fossil is closer to *Bolodon* than *Plagiaulax*. Despite the differences in jaw size, the sample is more massive and bulkier, especially in its anteroventral portion, compared to *Bolodon*. Its diastema is also distinct, being flatter and longer. The studied

fossil does not have one of the most distinguishable apomorphies of plagiaulacids: the elongated p_4, about twice as long as p_3, bearing five to seven ridged projections on the serrated crest (Kielan-Jaworowska & Ensom, 1992). Even though the p_4 of the specimen also has five projections on its crest and is longer (1.6 times) than its p_3, it does not reach the measurements found in Plagiaulacidae. In this family, the p_3 has four projections forming the shearing edge, one less than in the new fossil (Owen, 1871; Simpson, 1928). This one shares with *Bolodon* the high, subtriangular aspect of the crowns of p_3. The prolongation of the triangular lobe, its shape and proportion about the crown height of p_3 within *Bolodon* specimens and species vary immensely. For that reason, it is not possible to make a precise morphological comparison with the new fossil (e.g., Kielan-Jaworowska & Ensom, 1992: Pl. 2, Figs. 4 and 7; p3, DORCM GS 201, p3 of BMNH 48399). Plagiaulacids have no basal cusps on the labial side of p_3, whereas it has a row of basal cusps on p_4 (Kielan-Jaworowska & Hurum, 2001).

The Allodontidae family is known from two genera, *Ctenacodon* and *Psalodon*, from the Late Jurassic Morrison Formation in the United States (Marsh, 1879; Simpson, 1926; Kielan-Jaworowska *et al.*, 2004). Yet, *Psalodon* is known only from the upper jaws. Compared to *Psalodon? marshi* (USNM V 2684), the jaw of the new fossil has a more robust gestalt, mainly in its anteroventral portion, joining to the alveolar socket margin of the incisor via a more pronounced curvature. The diastema of both multituberculates appears to be similar in size. A more precise comparison is not possible due to the state of preservation of the allondontid dentary, which also hinders the identification of morphological characters on the teeth. Nevertheless, it is possible to discern two lobes on its p_3 and more pronounced lobes on its p_4, which are incompatible traits with the teeth morphology of the specimen. The growth of p_4 concerning p_3 is also present in this family. In Allodontidae, p_4 tends to be 1.5 times longer than p_3, a ratio close to that found in the studied material (1.6).

According to Kielan-Jaworowska and Hurum (2001), allodontids, and paulchoffatiids, have the distal lower premolars quadrangular in labial view instead of the sub-triangular shape found in the sample and plagiaulacids. This characteristic is present in *Psalodon? marshi* (USNM V 2684) and *Ctenacodon serratus* (USNM V 2688). However, some specimens diagnosed as *Ctenacodon* can show different traits. One example is *Ctenacodon* sp. (USNM PAL 619515), which displays massive subtriangular lobes on the labial side of its premolars that, although basally longer, resemble those of the new fossil. The length of the diastema is also similar in both specimens, but it is more angled in the allodontid jaw, contrasting with the new

fossil diastema. Posteriorly, the diastema of *Ctenacodon* sp. (USNM PAL 619515) maintains its angle until it reaches the alveolar line of the premolars, forming an arch that descends basally along the distal root line of the p_4, which contrasts to the flat alveolar line observed in the new fossil. *Ctenacodon* sp. also differs from the new fossil by having three (possibly four) projections on the crest of p_3; the mesial lobe of p_4 more prominent, making the gap between it and the distal lobe more carved; the masseteric fossa less anteriorly extended, orthogonal to m_1. Compared to the sample, *C. serratus* (USNM V 2688) differs in having shorter and more squared premolars with smaller subtriangular lobes on the labial side, bearing a small lobe over the distal root of p_3; three projections on p_3; the distal lobe of p4 rounder and more conspicuous; a more compact and delicate overall shape of the jaw; a more posterior extended masseteric fossa. The diastema of *C. serratus* is shorter. However, it is as flat as in the specimen, as is the alveolar line of the premolars.

Based on Kielan-Jaworowska *et al.* (2004), allodontids share with plagiaulacids the loss of labial cusps on p_3, thus differing from the new fossil. However, it is necessary to point out that although the descriptions of the holotypes do not mention any basal cusps on p_3, some specimens analysed through this research appear to have had them already, but apparently, they are worn (e.g., USNM PAL 619515; YPM 11832). In p_4, both allondontid genera share six projections on their crests and a row of basal cusps, which are usually almost entirely abraded by wear despite the tooth being unworn. This feature, mentioned by Simpson (1929), is similar to the one found in the new fossil, i.e., the crest projections are better preserved while the basal cusps are worn. In *Psalodon? marshi,* the row of basal cusps, mesial to a single bulky protuberance, grows in size progressively in a line oblique to the crown. According to Simpson (1929), *Ctenacodon* has a similar structure of small accessory basal cusps on p_4. Unfortunately, this characteristic cannot be compared with the new fossil.

Comparative anatomy with (other multituberculate *taxa*). *Zofiabaatar pulcher* was discovered in the latest Morrison fauna, making it the youngest specimen of multituberculate known from that Formation (Bakker *et al.*, 1990; Carpenter, 1998). This species is placed in a monotypic family called Zofiabaataridae (Bakker, 1992; but see Carpenter, 1998). *Zofiabaatar* differs from the new fossil for having a shorter and slopped diastema, forming a small step distal to p_1, and an inclined alveolar line of premolars. *Zofiabaatar* also differs from the new fossil in having possibly four projections on p_3, which is bilobed and, for that reason, also lacks the curvature on the

posterior edge of the crown; and a p_4 with seven serrations on its crest, almost as long as p_2 and p_3 together. *Zofiabaatar* p_4 also contrasts with the new fossil for having an arched occlusal surface, whose highest point is above the posterior part of its anterior root (Carpenter, 1998).

Glirodon grandis has been considered an *incertae sedis* multituberculate (but see phylogenetics section) also found in the Late Jurassic Morrison Formation known from upper and lower dentition (Gillette, 1999; Kielan-Jaworowska *et al.*, 2004). *Glirodon* differs from the new fossil for having a pronounced shorter and concave diastema; a less anteriorly extended, but laterally prominent well-developed masseteric fossa; the alveolar line of the premolars forming an angle, reaching the highest point under the p_4; three projections on the crest of p_3, which lacks any basal cusp. *G. grandis* shares with the specimen a lengthy triangular lobe on the labial surface of p_3, which is also not bilobed, and five projections on the occlusal crest of p4 (Gillette, 1999).

Following the aforementioned morphological comparisons, it is evident that the examined specimen does not correspond to any known species (Fig. 4.8).

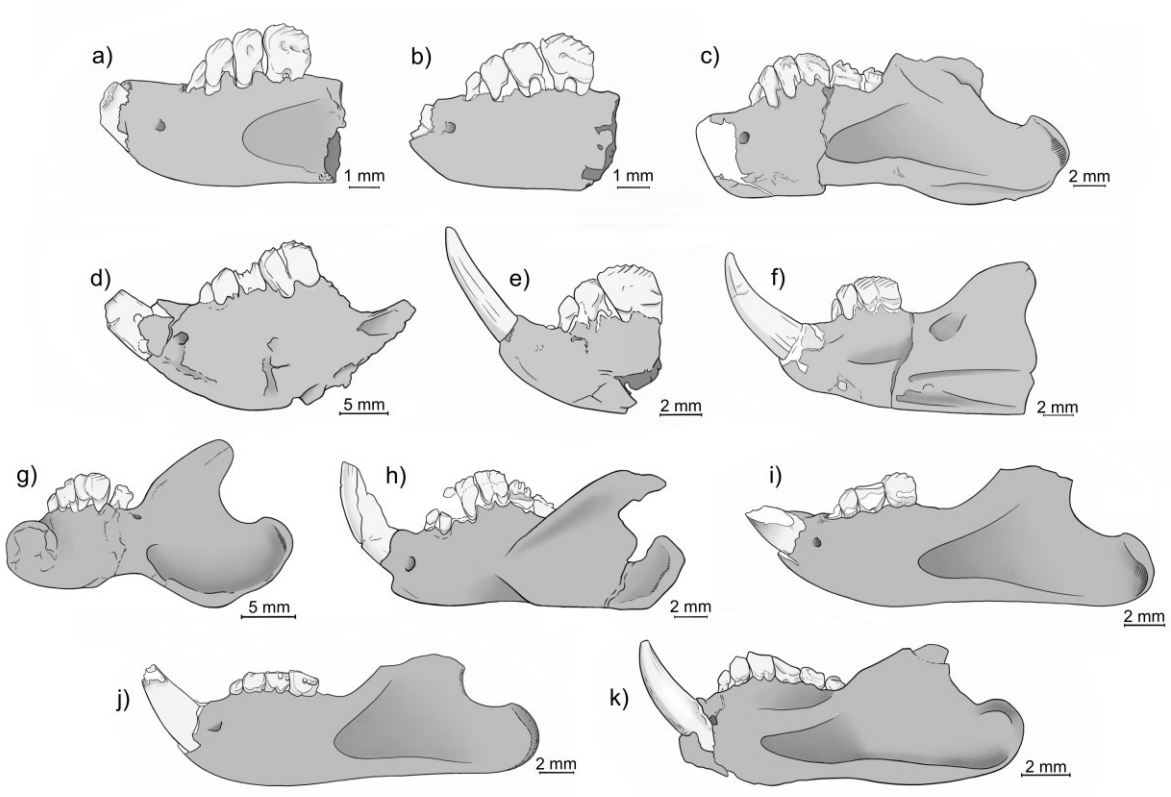

Figure 4.8 — Comparison between the right mandible (mirrored lateral view) of the new specimen a) and the following multituberculates: b) *Ctenacodon serratus* (USNM V 2688), mirrored lateral view; c) *Ctenacodon* sp. (USNM PAL 619515), lateral view; d) *Psalodon? marshi* (USNM V 2684), lateral view; e) *Bolodon falconeri* (NHMUK PV OR 47730), mirrored lateral view; f) *Plagiaulax becklesii* (NHMUK PV OR 47731), mirrored lateral view; g) *Zofiabaatar pulcher* (UCM 42329), mirrored medial view; h) *Glirodon grandis* (LACM 120452), mirrored lateral view; i) *Kuehneodon dietrichi* (V. J. 4 -155), mirrored lateral view; j) *Paulchoffatia delgadoi* (V. J. 1 -155), lateral view; k) *Meketibolodon robustus* (IPFUB Gui Mam 89/76), lateral view.

4.2 Palynological Taxonomy

4.2.1 Pollen

Family Cheirolepidiaceae Turutanova-Ketova, 1963

Genus *Classopollis* Pflug, 1953

Species *Classopollis* sp.

Remarks: The genus *Classopollis* (Fig. 4.9) is the most dominant *taxon*. On average, *Classopollis* represents 41% of the palynomorphs found in every sample from the Ulsa quarry. This spherical pollen, which generally occurs isolated (monad) or in tetrads, was produced by the extinct conifer family Cheirolepidiaceae, one of the most diverse conifer groups throughout the Mesozoic (Srivastava, 1976; Kürschner *et al.*, 2013). Fossil evidence of this family first emerged in the Late Triassic period in western North America (Tosolini *et al.*, 2015), while the latest records are dated to the Paleocene (Barreda *et al.*, 2012), The genus *Classopollis*, considered cosmopolitan pollen (Traverse, 2007), is characterised by a thickened equatorial band, a distal circular aperture through which the pollen can interact with its environment (cryptopore) and a proximal tetrad scar (Srivastava, 1976).

Figure 4.9 — *Classopollis* sp., the predominant palynomorph in all samples (CBL5, CBL6 and CBL7), appears as isolated grains and as in tetrads. Scale bar: 25 µm.

Family Cheirolepidiaceae Turutanova-Ketova, 1963

Genus *Spheripollenites* Couper, 1958

Species *Spheripollenites* sp.

Remarks: *Spheripollenites* (Fig. 4.10) are pollen grains originally spherical, possessing an equidimensional germinal aperture that can sometimes be indistinct (Burger, 1965). This genus was the second most frequently encountered palynomorph across the samples. The highest frequency of this pollen was found in sample CBL7, which accounted for approximately 33% of it. In sample CBL6, *Spheripollenites* represented 18% of the identified palynomorphs, and in CBL5 only 2%. According to Santos *et al.* (2022), this alete pollen is typically associated with conifers. However, its biological affinity is ambiguous since distinct authors frequently assign them to different families, such as Cheirolepidiaceae, Cupressaceae or Araucariaceae. However, in their more recent work, Santos *et al.* (2024) associated this genus with Cheirolepidiaceae.

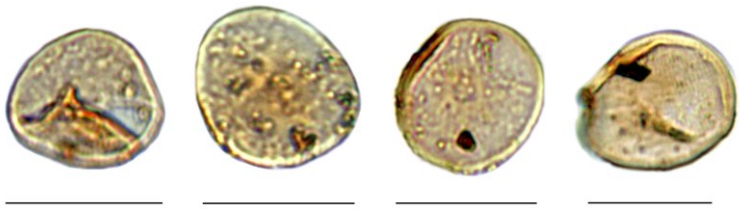

Figure 4.10 — *Spheripollenites* sp., the second most frequent palynomorph found in all samples (CBL5, CBL6 and CBL7). Scale bar: 25 µm.

Genus *Exesipollenites* Balme, 1957

Species *Exesipollenites* sp.

Remarks: The *Exesipollenites* genus (Fig. 4.11) is present in all the samples collected, being more abundant in CBL5, representing 20% of it. In CBL6 it composes 5% of this sample and 14.5% of CBL5. *Exesipollenites* is a monosporate pollen from a plant likely belonging to the Bennettitales, a group of gymnosperms similar to cycads that existed from about 250 to 70 million years ago (Peñalver *et al.*, 2015). As Watson *et al.* (1991) and Abbink (1998) noted, Bennettitales flourishes in dry, warm environments.

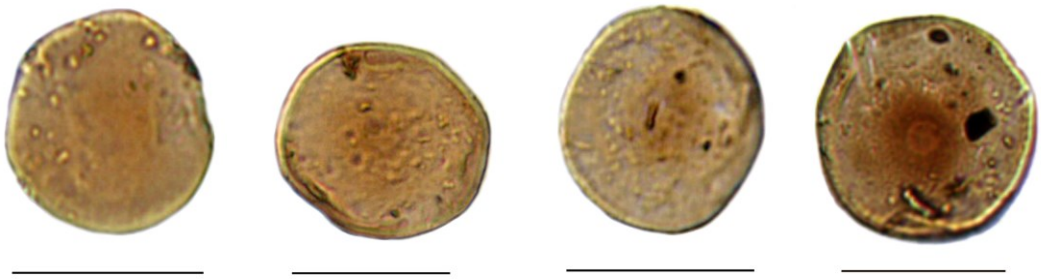

Figure 4.11 — *Exesipollenites* sp., a genus of pollen present in all the collected samples (CBL5, CBL6 and CBL7). Scale bar: 25 µm.

4.2.2 Spores

Family Schizaeaceae Kaulfuss, 1827

Genus *Cicatricosisporites* Potonié and Gelletich, 1933

Species *Cicatricosisporites* sp.

Remarks: The *Cicatricosisporites* (Fig. 4.13) is a trilete fern spore characterised by its radial symmetry and triangular outline, with sides that are either straight or slightly convex (Backhouse, 1988). The slits in the outer layer, or *laesura*, are elevated, exhibiting a gentle wave-like pattern, and stretching up to three-quarters of the spore radius, from the centre of the pollen grain to its outer edge. The *Cicatricosisporites* displays a cicatricose enxine ornamentation (Legrand *et al.*, 2011). This spore was only found in sample CBL5, representing 2% of its palynomorphs, following the pattern described by Duarte *et al.* (2021) that when in correlation with markers of dry climate, their presence is typically not statistically significant. According to the same authors, other researchers have attributed the association between *Cicatricosisporites* and *Classopollis* to hot and arid paleoclimates. For instance, Choi (1985) suggested a dry and warm paleoclimate based on the presence of *Classopollis* and *Ephedripites* and a limited occurrence of *Cicatricosisporites*. Schrank (2010) reported similar climatic conditions, identifying *Cicatricosisporites* and *Classopollis* in the Upper Jurassic and Lower Cretaceous sediments of Tanzania. Nichols (2003) also associated *Cicatricosisporites* with arid climates, citing its presence alongside *Classopollis* and *Exesipollenites*, among others, in the Cretaceous layers of China.

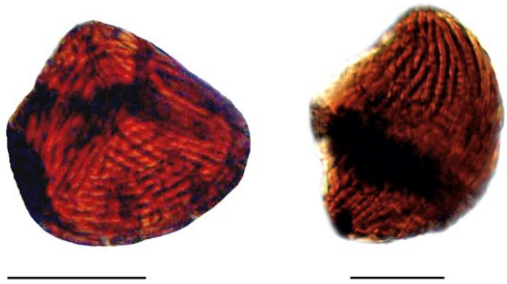

Figure 4.12 — *Cicatricosisporites* sp., a trilete fern spore collected only in the sample CBL5. Scale bar: 25 µm.

Family Matoniaceae Presl, 1847

Genus *Matonisporites* Couper, 1958

Species *Matonisporites* sp.

Remarks: Trilete spores (Fig. 4.14) featuring a biconvex shape with straight or concave sides. The *suturae* nearly reach the radial thicker crassitudes, i.e., the thickened areas of the exine, which is the outer layer of the spore or pollen grain (Backhouse, 1988; Legrand *et al.*, 2011). This spore was found only in the sample CBL6 representing 3% of its content. This genus belongs to the Matoniaceae, a family of ferns that could live in drier areas of the lowlands, not needing to stay in shady and humid regions such as freshwater bodies. However, this family of ferns had a wider range of distribution and a greater variety of potential habitats during the Mesozoic (Santos *et al.*, 2022).

Figure 4.13 — *Matonisporites* sp., a trilete fern spore found only in the sample CBL6. Scale bar: 25 µm.

Family Schizaeaceae Kaulfuss, 1827

Genus *Ischyosporites* Balme, 1957

Species *Ischyosporites* sp.

Remarks: *Ischyosporites* (synonym of the *Klukisporites* genus) (Fig. 4.15) is a strongly ornamented subtriangular trilete spore (Backhouse, 1988). This genus was found in samples CBL5 and CBL6, being more numerous in the former, representing 3% of its palynomorphs. According to Waksmundzka (2014), Guy-Ohlson (1971), based on observation of modern spore material of Schizaeaceae and Dicksoniaceae, suggested including the genus *Ischyosporites* into the family Schizaeaceae. Cranwell and Srivastava (2009) recognise *Klukisporites* as having botanical affinities with Schizaeaceae, reaffirming the taxonomy proposed by Guy-Ohlson, since the two are synonymous.

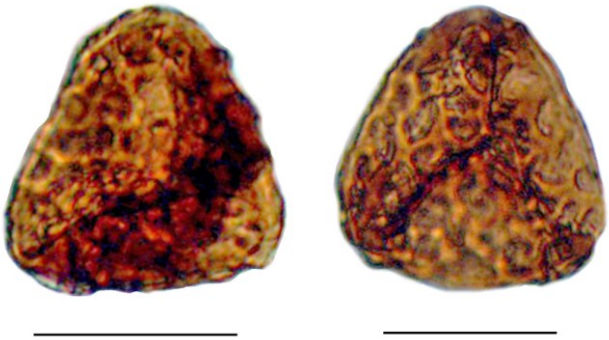

Figure 4.14 — *Ischyosporites* sp., a highly ornamented, subtriangular trilete spore, found in both the samples CBL5 and CBL6. Scale bar: 25 µm.

Family Cyatheaceae Kaulfuss, 1827

Genus *Deltoidospora* Miner, 1935

Species *Deltoidospora* sp.

Remarks: *Deltoidospora* is a trilete (Fig. 4.16) fern spore that likely grew in humid environments with moderate temperatures (Schrank, 2010). This genus is distinguished by its triangular shape characterised by straight to gently, concave sides with rounded corners. The *laesurae* are straight and simple, frequently remaining open, and extend up to three-quarters of the radius of the spore. (Baldoni, 1992). *Deltoidospora* was detected in all the samples, being more common in CBL7, representing 6% of its palynomorphs.

Figure 4.15 — *Deltoidospora* sp., a triangular trilete fern spore, was detected in all the samples. Scale bar: 25 µm.

Family Cyatheaceae Kaulfuss, 1827

Genus *Staplinisporites* Pocock, 1962

Species *Staplinisporites* sp.

Remarks: In conformity with Santos *et al.* (2022), *Staplinisporites* (Fig. 4.17) are among the species related to river sporomorphs that would be found in freshwater fluvial channels, such as Bryophytes and Lycopodiaceae-Selaginellaceae. These groups demonstrate significant water demands that correspond with riverbank ecosystems, which offer constant humidity and are likely subject to occasional flooding leading to submergence. Schrank (2010) also places this trilete spore amid Bryophytes and Lycophytes. This spore was found only in the sample CBL5.

Figure 4.16 — *Staplinisporites* sp., a trilete spore linked to groups that exhibit substantial water requirements, found only in the sample CBL5. Scale bar: 25 µm.

Family Pteridaceae Kirchner, 1831

Genus *Striatella* Mädler, 1964

Species *Striatella* sp.

Remarks: *Striatella* (Fig. 4.18) is a cingulate trilete spore belonging to the Pteridaceae family of ferns. This genus would thrive in lowland habitats, composed of vegetation that grows around ponds and freshwater marshes in floodplains (Santos *et al.*, 2022). This spore was found in samples CBL6 and CBL7, with a higher concentration in CBL7, constituting 3% of its palynomorphs.

Figure 4.17 — *Striatella* sp., a cingulate, trilete spore belonging to ferns. This genus was found in both the samples CBL6 and CBL7. Scale bar: 25 µm.

Some spore genera are represented in the samples by a single specimen:

Family Zygopteridaceae Scott, 1912

Genus *Verrucosisporites* Ibrahim, 1933

Species *Verrucosisporites* sp.

Remarks: *Verrucosisporites* (Fig. 4.19 a) is recognised as a trilete spore, which displays rugae and verrucae ornamentation and is associated with various fern *taxa*. It is also linked to botryopterids and can be seen as pre-pollen of seed ferns such as the lyginopterid *Schopfiangium* (Traverse, 2007; Ingrams *et al.*, 2020). This genus was present only in sample CBL5.

Family Schizaeaceae Kaulfuss, 1827

Genus *Trilobosporites* Potonié, 1956

Species *Trilobosporites* sp.

Remarks: *Trilobosporites* (Fig. 4.19 b) are verrucate spores, which can be distinguished morphologically by their size, the proportional size of their *verrucae*, and the variance in *verrucae* dimensions. This genus is believed to have been produced by ferns with significant affinities to the extant *Lygodium*, a genus known for typically thriving in warm and humid environments (Polette *et al.*, 2018). It is plausible that they grew on the peripheries of swamps and subsequently dispersed extensively across the developing floodplains (Néraudeau *et al.*, 2012). Santos *et al.* (2022) also connect this genus to lowland ecosystems, composed of vegetation that thrives near freshwater swamps and ponds within floodplains. Unfortunately, the specimen found in sample CBL5 is not well preserved, making it difficult to identify.

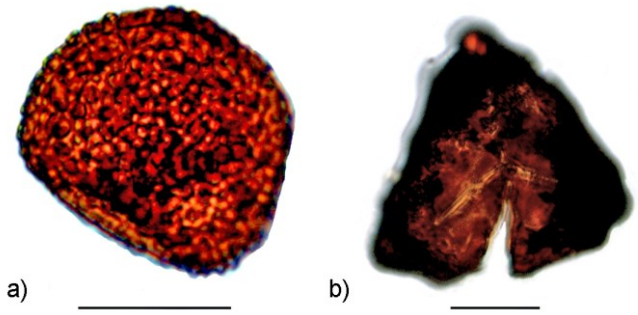

Figure 4.18 — a) *Verrucosisporites* sp., a trilete spore featuring rugae and verrucae ornamentation. b) *Trilobosporites* sp., a verrucate fern spore recognised for flourishing in warm and humid climates. Both genera were only found in the sample CBL5. Scale bar: 25 µm.

5

PHYLOGENETIC ANALYSIS

The phylogeny established by Smith *et al.* (2021) was used as the backbone data matrix. Smith *et al.* (2021) implemented 113 revisions to the phylogeny proposed by Weaver *et al.* (2020). These revisions were necessary to correct scores that had arisen since the phylogeny proposed by Kielan-Jaworowska and Hurum (2001), one of the first to suggest a detailed phylogeny for multituberculates. Only one modification in Character 35 was made to the matrix provided by Smith *et al.* (2021). Additionally, eight new characters and five *taxa* were introduced, including the new fossil. As a result, the changes are described in detail and explained here.

The five *taxa* added to the matrix were: the pinheirodontids *Pinheirodon pygmaeus*, *Bernardodon atlanticus* and *Iberodon quadrituberculatus*, the paulchoffatiid *Kielanodon hopsoni* and the new fossil. Although based on isolated materials, the species belonging to Pinheirodontidae were included in the matrix due to their geographical and morphological proximity to the new specimen. Notably, *K. hopsoni* is a key species for understanding both its phylogenetic relationship with the studied fossil and tooth replacement patterns in Multituberculata. This inclusion is particularly significant because the new fossil, *K. hopsoni* and *Rugosodon eurasiaticus* are the only multituberculate genera known to share the alternate posteroanterior teeth replacement (Hahn and Hahn, 1998a; Yuan *et al.*, 2013; see discussion section below).

The new characters are the following:

Character 35 (Lower p_3, or penultimate premolar, presence vs. absence) was changed from 0 to [0 1] in the *taxon Kuehneodon*, as this genus can display either three or four p_3 (e.g. *Kuehneodon guimarotensis*, does not display the p_1, Hahn, 1978a; Hahn 1987).

Character 131 (Teeth replacement pattern: anteroposterior 0, alternate posteroanterior replacement pattern 1, has been introduced to distinguish between species exhibiting an anteroposterior tooth replacement pattern and those with an alternate posteroanterior replacement pattern (Fig. 5.1).

Character 132 (Diastema size difference: short diastema 0, diastema ≥ p_1 and p_2 1, diastema ≥ p_4, when p_2 and p_3 are missing 2) compares the various diastema lengths in the jaws of multituberculates. Diastemas as long as the p_1 and p_2 in multituberculates possessing four premolars, and the p_4 in multituberculates lacking p_1 and p_2, were classified as long (Fig. 5.2).

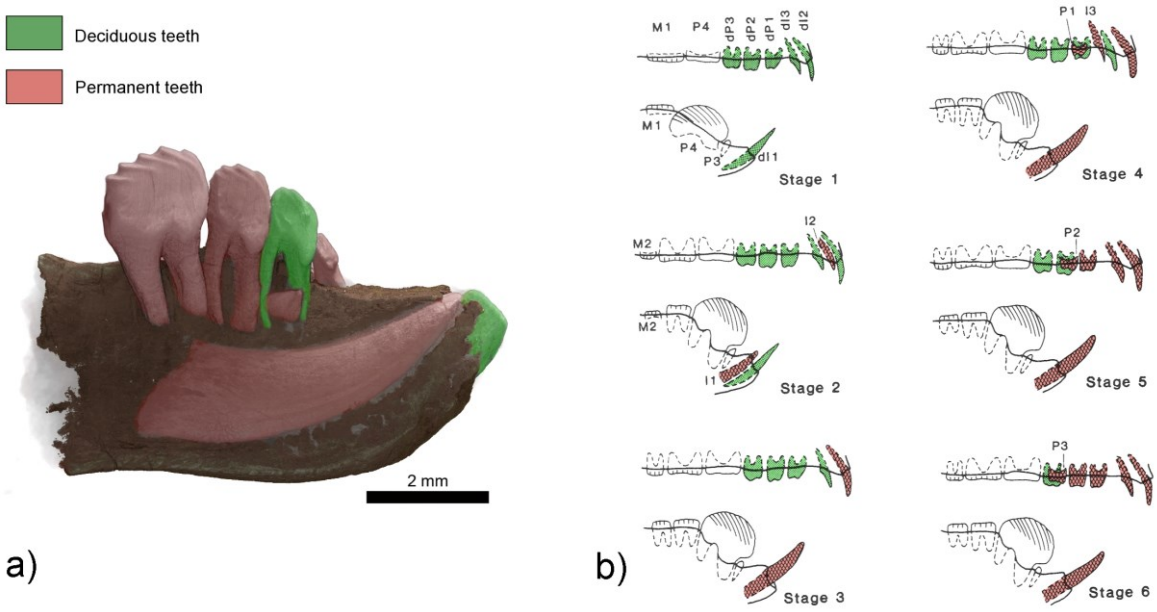

Figure 5.1 — The two different tooth replacement patterns found in multituberculates: a) the alternate posteroanterior teeth replacement of the studied fossil (mirrored picture) and b) the most common anteroposterior diphyodont replacement present in the majority of known *taxa* of multituberculates (modified from Greenwald, 1988).

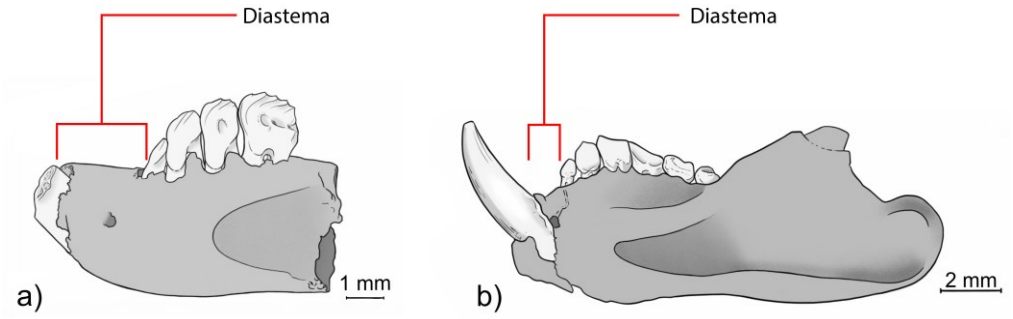

Figure 5.2 — The diastema size difference between a) the new fossil and b) the paulchoffatiid *Meketibolodon robustus.*

Character 133 (Outline of the alveolar line of the jaw: flat outline 0, arched outline 1, ladder-shaped outline 2) differentiates between the three distinct dorsal outlines of the multituberculate jaw: straight, arched, and ladder-shaped alveolar lines (Fig. 5.3).

Character 134 (Subtriangular lobe on p_2: absent 0, present 1) has been introduced to distinguish the presence or absence of the subtriangular lobe on the labial side of p_2, whilst character 135 (Subtriangular lobe on p_3: absent 0, present 1) differentiates between the presence or absence of the subtriangular lobe on the labial side of p_3 (Fig. 4.6).

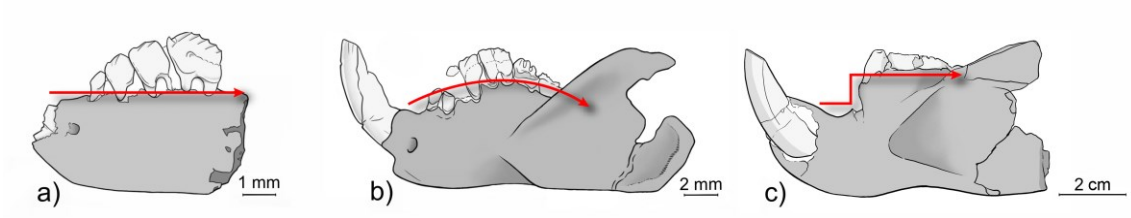

Figure 5.3 — The three main different alveolar lines of the jaw: a) straight, *Ctenacodon serratus* (USNM V 2688), mirrored lateral view; b) arched, *Glirodon grandis* (LACM 120452), mirrored lateral view; c) ladder-shaped, *Taeniolabis taoensis* (AMNH 16310), lateral view.

Character 136 (Lobe over the distal root of p_2: absent 0, present 1) compares the presence or absence of a second lobe at the crown-root junction over the distal root of p_2, meanwhile, character 137 (Lobe over the distal root of p_3: absent 0, present 1) compares the same trait over the distal root of p_3 (Fig. 4.6).

Character 138 has been introduced to distinguish the angle between the premolar row and the dentary axis of the jaw. Three ranges were established: angle smaller than 12° 0, angle between 12° and 17° 1, and angle between 18° and 22° 2 (Fig. 5.4).

The new matrix was analysed through a "New Technology search" in TnT version 1.5 software. After incorporating the new characters and *taxa*, and subsequent comparison of the revised phylogenetic tree with the framework proposed by Smith *et al.* (2021), it is evident that both phylogenies exhibit a similar picture of multituberculate evolutionary relationships (Fig. 5.6). Minor variations are observed in the branching order of several *taxa* within each major group. Nonetheless, the branching pattern of higher-level groups is essentially the same. Despite differences in their internal relationships, both phylogenies consistently place these families (Kogaionidae, Taeniolabidoidea, Ptilodontoidea, and Djadochtatherioidea) in similar topological positions.

Figure 5.4 — The angle between the premolar row and the dentary axis of the jaw of the new fossil is approximately 16 degrees.

The revised phylogenetic tree presents a new hypothetical framework elucidating aspects of the evolutionary relationships within Pinheirodontidae (Fig. 5.5). The phylogeny of this family has always been poorly known, mainly due to the scarce and isolated material, e.g., *Gerhardodon purbeckensis* (Kielan-Jaworowska & Ensom, 1992), *Lavocatia alfambrensis* (Canudo & Cuenca-Bescós, 1996) the already mentioned pinheirodontids from Porto Dinheiro, Portugal (Hahn & Hahn, 1999), *Ecprepaulax anomala* (Hahn & Hahn, 1999) and others. This

factor resulted in the exclusion of this family from the most recent phylogenies, e.g., Xu *et al.* (2015), Weaver *et al*. (2020), Smith *et al.* (2021), and Mao *et al.* (2023).

Through detailed comparative morphological analyses, the newly discovered fossil already exhibited a pronounced phylogenetic relationship with Pinheirodontidae, particularly *Iberodon*. After the phylogenetic analysis, not only was this relationship supported, but there was also a strengthening of the Pinheirodontidae family, showing that the Portuguese *taxa* have taxonomic affinities, despite their relatively incomplete preservation. The classification of the studied fossil within Pinheirodontidae, based on the new phylogenetic analysis, indicates that this is the first instance of encountering more complete material from this family, rather than isolated teeth.

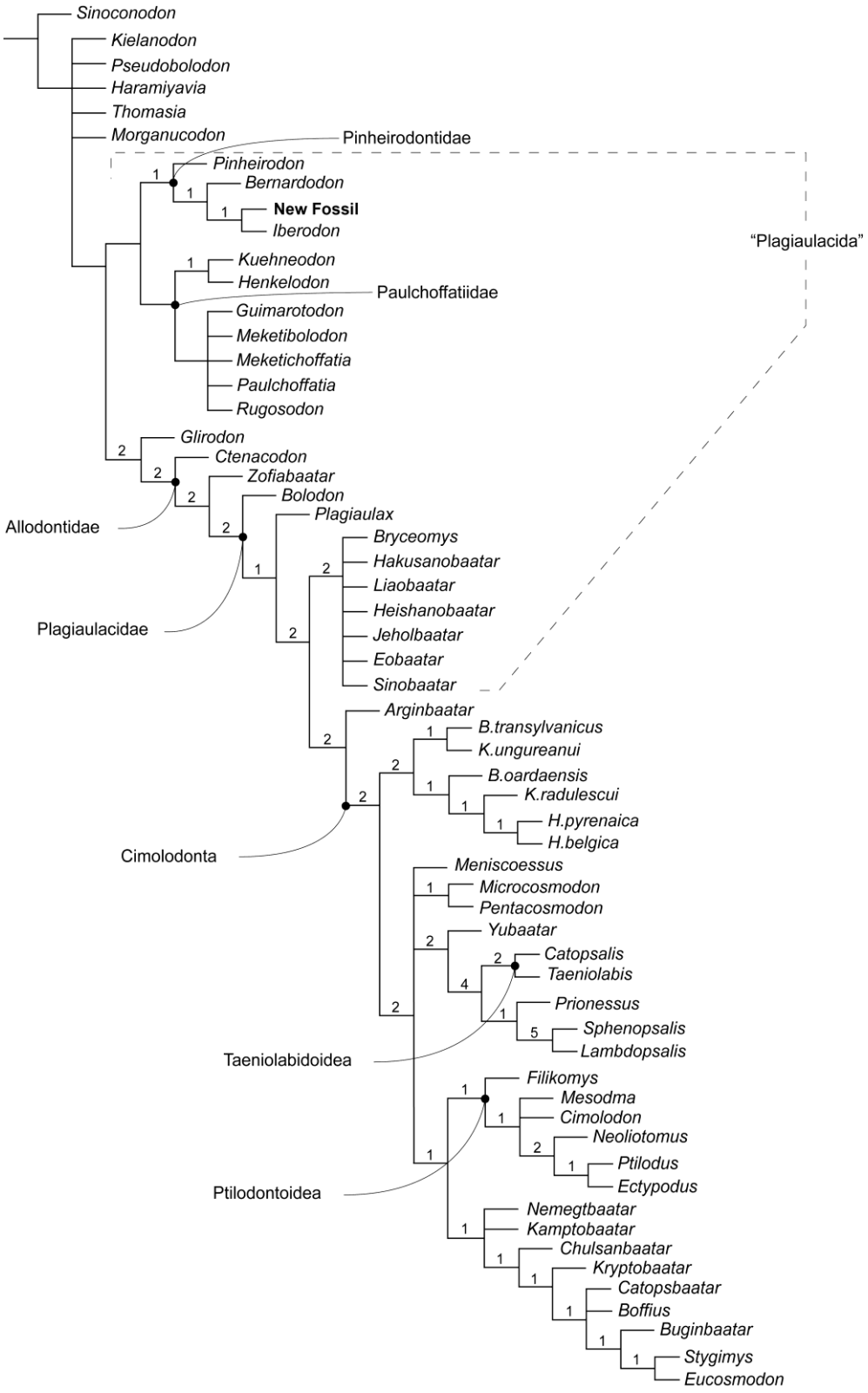

Figure 5.5 — The strict consensus tree, annotated with absolute Bremer support values above the branches, was generated by integrating newly acquired data into the matrix from Smith et al. (2021)

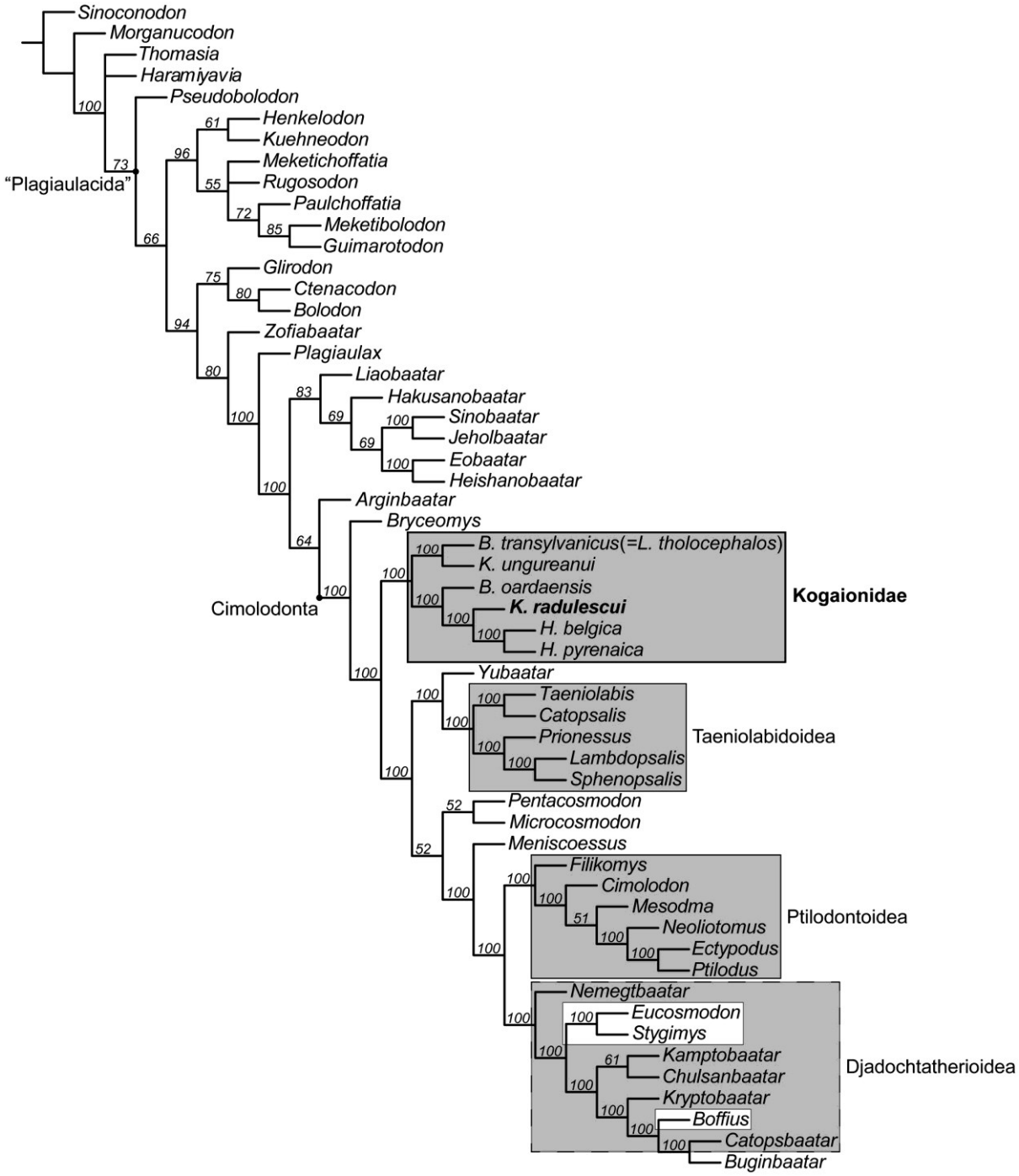

Figure 5.6 — Phylogenetic tree proposed by Smith *et al.* (2021).

6

DISCUSSION

6.1 Teeth Replacement Patterns

The specimen clearly shows all the distinct dental specialisations of a multituberculate, which are unique among Mesozoic mammals (Zachos & Asher, 2018). The most conspicuous is the modified multicuspid lower premolars forming a blade-like structure (Szalay, 1981; Kielan-Jaworowska *et al.*, 2004). Over the last decades, some rare fossils of odontologically immature multituberculates from different geological periods have been described (Clemens, 1963; Krause, 1980; Archibald, 1982). These specimens were in a more advanced ontogenetic stage than the new fossil, having what Greenwald (1988) calls "alveolar gap". This characteristic appears after the loss of di_x mesial to i_x, which is in a recent state of eruption, leaving the alveolus empty to be gradually filled by i_x. Considering this information, it is possible to infer the final insertion position of i_x from di_x.

The pattern variations found in the dental ontogeny of different multituberculates families can be relevant for systematic purposes. Based on several North American Late Cretaceous-Early Paleogene multituberculates *taxa*, Greenwald (1988) suggested a sequential anteroposterior diphyodont replacement of the anterior dentition similar to the one found in Theria. This replacement pattern is comparable to that found among paulchoffatiids, with only one difference: the replacement of p_4. While p_4 in Paulchoffatiidae is diphyodont (Hahn, 1978c: Figs. 1-5), in the Late Cretaceous-Early Paleogene multituberculates, it is monophyodont (Greenwald, 1988). The first exception to this pattern was proposed by Hahn and Hahn (1998a) when they described a specimen of a young paulchoffatiid known only for its upper dentition, *Kielanodon hopsoni*. According to these authors, in the right maxillary bone of *K. hopsoni*, the p^3 erupts between a dp^2 and a dp^4. The dp^2 is preceded by a dp^1, upon which the p^1, still in its

cavity, prepares to erupt (Fig. 6.1). This specimen of paulchoffatiid suggests that the tooth replacement took place alternately in two waves, with one tooth skipped individually at a time instead of being replaced one after the other, and that the replacement was posteroanterior.

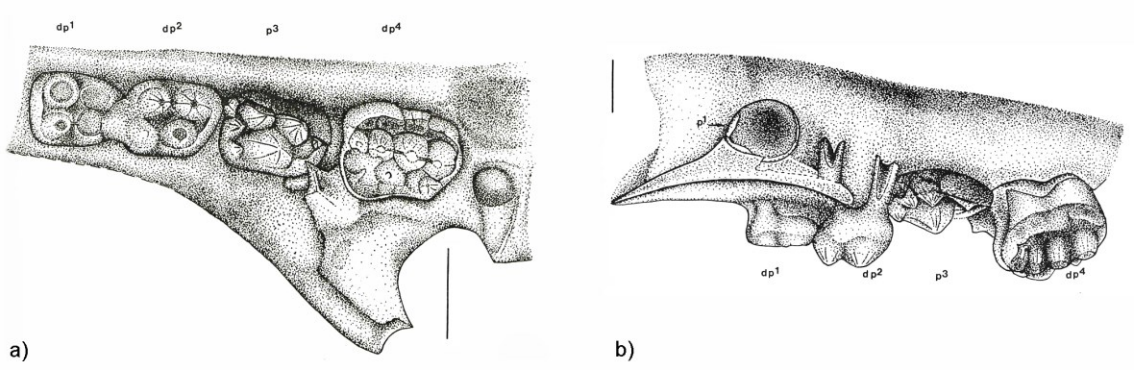

Figure 6.1 — The alternate posteroanterior teeth replacement found in the right maxilla of *Kielanodon. hopsoni*: a) occlusal view; b) lingual view (modified from Hahn and Hahn, (1998a)). Scale bar: 1mm.

The replacement pattern observed in *K. hopsoni*, which contradicts the usual anteroposterior pattern of mammals, is the same found in the more recently described *Rugosodon eurasiaticus* (Yuan *et al.*, 2013). The dentary presented in this research is the third specimen of multituberculate in the fossil record to display an alternate posteroanterior teeth replacement. Two of its three most anterior teeth are deciduous. The only exception is the already replaced p_1, which intercalates with them. In the meantime, p_3 and p_4 suggest they have already shed, being the first to be replaced. The p_1, p_3 and p_4 are described as definitive teeth due to the lack of evidence of erupting deciduous teeth apical to them and the level of wear on their projections, which, compared to dp_2, are sharper. Furthermore, as mentioned in the description, from all premolars, dp_2 has, on its occlusal crest, the most evident deciduous morphology similar to the Kimmeridgian multituberculates. Among the deciduous teeth of the studied material, the incisor is almost erupting in contrast to p_2, which is still deep into its cavity attached to the shallow depression on the mesial root of dp_2. Due to the advanced developmental stage of the incisor concerning p_2, it is deducible that di will probably be replaced before dp_2. Based on the presented evidence, it is possible to conclude that the studied fossil presents an alternate posteroanterior teeth replacement (see Fig. 4.2 and Fig. 5.1).

According to Hahn and Hahn (1998a), this alternate pattern presented in Paulchoffatiidae is a primitive feature similar to that of cynodonts, dryolestids and Mesozoic mammaliaforms such as *Sinoconodon*. This shared trait would, therefore, indicate the basal condition

of all multituberculates. Thus, the transition of alternate posteroanterior to continuous anteroposterior teeth replacement would have happened individually twice, i.e., in this order and in modern mammals. Two specimens of paulchoffatiids are a good example of anteroposterior sequential teeth replacement in this family: *Kuehneodon dietrichi* (MSG V.J. 441-155) and *Kuehneodon guimarotensis* (MSG V.J. 440-155) (Hahn, 1978c). Therefore, following this hypothesis proposed by Hahn and Hahn (1998a), these paulchoffatiid species would have already transitioned to an anteroposterior sequential teeth replacement.

The authors Kielan-Jaworowska *et al.* (2004) suggested three possible scenarios regarding the evolutionary relationship of tooth replacement patterns in multituberculates: the alternate posteroanterior teeth replacement is indeed a plesiomorphic condition among multituberculates, indicating that multituberculates possibly inherited a cynodont-like replacement pattern, therefore, the anteroposterior sequential replacement of the North American Late Cretaceous-Early Paleogene multituberculates would be a secondarily derived trait; the anteroposterior sequential replacement is a plesiomorphic condition for multituberculates and the pattern observed in *K. hopsoni* and *R. eurasiaticus*, and now as well as in the new specimen, is convergent with that of distant cynodonts; the conditions were independently derived in both paulchoffatiids and the Late Cretaceous-Early Paleogene multituberculates. In other words, the third interpretation suggests that each group developed its tooth replacement pattern independently, without one pattern being derived from the other.

The new analyses have revealed the alternate posteroanterior pattern in the Pinheirodontidae family, previously identified only in the Paulchoffatiidae. Additionally, the temporal range of this trait has been extended including now the Tithonian Multituberculata, whereas it was previously only known among Oxfordian and Kimmeridgian multituberculates. Furthermore, *K. hopsoni* was identified as the most basal multituberculate in the recently proposed phylogeny, indicating that the pattern of alternating tooth replacement was present in the basal *taxa*. However, any further hypotheses suggesting whether or not this feature is plesiomorphic for all multituberculates would be mere speculation. Future evidence and additional findings will be required to determine with certainty whether the alternating replacement of posteroanterior teeth is a plesiomorphic trait among multituberculates or a result of convergent evolution with cynodonts.

6.2 Palaeoenvironmental Aspects

The initial paleoclimatic indicators were derived from the geological features of the Ulsa quarry. As discussed in Chapter Two, the sedimentary composition of the area predominantly consists of reddish mudstone and siltstone layers displaying substantial carbonate concretions (caliche). According to Suguio (2003), caliche forms in soils in semiarid to arid climates, where the primary direction of soil moisture movement is upward due to excessive evaporation, which exceeds precipitation, and capillary action during dry periods. These carbonate concretions are valuable palaeoclimatic indicators due to their formation processes, found in climates with high evaporation rates and low annual precipitation, indicating seasonal variability.

Another indicator of an arid palaeoclimate was the presence of desert roses within the deposit containing the articulated assemblage of macrofossils. In conformity with Hope *et al.* (2015), desert roses are evaporites whose formation resembles that of caliche, i.e., the crystal formation results from the influx of water containing dissolved minerals (calcium sulfate), balanced by the outflow of water driven by evaporation. These minerals serve as indicators of arid climatic conditions during their formation.

Subsequent palynological analyses conducted near the Ulsa quarry have substantiated the initial paleoclimatic indicators. The most dominant palynomorph belongs to the genus *Classopollis*. This pollen is extensively distributed within Jurassic and Cretaceous strata, reaching its distribution peak during the Upper Jurassic. Consequently, this period also marks the maximum distribution of the Cheirolepidiaceae family (Vakhrameev, 1981). The Cheirolepidiaceae conifers displayed xeromorphic epidermal features as part of their physiological adaptations, which were particularly advantageous during times of water scarcity (Haworth & McElwain, 2008). Based on Vakhrameev (1970), the xeromorphic vegetative morphology present in the Cheirolepidiaceae family is an adaptational mechanism against excessive water loss, indicating a hot and dry climate. Since *Classopollis* pollen deposits predominantly concentrate along the shorelines of Jurassic and Cretaceous seas, yet are also present in intracontinental basins, it suggests that this family possesses halophytic adaptations. Such a trait would enable this genus to thrive in environments with highly saline soils or waters (Vakhrameev, 1981; Santos *et al.*, 2022). For this reason, this pollen is predominantly associated with shallow-water, nearshore marine, and deltaic deposits (Vakhrameev, 1981). The presence of unseparated tetrads of *Classopollis* in the Ulsa quarry, implies minimal transport from their

origin plants, suggesting that they likely represent autochthonous vegetation. (Santos *et al.*, 2022). This evidence could indicate a saline or highly stressed environment in the Ulsa quarry.

The second most abundant palynomorph was the pollen *Spherinopollenites*. Its frequent occurrence alongside *Classopollis* in certain samples was often associated with a more pronounced annual dry season Santos *et al.* (2022). The third most common palynomorph was also an additional marker of a dry palaeoclimate, the *Exesipollenites* pollen. This genus as mentioned previously, belongs to Bennettitales, which according to Watson *et al.* (1991) and Abbink (1998) would flourish in dry, warm environments. Like cheirolepidids, Bennettitales adapted well to dry conditions. They thrived in environments where other plant groups, particularly ferns and moisture-loving gymnosperms, could not cope with the arid climate and eventually diminished. They were often found alongside cheirolepidid conifers in environments that were transitioning from humid to semiarid and arid conditions, forming part of the low sparse forests that dominated these dry climates (Vakhrameev, 1981).

Although the number of spore specimens found in the sample is not statistically significant, thus demonstrating the predominance of dry climate pollen, according to Santos *et al.* (2022), the association of *Matonisporites* with *Cicatricosisporites*, *Deltoidosora*, *Striatella*, *Ischyosporites* or *Trilobosporites*, among others, would consist in lowland communities. They probably would be vegetation that thrived close to freshwater and ponds in flood plains, combined with *taxa* adapted to drier and wetter environmental conditions, without the influence of salt water.

In conclusion, the paleoenvironment represented by the evidence is characterised by a terrestrial landscape with sporadic fluvial activity. The presence of reddish mudstone and siltstone sediments, along with caliche concretions and sparse micro desert roses, suggests a depositional environment with periodic episodes of soil formation under arid or semi-arid conditions, where evaporation rates were high and water availability was limited. Furthermore, the significant occurrence of *Classopollis* pollen, known for its halophytic adaptations, supports the inference of a saline or highly stressed environment, likely with intermittent wet and dry periods. Meanwhile, the presence of other dry climate pollen indicates a community which, for the most part, was also adapted to similar environmental stresses.

6.3 Microvertebrates Taphonomy

Following the criteria proposed by Rogers *et al.* (2008), the Ulsa quarry up to this point can be referred to as a "mixed bonebed", since the analysis of all its contents has not been completed. This designation is used for sites containing significant mixtures of macrofossils and microfossils. It remains uncertain whether the macrofossils found in the upper layers of the block represent juvenile individuals. Nonetheless, these specimens are notably small in size. As previously mentioned, both macro- and microfossils display some degree of articulation. For Brett and Thomka (2013), certain taphonomic features, such as the articulation of delicate skeletal elements, unequivocally indicate episodes of very rapid sedimentation. Since disarticulation occurs only after scavenging or decomposition of the connective tissues that hold the skeleton together, these individuals were likely buried before these biotic agents could take effect (Benton & Harper, 2009).

According to Brett and Baird (1986), the extent of reorientation and transport of various skeletal elements is influenced by the energy of the surrounding environment and the density and shape of the skeletal elements. The degree of articulation observed in the individuals, including the highly delicate microvertebrate fossils, suggests that the depositional environment of the fossiliferous material was of low energy, probably a floodplain setting. This inference is supported by lenticular sandstone layers near the quarry, which are interpreted as channel deposits.

Environments characterised by wet and soft, muddy substrates, particularly those found in floodplains, could frequently be transformed into mires or mud traps. These areas, subject to periodic inundation and subsequent drying, became hazardous zones where animals, already debilitated by the extended dry seasons, as indicated by palynological evidence, were prone to entrapment and death (Benton *et al.*, 2012). In this fluvial context, the existence of a spring or seep is highly plausible (Roger M.S. Smith personal communication 2024). Such a water source would have served as a crucial attractant for both large and small animals during dry periods. However, the sporadic and insufficient water supply would not have sustained a permanent aquatic ecosystem, explaining the absence of exclusively aquatic fauna within the sedimentary record.

Furthermore, the cyclic nature of wet and dry seasons would exacerbate the vulnerability of these animals, particularly during the transition phases when weakened individuals

were more likely to seek out these temporary water sources. The subsequent entrapment in soft sediments would result in a higher likelihood of preservation within the fossil record (Smith & Botha-Brink, 2014).

7

CONCLUSION

The bone bed from the Ulsa quarry has proven to be a small yet rich and significant fossiliferous deposit, distinguished by unique fossilization characteristics within the Portuguese fossil record, and it promises substantial material for future study. The specimen unearthed in a "mixed bonebed" of macro and microfossils exhibits remarkable features: high premolars with sturdy subtriangular lobes, an elongated diastema, and a pronounced masseteric fossa projecting more anteriorly than any other analysed Mesozoic multituberculate. Detailed morphological and phylogenetic analysis has unequivocally established this specimen from Cambelas, Portugal, as a new species of Pinheirodontidae. This juvenile multituberculate reveals for the first time the jaw anatomy of this family, which was previously known only from isolated teeth, and also elucidates the teeth replacement pattern of this family.

The alternate posteroanterior teeth replacement pattern, previously observed only in Paulchoffatiidae, has now been identified in Pinheirodontidae, broadening the temporal range of this trait to include Tithonian multituberculates. This pattern was previously known only among Oxfordian and Kimmeridgian multituberculates *taxa*. The new phylogenetic analysis strengthens the Pinheirodontidae family, demonstrating that the Portuguese *taxa* have a clear taxonomic affinity.

Palynological analyses, combined with geological studies of the Ulsa quarry strata, have yielded significant insights, facilitating the reconstruction of potential palaeoenvironments and palaeoclimates. The predominance of xeromorphic conifer pollen and caliche concretions in the reddish mudstone indicates a stressed depositional environment with periodic episodes

of soil formation under arid or semi-arid conditions, marked by high evaporation rates and limited water availability. The degree of articulation found in the fossils of the bonebed, in both macro and micro remains, including delicate microvertebrate bones, suggests a low-energy depositional environment, likely a floodplain.

In this fluvial setting, spring or seep may have been one of the few water sources available during prolonged droughts, drawing diverse *taxa* to these moist, soft mud substrates. These areas frequently transformed into mires or mud traps, becoming hazardous zones. The exclusive presence of small animals, including non-dryosaurid dryomorph dinosaurs, implies that these creatures, already weakened by the extended dry season, became entrapped and perished in the mud.

While the new Pinheirodontidae species does not fully resolve the origins of the basal teeth replacement pattern among multituberculates, it significantly contributes to filling gaps in the multituberculate fossil record, which remains incomplete. This discovery enhances the understanding of the phylogenetic relationships; however, it extends beyond taxonomy, offering a deeper comprehension of the evolutionary and ecological dynamics that shaped the ancient environments of the Iberian Peninsula, highlighting once again the significant role of Portugal in paleontological research.

REFERENCES

Abbink, O. A. (1998). Palynological investigations in the Jurassic of the North Sea region: Palynologisch Onderzoek in de Jura Van Het Noordzeegebied, 192 pp.

Alves, T. M., Gawthorpe, R. L., Hunt, D. W., & Monteiro, J. H. (2002). Jurassic tectono-sedimentary evolution of the Northern Lusitanian Basin (offshore Portugal). Marine and Petroleum Geology, 19(6), 727-754.

Alves, T. M., Moita, C., Sandnes, F., Cunha, T., Monteiro, J. H., & Pinheiro, L. M. (2006). Mesozoic–Cenozoic evolution of North Atlantic continental-slope basins: The Peniche basin, western Iberian margin. AAPG bulletin, 90(1), 31-60.

Ameghino, F. (1889). Contribucion al conocimiento de los mamiferos fosiles de la República Argentina: Obra escrita bajo los auspicios de la Academia nacional de ciencias de la República Argentina para ser presentada á la Exposicion universal de Paris de 1889, Actas de la Academia nacional de ciencias de la República Argentina en Cordoba, Vol. 6, 1027 pp. https://doi.org/10.5962/bhl.title.121288

Antunes, M. T. (1998). A new Upper Jurassic Paulchoffatiid multituberculate (Mammalia) from Pai Mogo, Portugal. Memórias da Academia de Ciências de Lisboa, 37, 125-153.

Araújo, R., David, R., Benoit, J., Lungmus, J. K., Stoessel, A., Barrett, P. M., Maisano, J. A., Ekdale, E., Orliac, M., Luo, Z., Martinelli, A. G., Hoffman, E. A., Sidor, C. A., Martins, R. M. S., Spoor, F., & Angielczyk, K. D. (2022). Inner ear biomechanics reveals a Late Triassic origin for mammalian endothermy. Nature, 607(7920), 726–731. https://doi.org/10.1038/s41586-022-04963-z

Archibald, J. D. (1982). A study of mammalia and geology across the Cretaceous-Tertiary boundary in Garfield County, Montana. http://ci.nii.ac.jp/ncid/BA04126900

Armstrong, H., & Brasier, M. (2005). Microfossils. Blackwell Publishing, 296 pp.

Ash, S. R. (1978). Geology, Paleontology and Paleoecology of a Late Triassic lake, Western New Mexico (ed. Ash SR) Coprolites. Brigham Young University Geology Studies, 69-73.

Askin, R. A., & Jacobson, S. R. (2003). Palynology. Elsevier Books, 563–578. https://doi.org/10.1016/b0-12-227410-5/00930-3

Averianov, A. O., Martin, T., Лопатин, А. В., Schultz, J. A., Schellhorn, R., Krasnolutskii, S., Skutschas, P. P., & Ivantsov, S. V. (2020). Multituberculate mammals from the Middle Jurassic of Western Siberia, Russia, and the origin of Multituberculata. Papers in Palaeontology, 7(2), 769–787. https://doi.org/10.1002/spp2.1317

Backhouse, J. (1988). Late Jurassic and early Cretaceous palynology of the Perth Basin, western Australia, 135, State Print. Division, 244 pp.

Badiola, A., Canudo, J. I., & Cuenca-bescós, G. (2008). New Multituberculate Mammals from the Hauterivian/Barremian Transition of Europe (Iberian Peninsula). Palaeontology, 51(6), 1455–1469. https://doi.org/10.1111/j.1475-4983.2008.00822.x

Baldoni, A. M. (1992). Palynology of the Lower Lefipan Formation (Upper Cretaceous) of Barranca de Los Perros, Chubut Province, Argentina. Part I. Cryptogam Spores and Gymnosperm Pollen. Palynology, 16, 117–136. http://www.jstor.org/stable/3687656

Balme, B. E. (1957). Spores and pollen grains from the Mesozoic of Western Australia. Commonwealth Scientific and Industrial Research Organization, Coal Research Section, 25, 1-48.

Bakker, R. T., Carpenter, K., Galton, P., Siegwarth, J., & Filla, J. (1990). A new latest Jurassic vertebrate fauna from the highest levels of the Morrison Formation at Como Bluff, Wyoming, with comments on Morrison biochronology. Hunteria, 2(6), 1-19.

Bakker, R. T. (1992). Zofiabaataridae, a new family of multituberculate mammals from the Breakfast Bench fauna at Como Bluff. Hunteria, 2(9), 24-24.

Barbarand, J., Marques, F., Hildenbrand, A., Pinna-Jamme, R., & Nogueira, C. R. (2021). Thermal evolution of onshore West Iberia: A better understanding of the ages of breakup and rift-to-drift in the Iberia-Newfoundland Rift. Tectonophysics, 813, 228926. https://doi.org/10.1016/j.tecto.2021.228926

Barreda, V., Cúneo, N. R., Wilf, P., Currano, E. D., Scasso, R. A., & Brinkhuis, H. (2012). Cretaceous/Paleogene floral turnover in Patagonia: drop in diversity, low extinction, and a classopollis spike. PloS One, 7(12), e52455. https://doi.org/10.1371/journal.pone.0052455

Behrensmeyer, A. K. (1992). Terrestrial ecosystems through time: Evolutionary Paleoecology of Terrestrial Plants and Animals. University of Chicago Press, 588 pp.

Behrensmeyer, A. K., Kidwell, S. M., & Gastaldo, R. A. (2000). Taphonomy and paleobiology. Paleobiology, 26(sp4), 103–147. https://doi.org/10.1666/0094-8373(2000)26

Benton, M. J. (2014). Vertebrate palaeontology. John Wiley & Sons, 480 pp.

Benton, M., & Harper, D. A. T. (2009). Introduction to paleobiology and the fossil record. Wiley-Blackwell, 592 pp.

Benton, M. J., Newell, A. J., Khlyupin, A. Y., Shumov, I. S., Price, G. D., & Kurkin, A. A. (2012). Preservation of exceptional vertebrate assemblages in Middle Permian fluviolacustrine mudstones of Kotel'nich, Russia: stratigraphy, sedimentology, and taphonomy. Palaeogeography, Palaeoclimatology, Palaeoecology, 319–320, 58–83. https://doi.org/10.1016/j.palaeo.2012.01.005

Benton, M. J., Donoghue, P. C. J., Asher, R. J., Friedman, M., Near, T. J., & Vinther, J. (2015). Constraints on the timescale of animal evolutionary history. Palaeontologia Electronica. https://doi.org/10.26879/424

Bercovici, A., & Vellekoop, J. (2017). Methods in paleopalynology and palynostratigraphy. Elsevier Books, 127–164. https://doi.org/10.1016/b978-0-12-803243-5.00003-0

Bi, S., Wang, Y., Guan, J., Sheng, X., & Meng, J. (2014). Three new Jurassic euharamiyidan species reinforce early divergence of mammals. Nature (London), 514(7524), 579–584. https://doi.org/10.1038/nature13718

Bignot, G. (Ed.) (1985). Elements of micropalaeontology. Springer Science & Business Media. https://doi.org/10.1002/gj.3350210122

Brand, N., Heckert, A., Sánchez, I. M., Foster, J. B., Hunt-Foster, R., & Eberle, J. J. (2022). New Upper Cretaceous Microvertebrate Assemblage from the Williams Fork Formation, northwestern Colorado, U.S.A., and its Paleoenvironmental Implications. Acta Palaeontologica Polonica, 67, 600 pp. https://doi.org/10.4202/app.00934.2021

Brett, C. E., & Baird, G. C. (1986). Comparative Taphonomy: A key to paleoenvironmental interpretation based on fossil preservation. Palaios, 1(3), 207. https://doi.org/10.2307/3514686

Brett, C. E., & Thomka, J. R. (2013). Fossils and fossilisation. Encyclopedia of Life Sciences. https://doi.org/10.1002/9780470015902.a0001621.pub2

Brilha, J., Andrade, C., Azerêdo, A. C., Barriga, F., Cachão, M., Couto, H. a. R. D., Cunha, P. P., Crispim, J., Dantas, P., Duarte, L. V., Freitas, M. C., Granja, H. M., Henriques, M. H., Henriques, P. a. M., Lopes, L. a. C., Madeira, J., Matos, J. X., Noronha, F., Pais, J. & Terrinha, P. (2005). Definition of the Portuguese frameworks with international relevance as an input for the European geological heritage characterisation. Episodes, 28(3), 177–186. https://doi.org/10.18814/epiiugs/2005/v28i3/004

Brusatte, S. (2022). The rise and reign of the mammals: A New History, from the Shadow of the Dinosaurs to Us. Mariner Books, 528 pp.

Bryant, V. M., & Jones, G. D. (2006). Forensic palynology: Current status of a rarely used technique in the United States of America. Forensic Science International, 163(3), 183-197.

Burger, D. (1965). Palynology of uppermost Jurassic and lowermost Cretaceous strata in the Eastern Netherlands. Leidse Geologische Mededelingen, 35(1), 209–276.

Butler, P. M. (2000). Review of the early allotherian mammals. Acta Palaeontologica Polonica, 45(4), 317-342.

Butler, P. M. & Hooker, J. J. (2005). New teeth of allotherian mammals from the English Bathonian, including the earliest multituberculates. Acta Palaeontologica Polonica 50, 185–207.

Canudo, J. I., & Cuenca-Bescós, G. (1996). Two new mammalian teeth (Multituberculata and Peramura) from the Lower Cretaceous (Barremian) of Spain. Cretaceous Research, 17(2), 215–228. https://doi.org/10.1006/cres.1996.0016

Carpenter, K. (1998). Redescription of the multituberculate, Zofiabaatar and the paurodont, Foxraptor, from Pine Tree Ridge, Wyoming. Modern Geology, 23, 393–405.

Carroll, R. L. (1997). Patterns and processes of vertebrate evolution. Cambridge University Press, 464 pp.

Carvalho, I. S. (2004). Paleontologia Vol. 2. Editora Interciência, 1119 pp.

Castro, L. (2006). Dinoflagelados e outros palinomorfos do Miocénico do sector distal da Bacia do Baixo-Tejo. Tese de Doutoramento, Faculdade de Ciências e Tecnologia da Univ. Nova Lisboa: 380 pp., 241 figs. https://run.unl.pt/bitstream/10362/29907/1/Castro_2006.pdf

Choi, D. K. (1985). Spores and pollen from the Gyeongsang supergroup, southeastern Korea and the chronologic and paleoecologic implications. J. Paleontol. Soc. Korea 1, 33–50

Cifelli, R. L., Davis, B. M., & Sames, B. (2012). Earliest Cretaceous mammals from the western United States. Acta Palaeontologica Polonica. https://doi.org/10.4202/app.2012.0089

Clark, J. M. (1992). Review of Origins of the Higher Groups of Tetrapods: Controversy and Consensus, by H. -P. Schultze & L. Trueb. Journal of Vertebrate Paleontology, 12(4), 532–536. http://www.jstor.org/stable/4523478

Clemens, W. A. (1963). Fossil mammals of the type Lance Formation. Part I. Introduction and Multituberculata. University of California Publications in Geological Sciences 48, 1-105.

Close, R. A., Friedman, M., Lloyd, G. T., & Benson, R. B. J. (2015). Evidence for a Mid-Jurassic adaptive radiation in mammals. Current Biology, 25(16), 2137–2142. https://doi.org/10.1016/j.cub.2015.06.047

Codrea, V., Solomon, A., Venczel, M., & Smith, T. (2017). First mammal species identified from the Upper Cretaceous of the Rusca Montană Basin (Transylvania, Romania). Comptes Rendus Palevol, 16(1), 27–38. https://doi.org/10.1016/j.crpv.2016.04.002

Cope, E. D. (1884). The tertiary marsupialia. The American Naturalist, 18(7), 686–697. https://doi.org/10.1086/273711

Couper, R. A. 1958. British Mesozoic microspores and pollen grains. A systematic and stratigraphic study. Palaeontographica Abt. B., 103, 75 -179

Cranwell, L. M., & Srivastava, S. K. (2009). An early cretaceous (Hauterivian) spore-pollen assemblage from southern Chile. Palynology, 33(1), 241–280. https://doi.org/10.1080/01916122.2009.9989675

Croneis, C. (1941). Micropaleontology--Past and Future. AAPG Bulletin, 25(7), 1208-1255.

De Wever, P. (2020). Marvelous microfossils: creators, timekeepers, architects. In HAL (Le Centre pour la Communication Scientifique Directe). https://hal.science/hal-03530219

Drewes, C. (2006). Discovering Devonian Microfossils. In 27th Conference/Workshop of the Association for Biology Laboratory Education (ABLE), Purdue University, Vol 27, 47-55.

Duarte, S. G., Da Silva, F. J., Arai, M., Da Silva Sylvestre, L., Wanderley, M. D., Jha, N., Joshi, H., Masure, E., & Atfy, H. E. (2021). Paleoclimatic and paleoecological inferences of the Family Anemiaceae: A palynological investigation from variable spatial and temporal strata in some lithostratigraphic units of Brazil, India and France. Review of Palaeobotany and Palynology, 285, 104316. https://doi.org/10.1016/j.revpalbo.2020.104316

Eberth, D. A., Shannon, M., & Noland, B. C. (2007). A Bonebeds database. In University of Chicago Press eBooks, 103–220. https://doi.org/10.7208/chicago/9780226723730.003.0003

Falconer, H. (1857). Description of two species of the fossil mammalian genus Plagiaulax from Purbeck. Quarterly Journal of the Geological Society, 13(1-2), 261-282.

Farjon, A. (2017). A handbook of the world's conifers, 1154 pp.

Feagri, I., & Iverson, J. (1964). Textbook of Pollen Analysis. London: Blackwell.

Ferriday, T., & Montenari, M. (2016). Chemostratigraphy and chemofacies of source rock analogues. In Stratigraphy & timescales, 123–255. https://doi.org/10.1016/bs.sats.2016.10.004

Fraser, N., & Sues, H. (2018). Terrestrial Conservation lagerstatten: Windows into the Evolution of Life on Land. Liverpool University Press.

Fürsich, F. T., Schneider, S., Werner, W., Lopez-Mir, B., & Pierce, C. (2021). Life at the continental–marine interface: palaeoenvironments and biota of the Alcobaça Formation (Late Jurassic, Central Portugal), with a formal definition of the unit appended. Palaeobiodiversity and Palaeoenvironments. https://doi.org/10.1007/s12549- 021-00496-x

Garwood, R. J., & Edgecombe, G. D. (2011). Early terrestrial animals, evolution, and uncertainty. Evolution: Education and Outreach, 4, 489-501.

Gill, T. N. (1872). Arrangement of the families of mammals. With analytical tables. Smithonian Miscellaneous Collections 11, 1–98.

Gillette, D. D. (1999). Vertebrate paleontology in Utah. Utah Geological Survey Miscellaneous Publication, 553 pp.

Greenwald, N. S. (1988). Patterns of tooth eruption and replacement in multituberculate mammals. Journal of Vertebrate Paleontology, 8(3), 265–277. https://doi.org/10.1080/02724634.1988.10011709

Göppert, J. H. R. (1837). De floribus in statu fossili commentatio botanica. Typis Grassii, Barthii et sociorum.

Green, O. (2001). A manual of practical laboratory and field techniques in palaeobiology. Springer, 552 pp.

Guy-Ohlson, D. (1971). Palynological investigations in the Middle Jurassic of the Vilhelmsfalt Boring Southern Sweden. Publ. from The Institutes of Mineralogy, Paleontology and Quaternary Geol. Univ. of Lund., 168, 1–104.

Hahn, G. (1969). Beiträge zur Fauna der Grube Guimarota Nr. 3. Die Multituberculata. Palaeontographica Abteilung A Band A133 Lieferung (1/3), 1-100.

Hahn, G. (1971). The dentition of the Paulchoffatiidae (Multituberculata, upper Jurassic). Memória dos Serviços Geológicos de Portugal, 17, 7-39.

Hahn G. (1978a). Neue Unterkiefer von Multituberculaten aus dem Malm Portugals. Geologica et Palaeontologica, 12, 77-212.

Hahn, G. (1978b). Die Multituberculata, eine fossile SãugetierOrdnung. Sonderband des naturwissenschaftlichen Vereins Hamburg, 3, 61-95.

Hahn, G. (1978c). Milch-Bezahnungen von Paulchoffatiidae (Multituberculata ; Ober-Jura). N. Jb. Geol. Paläont. Stuttgart, Mh., 25-34.

Hahn, G. (1987). Neue Beobachtungen zum Schädel -und Gebiss- Bau der Paulchoffatiidae (Multituberculata, Ober-Jura). Palaeovertebrata 17, 155–196.

Hahn, G., & Hahn, R. (1983). Multituberculata. Fossilium Catalogus, I: Animalia, Pars 127. Kugler Publications, Amsterdam, 1-409.

Hahn, G., & Hahn, R. (1998a). Neue Beobachtungen an Plagiaulacoidea (Multituberculata) des Ober-Juras 1. Zum ZahnWechsel bei Kielanodon. Berliner geowissenschaftliche Abhandlungen E, 28, 1-7.

Hahn, G., & Hahn, R. (1998b). Neue Beobachtungen an Plagiaulacoidea (Multituberculata) des Ober-Juras 3. Der Bau der Molaren bei den Paulchoffatiidae. Berliner geowissenschaftliche, Abhandlungen E 28, 39–84.

Hahn, G., & Hahn, R. (1999). Pinheirodontidae n. fam. (Multituberculata) (Mammalia) aus der tiefen Unter-Kreide Portugals. Palaeontographica Abteilung A-palaozoologie-stratigraphie, 253(4–6), 77–222. https://doi.org/10.1127/pala/253/1999/77

Hahn, G., & Hahn, R. (2001). Multituberculate teeth from the Upper Jurassic of Porto das Barcas (Portugal). Paläontologische Zeitschrift, 74, 583-586.

Halbritter H, Ulrich S, Grímsson F, Weber M, Zetter R, Hesse M, Buchner R, Svojtka M, Frosch-Radivo A (2018) Ornamentation. In: Halbritter H, Ulrich S, Grímsson F, Weber M, Zetter R, Hesse M, Buchner R, Svojtka M, Frosch-Radivo A (eds) Illustrated Pollen Terminology. Springer eBooks, 295–378. https://doi.org/10.1007/978-3-319-71365-6_10

Haworth, M., & McElwain, J. (2008). Hot, dry, wet, cold or toxic? Revisiting the ecological significance of leaf and cuticular micromorphology. Palaeogeography, Palaeoclimatology, Palaeoecology, 262(1–2), 79–90. https://doi.org/10.1016/j.palaeo.2008.02.009

Heckert, A. B. (2004). Late Triassic microvertebrates from the lower Chinle Group (Otischalkian-Adamanian: Carnian), southwestern USA: Bulletin 27 (Vol. 27). New Mexico Museum of Natural History and Science.

Hill, G. (1988). The sedimentology and lithostratigraphy of the Upper Jurassic Lourinha Formation, Lusitanian Basin, Portugal [Ph. D. dissertation]. Milton Keynes: The Open University, 408 pp.

Hodgkinson, R. (1991). Microfossil processing: a damage report. Micropaleontology, 37(3), 320. https://doi.org/10.2307/1485894

Holbourn, A. E., & Henderson, A. S. (2002). Re-illustration and revised taxonomy for selected deep-sea benthic foraminifers. Palaeontologia Electronica, 4(2), 34.

Hope, S. M., Kundu, S., Roy, C., Manna, S. S., & Hansen, A. (2015). Network topology of the desert rose. Frontiers in Physics, 3. https://doi.org/10.3389/fphy.2015.00072

Hu, Y., Meng, J., Wang, Y., & Li, C. (2005). Large Mesozoic mammals fed on young dinosaurs. Nature (London), 433(7022), 149–152. https://doi.org/10.1038/nature03102

Hyde, H. A., & Williams, D. A. (1944). The right word. Pollen Analysis. Circular no. 8, p. 6.

Ibrahim, A. C. (1933). Sporenformen des Aegir-horizonts des RuhrReviers. Dissertation, University of Berlin.

Ingrams, S., McLean, D., Booth, M., & Bodman, D. J. (2020). Biostratigraphy and paleoecology of Asbian–Brigantian (Mississippian) miospores from Berwick-upon-Tweed, Northumberland, UK: Preliminary results. Review of Palaeobotany and Palynology, 276, 104206. https://doi.org/10.1016/j.revpalbo.2020.104206

Jain, S. (2020). Fundamentals of Invertebrate Palaeontology. Springer India, 340 pp.

Jolivet, J. L., Bonnin, J., Beuzart, P., & Auzende, J. M. (1984). Cinématique de l'Atlantique nord et central.

Jurigan, I., Ricardi-Branco, F., & Dantas, M. V. B. (2023). Taphonomic analysis of microfossil bonebeds from Western Gondwana: a case study from the late Permian Corumbataí Formation (Paraná Basin, Brazil). Historical Biology, 1–18. https://doi.org/10.1080/08912963.2023.2272682

Kaulfuss, G. F. (1827). Das Wesen der Farrenkraüter: besonders ihrer Fruchttheile zugleich mit Rücksicht auf systematische Anordnung betrachtet und mit einer Darstellung der Entwickelung der Pteris serrulata aus dem Samen begleitet. Erste Hälfte (Vol. 1). C. Cnobloch.

Kanungo, S., Young, J. R., & Skowron, G. (2017). Microfossils: calcareous nannoplankton (Nannofossils). Techniques in Dentistry and Oral & Maxillofacial Surgery, 1–18. https://doi.org/10.1007/978-3-319-02330-4_4-2

Kemp, T. S. (2005). The origin and evolution of mammals. Oxford University Press on Demand, 344 pp.

Kielan-Jaworowska, Z., & Ensom, P. C. (1992). Multituberculate mammals from the Upper Jurassic Purbeck Limestone formation of southern England. Palaeontology 35, 95126.

Kielan-Jaworowska, Z., & Nessov, L. A. (1992). Multituberculate mammals from the Cretaceous of Uzbekistan. Acta Palaeontologica Polonica, 37(1), 1–17. http://www.app.pan.pl/archive/published/app37/app37-001.pdf

Kielan-Jaworowska, Z., & Hurum, J. H. (2001). Phylogeny and systematics of multituberculate mammals. Palaeontology, 44(3), 389–429. https://doi.org/10.1111/1475-4983.00185

Kielan-Jaworowska, Z., Cifelli, R. L., & Luo, Z. X. (2004). Mammals from the Age of Dinosaurs. Columbia University Press. https://doi.org/10.7312/kiel11918

Kirchner, E. D. M. (1831). Schul-Botanik oder kurze Naturgeschichte der Pflanzen überhaupt, und derer insbesondere, welche zur Erklärung des Pflanzenlebens, ferner in der Haushaltung, Gesundheitslehre, in Künsten und Gewerben [et] c [etera] wichtig sind. Nauck.

Kleinpell, R. M. (1971). California's early "oil bug" profession. Journal of the West, 10(1), 72-101.

Krause, D. W. (1980). Multituberculates from the Clarkforkian land-mammal age, late Paleocene-early Eocene, of western North America. Journal of Paleontology, 54(6), 1163–1183.

Krause, D. W., Hoffmann, S., Wible, J. R., Kirk, E. C., Schultz, J. A., von Koenigswald, W., ... & Andriamialison, H. (2014). First cranial remains of a gondwanatherian mammal reveal remarkable mosaicism. Nature, 515(7528), 512-517.

Kullberg, M. C. & Kullberg, J. C. (2000). Tectónica da Região de Sintra. In: Tectónica das regiões de Sintra e Arrábida. Mem. Geociências, Univ. Lisboa, 2, 1-34.

Kullberg, J. C., Machado, S., & Ramalho, M. M. (2006). Legenda da Carta Geológica de Portugal na escala 1: 100 000 da Área Metropolitana de Lisboa, Folhas Norte e Sul. Carta Geológica de Portugal na escala, 1(100), 000.

Kullberg, J. C., Rocha, R. B., Soares, A. F., Rey, J., Terrinha, P., Azerêdo, A. C., Callapez, P., Duarte, L. V., Kullberg, M. C., Martins, L., Miranda, R., Alves, C., Mata, J., Madeira, J., Mateus, O., Moreira, M. & Nogueira, C. R. (2013). A Bacia Lusitaniana: Estratigrafia, Paleogeografia e Tectónica. In Dias, R. *et al.* – Geologia de Portugal, Volume II, Geologia Meso-cenozóica de Portugal. Escolar Editora, Lisboa, 195-348. https://docentes.fct.unl.pt/omateus/files/kullberg_et_al_2013_a_bacia_lusitaniana.pdf

Kürschner, W. M., Batenburg, S. J., & Mander, L. (2013). Aberrant Classopollis pollen reveals evidence for unreduced (2 n) pollen in the conifer family Cheirolepidiaceae during the Triassic–Jurassic transition. Proceedings - Royal Society. Biological Sciences/Proceedings - Royal Society. Biological Sciences, 280(1768), 20131708. https://doi.org/10.10 98/rspb.2013.1708

Lazzari, V., Schultz, J. A., Tafforeau, P., & Martin, T. (2010). Occlusal Pattern in Paulchoffatiid Multituberculates and the Evolution of Cusp Morphology in Mammaliamorphs with Rodent-

like Dentitions. Journal of Mammalian Evolution, 17(3), 177–192. https://doi.org/10.1007/s10914-010-9139-5

Legrand, J., Pons, D., Nishida, H., & Yamada, T. (2011). Barremian palynofloras from the Ashikajima and Kimigahama formations (Choshi Group, Outer Zone of south-west Japan). Geodiversitas, 33(1), 87–135. https://doi.org/10.5252/g2011n1a6

Leinfelder, R. (1993). A sequence stratigraphic approach to the Upper Jurassic mixed carbonate-siliciclastic successionof the Central Lusitanian Basin, Portugal. Profil 5, 119-140. http://userpage.fu-berlin.de/leinfelder/palaeo_de/leinfelder/pdfs/Leinfelder1993b.pdf

Leinfelder, R., & Wilson, R. C. (1999). Third-Order sequences in an Upper Jurassic Rift-Related Second-Order sequence, Central Lusitanian Basin, Portugal. In SEPM (Society for Sedimentary Geology) eBooks. https://doi.org/10.2110/pec.98.02.0507

Linnaeus, C. V. (1758). Systema Naturae, edition X, Vol. 1 (Systema naturae per regna tria naturae, secundum classes, ordines, genera, species, cum characteribus, differentiis, synonymis, locis. Tomus I. Editio decima, reformata). Holmiae Salvii, 824, 610-614.

Lipps, J. H. (1981). What, if anything, is micropaleontology? Paleobiology, 7(2), 167–199. https://doi.org/10.1017/s0094837300003973

Lovegrove, B. G. (2019). Fires of life. Yale University Press.

Luo, Z. (2007). Transformation and diversification in early mammal evolution. Nature, 450(7172), 1011–1019. https://doi.org/10.1038/nature06277

Luo, Z. X., Kielan-Jaworowska, Z., & Cifelli, R. L. (2002). In quest for a phylogeny of Mesozoic mammals. Acta Palaeontologica Polonica, 47(1). https://www.webpages.uidaho.edu/biol483/articles/Luo_et_al.pdf

Luo, Z., Gatesy, S. M., Jenkins, F. A., Amaral, W. W., & Shubin, N. H. (2015). Mandibular and dental characteristics of Late Triassic mammaliaform Haramiyavia and their ramifications for basal mammal evolution. Proceedings of the National Academy of Sciences of the United States of America, 112(51). https://doi.org/10.1073/pnas.1519387112

Mädler, K. (1964). Bemerkenswerte Sporenformen aus dem Keuper und unteren Lias. Geologisches Landesamt Nordrhein-Westfalen.

Manuppella, G., Antunes, M.T., Pais, J., Ramalho, M.M., & Rey, J. (1999). Notícia explicativa da Folha 30-A (Lourinhã). Departamento de Geologia do Instituto Geológico e Minerio, Lisboa.

Mao, F., Li, Z., Hooker, J. J., & Meng, J. (2023). A new euharamiyidan, Mirusodens caii (Mammalia: Euharamiyida), from the Jurassic Yanliao Biota and evolution of allotherian mammals. Zoological Journal of the Linnean Society, 199(3), 832–859. https://doi.org/10.1093/zoolinnean/zlad050

Marsh, O.C. (1879). Notice of new Jurassic mammals: American Journal of Science, 20, 396–398.

Marsh, O. C. (1880). Notice of Jurassic mammals representing two new orders. American Journal of Science, s3-20(117), 235–239. https://doi.org/10.2475/ajs.s3-20.117.235

Marsh, O. C. (1889). Discovery of Cretaceous Mammalia. Part II. American Journal of Science, 38, 177–180.

Martin, T., & Krebs, B. (2000). Guimarota: A Jurassic Ecosystem, 157 pp.

Martin, T., Averianov, A. O., Schultz, J. A., Schwermann, A. H., & Wings, O. (2019). Late Jurassic multituberculate mammals from Langenberg Quarry (Lower Saxony, Germany) and palaeobiogeography of European Jurassic multituberculates. Historical Biology, 33(5), 616–629. https://doi.org/10.1080/08912963.2019.1650274

Martin, T., Averianov, A. O., Schultz, J. A., & Schwermann, A. H. (2021). First multituberculate mammals from the Lower Cretaceous of Germany. Cretaceous Research, 119, 104699. https://doi.org/10.1016/j.cretres.2020.104699

Martinius, A., & Gowland, S. (2011). Tide-influenced fluvial bedforms and tidal bore deposits (Late Jurassic Lourinhã Formation, Lusitanian Basin, western Portugal). Sedimentology, 58, 285-324. doi:10.1111/j.1365-3091.2010.01185.x

Meng, J., Bi, S., Wang, Y., Zheng, X., & Wang, X. (2014). Dental and Mandibular Morphologies of Arboroharamiya (Haramiyida, Mammalia): A Comparison with Other Haramiyidans and Megaconus and Implications for Mammalian Evolution. PloS One, 9(12), e113847. https://doi.org/10.1371/journal.pone.0113847

Mildenhall, D. C., Wiltshire, P. E., & Bryant, V. (2006). Forensic palynology: Why do it and how it works. Forensic Science International, 163(3), 163–172. https://doi.org/10.1016/j.forsciint.2006.07.012

Milne, L. A., Bryant, V. M., & Mildenhall, D. C. (2004). Forensic palynology. Forensic Botany: Principles and Applications to Criminal Casework, CRC Press, Boca Raton, 217-252.

Milsom, C., & Rigby, S. (2009). Fossils at a glance. John Wiley & Sons.

Miner, E. L. (1935). Paleobotanical examinations of Cretaceous and Tertiary coals. American Midland Naturalist, 585-625.

Mocho, P., Royo-Torres, R., Escaso, F., Malafaia, E., De Miguel Chaves, C., Narváez, I., Pérez-García, A., Pimentel, N., Silva, B., & Ortega, F. (2017). Upper Jurassic sauropod record in the Lusitanian Basin (Portugal): Geographical and lithostratigraphical distribution. Palaeontologia Electronica. https://doi.org/10.26879/662

Montenat, C. H., Guery, F., Jamet, M., & Berthou, P. Y. (1988). Mesozoic evolution of the Lusitanian Basin: comparison with the adjacent margin. In Proceedings of the ocean drilling program, scientific results, 103, 757-775. Washington, College Station, TX: Ocean Drilling Program. https://doi.org/10.2973/odp.proc.sr.103.117.1988

Néraudeau, D., Allain, R., Ballèvre, M., Batten, D., Buffetaut, E., Colin, J., Dabard, M., Daviero-Gomez, V., Albani, A. E., Gomez, B., Grosheny, D., Lœuff, J. L., Leprince, A., Martín-Closas, C., Masure, E., Mazin, J., Philippe, M., Pouech, J., Tong, H., . . . Vullo, R. (2012). The Hauterivian–Barremian lignitic bone bed of Angeac (Charente, south-west France): stratigraphical, palaeobiological and palaeogeographical implications. Cretaceous Research, 37, 1–14. https://doi.org/10.1016/j.cretres.2012.01.006

Nichols, D. (2003). Biodiversity changes in Cretaceous palynofloras of eastern Asia and western North America. Journal of Asian Earth Sciences, 21(8), 823–833. https://doi.org/10.1016/s1367-9120(02)00091-3

Olivera, D. E., Zavattieri, A. M., & Quattrocchio, M. E. (2015). The palynology of the Cañadón Asfalto Formation (Jurassic), Cerro Cóndor depocentre, Cañadón Asfalto Basin, Patagonia, Argentina: palaeoecology and palaeoclimate based on ecogroup analysis. Palynology, 39(3), 362–386. https://doi.org/10.1080/01916122.2014.988382

Owen, P. (1871). Monograph of the fossil Mammalia of the Mesozoic formations. Monographs of the Palaeontographical Society, 24(110), v-115. https://doi.org/10.5962/bhl.title.14831.

Pena dos Reis, R.P.B., Proença Cunha, C.P., Dinis, J.L., & Trincão, P.R. (2000). Geologic evolution of the Lusitanian Basin (Portugal) during the late Jurassic. GeoResearch Forum, 6, 345-356. https://estudogeral.sib.uc.pt/bitstream/10316/15202/1/2000Reis_etal-Georesearch Forum.pdf

Peñalver, E., Arillo, A., La Fuente, R. P., Riccio, M. L., Delclòs, X., Barrón, E., & Grimaldi, D. A. (2015). Long-Proboscid flies as pollinators of cretaceous gymnosperms. CB/Current Biology, 25(14), 1917–1923. https://doi.org/10.1016/j.cub.2015.05.062

Pflug, H. D. (1953). Zur Entstehung und Enturicklung des angiospermiden pollens in der Erdgeschichte. Palaeontographica. 95B: 60- 171.

Piché, N., Bouchard, I., & Marsh, M. (2017). Dragonfly SegmentationTrainer - a general and User-Friendly machine learning image segmentation solution. Microscopy and Microanalysis, 23(S1), 132–133. https://doi.org/10.1017/s1431927617001349

Pinheiro, L. M., Wilson, R. C., Reis, R. P. D., Whitmarsh, R. B., & Ribeiro, A. (1996). The western Iberia Margin: a geophysical and geological overview. In Proceedings of the Ocean Drilling Program. https://doi.org/10.2973/odp.proc.sr.149.246.1996

Pocock, S. A. (1962). Microfloral analysis and age determination of strata at the Jurassic-Cretaceous boundary in the western Canada plains. Palaeontographica Abteilung B, 111, 1-95.

Polette, F., Batten, D. J., & Néraudeau, D. (2018). Re-examination of the palynological content of the Lower Cretaceous deposits of Angeac, Charente, south-west France: Age, palaeoenvironment and taxonomic determinations. Cretaceous Research, 90, 204–221. https://doi.org/10.1016/j.cretres.2018.04.017

Potonié, R. (1956). Synopsis der Gattungen der sporae dispersae I. Teil: Sporites (Vol. 23). Alexander Doweld.

Presl, C. (1847). In: Gefässb. Stipes Farrnkr, 32.

Puttick, M. N., O'Reilly, J., Tanner, A. R., Fleming, J. F., Clark, J., Holloway, L., Lozano-Fernandez, J., Parry, L. A., Tarver, J. E., Pisani, D., & Donoghue, P. C. J. (2017). Uncertain-tree: discriminating among competing approaches to the phylogenetic analysis of phenotype data.

Proceedings - Royal Society. Biological Sciences/Proceedings - Royal Society. Biological Sciences, 284(1846), 20162290. https://doi.org/10.1098/rspb.2016.2290

Rasmussen, E. S., Lomholt, S., Andersen, C., & Vejbæk, O. V. (1998). Aspects of the structural evolution of the Lusitanian Basin in Portugal and the shelf and slope area offshore Portugal. Tectonophysics, 300(1–4), 199–225. https://doi.org/10.1016/s0040-1951(98)00241-8

Riding, J. B. (2021). A guide to preparation protocols in palynology. Palynology, 45, 1–110. https://doi.org/10.1080/01916122.2021.1878305

Rocha, R., & Kullberg, J. C. (2017). Bacia Lusitânica ou Bacia Lusitaniana%? Ciências Da Terra. https://doi.org/10.21695/cterra/esj.v19i1.362

Rogers, R. R., Eberth, D. A., & Fiorillo, A. R. (2008). Bonebeds: Genesis, Analysis, and Paleobiological Significance. University of Chicago Press, 512 pp.

Rogers, R. R., & Brady, M. E. (2010). Origins of microfossil bonebeds: insights from the Upper Cretaceous Judith River Formation of north-central Montana. Paleobiology, 36(1), 80–112. doi:10.1666/0094-8373-36.1.80

Rogers, R. R., Rahantarisoa, L. J., Kemp, A. D., & Andriamialison, H. (2014). First cranial remains of a gondwanatherian mammal reveal remarkable mosaicism. Nature, 515(7528), 512–517. https://doi.org/10.1038/nature13922

Rost, T. L., Barbour, M. G., Murphy, T. M., & Stocking, C. R. (1998). Plant biology. Brooks Cole, 568 pp.

Rowe, T. (1988). Definition, Diagnosis, and Origin of Mammalia. Journal of Vertebrate Paleontology, 8(3), 241–264. http://www.jstor.org/stable/4523202

Rowe, T. (1993). Phylogenetic systematics and the early history of mammals. Springer Books, 129–145 https://doi.org/10.1007/978-1-4613-9249-1_10

Sánchez, M. (2012). Embryos in Deep Time: The Rock Record of Biological Development (1st ed.). University of California Press. http://www.jstor.org/stable/10.1525/j.ctt1pnhr2

Santos, A. A., Piñuela, L., Rodríguez-Barreiro, I., García-Ramos, J. C., & Diez, J. B. (2022). Jurassic Palynology from "The Dinosaur Coast" of Asturias (Lastres Fm., Northwestern Spain): Palynostratigraphical and Palaeoecological Insights. Biology, 11(12), 1695. https://doi.org/10.3390/biology11121695

Santos, A. A., Rodríguez-Barreiro, I., McLoughlin, S., Pons, D., Valenzuela-Ríos, J. I., & Diez, J. B. (2024). Plant colonization of isolated palaeoecosystems: Palynology of a Middle Jurassic extinct volcanic island (Camarena, eastern Spain). Palaeogeography, Palaeoclimatology, Palaeoecology, 639, 112081. https://doi.org/10.1016/j.palaeo.2024.112081

Saraswati, P. K., & Srinivasan. (2016). Micropaleontology. Springer Books. https://doi.org/10.1007/978-3-319-14574-7

Schneider, S., Fürsich, F. T., & Werner, W. (2009). Sr-isotope stratigraphy of the Upper Jurassic of central Portugal (Lusitanian Basin) based on oyster shells. International Journal of Earth Sciences, 98, 1949-1970. https://doi.org/10.1007/s00531-008-0359-3

Schrank, E. (2010). Pollen and spores from the Tendaguru Beds, Upper Jurassic and Lower Cretaceous of southeast Tanzania: palynostratigraphical and paleoecological implications. Palynology, 34(1), 3–42. https://doi.org/10.1080/01916121003620106

Scott, D. H. (1912). On a palaeozoic fern, the Zygopteris grayi of Williamson. Annals of Botany, os-26(1), 39–69. https://doi.org/10.1093/oxfordjournals.aob.a089389

Simpson, G. G. (1926). Mesozoic Mammalia, IV; the multituberculates as living animals. American Journal of Science, s5-11(63), 228–250. https://doi.org/10.2475/ajs.s5-11.63.228

Simpson, G. G. (1928). A catalogue of the Mesozoic Mammalia in the Geological Department of the British Museum. https://doi.org/10.5962/bhl.title.118972

Simpson, G. G. (1929). American mesozoic mammalia, 235 pp.

Simpson, M. G. (2010). Plant Systematics. Academic Press, 752 pp.

Smith, F. A. (2021). Mammalian paleoecology: Using the Past to Study the Present. JHU Press, 280 pp.

Smith, R. M., & Botha-Brink, J. (2014). Anatomy of a mass extinction: Sedimentological and taphonomic evidence for drought-induced die-offs at the Permo-Triassic boundary in the main Karoo Basin, South Africa. Palaeogeography, Palaeoclimatology, Palaeoecology, 396, 99–118. https://doi.org/10.1016/j.palaeo.2014.01.002

Smith, T., Codrea, V. A., Devillet, G., & Solomon, A. A. (2021). A New Mammal Skull from the Late Cretaceous of Romania and Phylogenetic Affinities of Kogaionid Multituberculates. Journal of Mammalian Evolution, 29(1), 1–26. https://doi.org/10.1007/s10914-021-09564-7

Sorkhabi, R. (Ed.). (2020). Encyclopedia of Petroleum Geoscience. Springer International Publishing. https://doi.org/10.1007/978-3-319-02330-4

Srivastava, S. K. (1976). The fossil pollen genus *Classopollis*. Lethaia, 9(4), 437–457. https://doi.org/10.1111/j.1502-3931.1976.tb00985.x

Stapel, G., Cloetingh, S., & Pronk, B. (1996). Quantitative subsidence analysis of the Mesozoic evolution of the Lusitanian basin (western Iberian margin). Tectonophysics, 266(1–4), 493–507. https://doi.org/10.1016/s0040-1951(96)00203-x

Suguio, K. (2003). Geologia sedimentar. Editora Blucher, 416 pp.

Sukh, D. (1961). The fossil flora of the Jubalpur series. III, Spores and pollen grains.

Szalay, F. S., Lillegraven, J. A., Kielan-Jaworowska, Z., & Clemens, W. A. (1981). Mesozoic Mammals, the first two thirds of mammalian history. University of California Press, Berkeley, California. Journal of Mammalogy, 62(2), 443–445. https://doi.org/10.2307/1380738

Taylor, A. M., Gowland, S., Leary, S., Keogh, K. J., & Martinius, A. W. (2013). Stratigraphical correlation of the Late Jurassic Lourinhã Formation in the Consolação Sub-basin (Lusitanian Basin), Portugal. Geological Journal, 49(2), 143–162. https://doi.org/10.1002/gj.2505

Tosolini, A. P., McLoughlin, S., Wagstaff, B. E., Cantrill, D. J., & Gallagher, S. (2015). Cheirolepidiacean foliage and pollen from Cretaceous high-latitudes of southeastern Australia. Gondwana Research, 27(3), 960–977. https://doi.org/10.1016/j.gr.2013.11.008

Traverse, A. (2007). Paleopalynology: Second Edition. Springer Science & Business Media, 813 pp.

Tschudy, R. H. (1961). Palynomorphs as indicators of facies environments in Upper Cretaceous and Lower Tertiary strata, Colorado and Wyoming.Symposium on Late Cretaceous rocks, 16. Annual Field Conference, Guide Book, Wyoming Geological Association, 53-59.

Turutanova-Ketova, A. I. (1963). Semejstvo Cheirolepidiaceae Hirmer und Hörhammer, 1934. Osnovy paleontologii, 15, 249-250.

Ungar, P. S. (2010). Mammal Teeth: Origin, Evolution, and Diversity. Johns Hopkins University Press, 320 pp.

Vakhrameev, V. A. (1970). Range and palaeoecology of Mesozoic conifers, the Cheirolepidiaceae. Paleontologicheskii zhurnal, 1, 19-34.

Vakhrameev, V. A. (1981). Pollen Classopolis: indicator of Jurassic and Cretaceous climates. Journal of Palaeosciences, 28, 301-307.

Venkatachala, B., Kar, R., & Raza, S. (1968). Palynology of the Mesozoic sediments of Kutch, w. India - 3. Morphological study and revision of the spore genus Trilobosporites Pant ex Potonie, 1956. Journal of Palaeosciences, 17(1-3), 123–126. https://doi.org/10.54991/jop.1968.788

Vergés, J., Kullberg, J. C., Casas-Sainz, A., De Vicente, G., Duarte, L. V., Fernàndez, M., Gómez, J. J., Gómez-Pugnaire, M. T., Sánchez, A. J., López-Gómez, J., Macchiavelli, C., Martín-Algarra, A., Martín-Chivelet, J., Muñoz, J. A., Quesada, C., Terrinha, P., Torné, M., & Vegas, R. (2019). A Geodynamic Approach. *Regional Geology Reviews*. Springer, Cham, 1-14. https://doi.org/10.1007/978-3-030-11295-0_1

Vullo, R. (2009). Taphonomy Of Vertebrate Microfossil Assemblages In Coastal Environments: In Search Of A Modern Analogous Model. Palaios, 24(11), 723–725. https://doi.org/10.2110/palo.2009.s06

Waksmundzka, M. (2014). Mesozoic spores of Poland – a revision of selected *taxa*. Biuletyn Państwowego Instytutu Geologicznego, 25–87. http://yadda.icm.edu.pl/yadda/element/bwmeta1.element.baztech-739e2046-c582-4f8a-ab88-134af0f2124a

Watson, J., Henderson, C. M. B., & Sincock, C. A. (1991). Bennettitales of the English Wealden. Monograph of the Palaeontographical Society, 145(588), 2–224. https://doi.org/10.1080/25761900.2022.12131771

Weaver, L. N., Varricchio, D. J., Sargis, E. J., Chen, M., Freimuth, W. J., & Mantilla, G. P. W. (2020). Early mammalian social behaviour revealed by multituberculates from a dinosaur nesting site. Nature Ecology & Evolution, 5(1), 32–37. https://doi.org/10.1038/s41559-020-01325-8

Wellborn, G. A., & Langerhans, R. B. (2014). Ecological opportunity and the adaptive diversification of lineages. Ecology and Evolution, 5(1), 176–195. https://doi.org/10.1002/ece3.1347

Williamson, T. E., Brusatte, S. L., Secord, R., & Shelley, S. L. (2015). A new taeniolabidoid multituberculate (Mammalia) from the middle Puercan of the Nacimiento Formation, New Mexico, and a revision of taeniolabidoid systematics and phylogeny. Zoological Journal of the Linnean Society, 177(1), 183–208. https://doi.org/10.1111/zoj.12336

Wilson, R. C. (1988). Mesozoic Development Of The Lusitanian Basin, Portugal. Revista de la Sociedad Geológica de España, 1(3), 393-407.

Xu, L., Zhang, X., Pu, H., Jia, S., Zhang, J., Lü, J., & Meng, J. (2015). Largest known Mesozoic multituberculate from Eurasia and implications for multituberculate evolution and biology. Scientific Reports, 5(1). https://doi.org/10.1038/srep14950

Yuan, C., Ji, Q., Meng, Q., Tabrum, A. R., & Luo, Z. X. (2013). Earliest evolution of multituberculate mammals revealed by a new Jurassic fossil. Science, 341(6147), 779–783. https://doi.org/10.1126/science.1237970

Zachos, F. E., & Asher, R. J. (2018). Mammalian Evolution, Diversity and Systematics. De Gruyter eBooks. https://doi.org/10.1515/9783110341553

Zheng, X., Bi, S., Wang, X., & Meng, J. (2013). A new arboreal haramiyid shows the diversity of crown mammals in the Jurassic period. Nature, 500(7461), 199–202. https://doi.org/10.1038/nature12353

Zhou, C., Wu, S., Martin, T., & Luo, Z. (2013). A Jurassic mammaliaform and the earliest mammalian evolutionary adaptations. Nature, 500(7461), 163–167. https://doi.org/10.1038/nature12429

A

Annexes

	1	2	3	4	5	6	7	8	9	10
Sinoconodon	0	0	0	0	0	0	0	0	0	0
Morganucodon	0	0	0	0	0	0	0	0	0	0
Thomasia	?	?	?	?	?	?	?	?	?	?
Haramiyavia	0	0	0	?	1	0	0	0	0	0
Rugosodon	1	1	1	?	1	?	0	1	0	1
Paulchoffatia	1	1	1	?	1	0	0	1	0	1
Meketichoffatia	?	?	?	?	?	?	?	?	?	?
Henkelodon	?	?	?	?	?	?	?	?	?	?
Meketibolodon	1	1	1	1	1	0	0	1	0	1
Guimarotodon	1	1	1	1	1	0	0	1	0	1
Kuehneodon	1	1	1	0	1	0	0	1	0	1
Pseudobolodon	?	?	?	?	?	?	?	?	?	?
Ctenacodon	1	1	1	1	0	?	1	1	1	1
Glirodon	1	1	1	1	0	0	1	1	1	1
Bolodon	1	1	1	1	1	?	1	1	?	?
Plagiaulax	1	1	1	1	0	0	1	1	1	1
Zofiabaatar	1	1	1	1	0	0	1	1	1	1
Sinobaatar	1	1	1	1	0	0	1	1	0	1
Eobaatar	1	1	?	1	?	?	?	1	?	1
Jeholbaatar	1	1	1	1	0	0	1	1	0	1
Heishanobaatar	1	1	1	1	0	0	1	1	0	1
Liaobaatar	1	1	1	1	0	0	1	1	0	1
Hakusanobaatar	?	?	?	?	?	?	?	?	?	?
Arginbaatar	?	1	2	1	0	?	?	1	?	?
Bryceomys	?	?	?	?	?	?	?	?	?	?
Boffius	?	?	?	?	?	?	?	?	?	?
Meniscoessus	1	1	2	1	1	?	0	1	?	1
Buginbaatar	1	1	1	1	1	0	0	1	?	?
Cimolodon	1	1	2	1	0	?	0	1	?	1
Ectypodus	1	1	2	1	0	?	0	1	1	1
Mesodma	1	1	2	1	0	?	0	1	?	1
Ptilodus	1	1	2	1	0	0	0	1	0	1
Neoliotomus	1	1	2	1	1	?	0	1	?	1
Filikomys	1	1	2	1	0	1	0	1	1	1
Pentacosmodon	1	1	2	1	0	0	1	1	1	1
Microcosmodon	1	1	2	?	0	?	1	1	1	1
Catopsbaatar	1	1	2	1	0	0	1	1	1	1
Kamptobaatar	1	1	2	1	1	1	0	1	1	1
Chulsanbaatar	1	1	2	1	1	0	1	1	0	1
Kryptobaatar	1	1	2	1	1	0	0	1	0	1
Nemegtbaatar	1	1	2	1	1	0	0	1	0	1
Eucosmodon	1	1	2	1	1	?	1	1	0	1
Stygimys	1	1	1	1	1	0	0	1	0	1
Taeniolabis	1	1	2	1	0	0	0	1	1	1
Lambdopsalis	1	1	2	1	0	1	1	1	1	1
Sphenopsalis	1	1	?	1	?	?	?	1	?	1
Prionessus	1	1	2	1	?	?	?	1	?	1
Catopsalis	1	1	2	1	0	0	0	1	[1 2]	1
Yubaatar	1	1	1	1	0	0	0	1	1	1
K.ungureanui	?	?	?	?	?	?	?	?	?	?
B.transylvanicus	1	1	2	1	0	1	1	1	0	1
B.oardaensis	?	?	?	?	?	?	?	?	?	?
K.radulescui	?	?	?	?	?	?	?	?	?	?
H.belgica	?	?	?	?	?	?	?	?	?	?
H.pyrenaica	?	?	?	?	?	?	?	?	?	?
Kielanodon	?	?	?	?	?	?	?	?	?	?
Iberodon	?	?	?	?	?	?	?	?	?	?
Pinheirodon	?	?	?	?	?	?	?	?	?	?
Bernardodon	?	?	?	?	?	?	?	?	?	?
New Fossil	?	1	2	?	?	?	0	?	?	?

	11	12	13	14	15	16	17	18	19	20
Sinoconodon	0	0	0	0	0	0	0	0	0	0
Morganucodon	0	0	0	0	0	0	0	0	0	0
Thomasia	0	1	?	?	0	0	0	?	0	0
Haramiyavia	0	1	0	0	0	0	0	1	0	0
Rugosodon	1	1	1	1	0	0	1	0	1	1
Paulchoffatia	1	1	0	1	0	0	?	?	?	?
Meketichoffatia	?	?	?	?	?	?	?	?	?	?
Henkelodon	?	?	?	?	?	?	1	0	1	2
Meketibolodon	1	1	0	1	0	0	?	?	?	?
Guimarotodon	1	1	0	1	0	0	?	?	?	?
Kuehneodon	1	1	1	1	0	0	1	0	1	2
Pseudobolodon	?	?	?	?	?	?	1	0	0	0
Ctenacodon	1	1	1	1	0	0	1	0	1	1
Glirodon	1	1	1	1	0	2	1	0	1	1
Bolodon	1	1	1	?	0	0	?	?	?	?
Plagiaulax	1	1	1	1	0	0	?	?	?	?
Zofiabaatar	1	1	?	1	0	?	?	?	?	?
Sinobaatar	1	1	1	1	0	0	1	1	0	1
Eobaatar	1	1	1	1	0	2	?	?	?	?
Jeholbaatar	1	1	1	1	0	0	1	1	1	0
Heishanobaatar	1	1	1	1	0	0	?	?	?	?
Liaobaatar	1	1	1	1	0	0	?	?	?	?
Hakusanobaatar	?	1	?	1	0	0	?	?	1	0
Arginbaatar	1	1	1	1	0	0	?	?	?	?
Bryceomys	?	?	?	?	?	?	?	?	?	?
Boffius	?	?	?	?	0	?	?	?	?	?
Meniscoessus	1	1	1	1	0	0	2	1	1	1
Buginbaatar	1	1	?	1	0	0	?	?	?	?
Cimolodon	1	1	1	1	?	0	?	?	?	?
Ectypodus	1	1	1	1	1	0	2	1	0	1
Mesodma	1	1	1	1	1	0	2	?	?	?
Ptilodus	1	1	1	1	1	0	2	1	0	0
Neoliotomus	1	1	1	1	0	2	?	?	0	?
Filikomys	1	1	1	1	1	0	2	1	0	0
Pentacosmodon	1	1	1	1	0	2	?	?	?	?
Microcosmodon	1	1	1	1	0	2	2	0	1	1
Catopsbaatar	1	1	1	1	0	2	2	1	0	1
Kamptobaatar	1	1	1	1	0	1	2	1	0	1
Chulsanbaatar	1	1	1	1	0	2	2	1	0	1
Kryptobaatar	1	1	1	1	0	2	2	1	0	1
Nemegtbaatar	1	1	1	1	0	2	2	1	0	1
Eucosmodon	1	1	1	1	0	2	2	?	1	1
Stygimys	1	1	1	1	0	2	2	1	1	1
Taeniolabis	1	1	1	1	0	2	2	[1 2]	1	0
Lambdopsalis	1	1	1	1	0	2	2	0	0	0
Sphenopsalis	1	1	1	1	0	2	2	0	0	0
Prionessus	1	1	1	1	0	2	2	?	?	?
Catopsalis	1	1	1	1	0	2	2	[1 2]	1	0
Yubaatar	1	1	1	1	0	2	?	?	?	?
K.ungureanui	?	?	?	?	?	?	2	0	?	0
B.transylvanicus	1	1	1	1	0	2	2	0	1	0
B.oardaensis	1	1	?	?	0	2	2	?	1	0
K.radulescui	1	1	1	1	0	2	2	0	?	0
H.belgica	?	?	?	?	?	?	?	?	?	?
H.pyrenaica	?	?	?	?	?	?	?	?	?	?
Kielanodon	?	?	?	?	?	?	?	?	?	?
Iberodon	1	1	?	?	1	?	?	1	?	?
Pinheirodon	1	1	?	?	1	?	?	1	?	?
Bernardodon	1	1	?	?	0	?	?	1	?	?
New Fossil	1	1	0	1	0	?	?	?	?	?

	21	22	23	24	25	26	27	28	29	30
Sinoconodon	0	0	0	0	0	0	0	0	2	?
Morganucodon	0	0	0	0	0	0	0	0	2	?
Thomasia	?	?	?	?	?	3	0	0	2	0
Haramiyavia	0	1	0	0	?	?	?	?	?	?
Rugosodon	0	1	1	1	0	0	0	?	0	0
Paulchoffatia	?	?	?	1	?	?	?	?	?	?
Meketichoffatia	?	1	1	?	0	0	0	1	0	0
Henkelodon	0	2	?	?	0	0	0	1	0	0
Meketibolodon	?	?	?	1	?	?	?	?	?	?
Guimarotodon	?	?	?	1	?	?	?	?	?	?
Kuehneodon	0	1	1	1	0	1	0	1	0	0
Pseudobolodon	?	0	1	?	?	0	0	0	?	1
Ctenacodon	0	1	?	1	0	0	0	1	0	1
Glirodon	0	1	0	1	0	0	0	1	0	1
Bolodon	?	1	?	1	?	0	0	1	0	1
Plagiaulax	?	?	?	1	?	?	?	?	?	?
Zofiabaatar	?	?	?	?	?	?	?	?	?	?
Sinobaatar	0	2	?	1	2	0	0	0	0	[2 3]
Eobaatar	?	?	?	1	?	0	0	0	0	0
Jeholbaatar	0	2	?	1	0	0	0	0	0	2
Heishanobaatar	?	?	?	1	?	?	?	?	?	?
Liaobaatar	?	?	?	?	?	?	?	?	0	?
Hakusanobaatar	0	2	?	1	?	0	0	0	0	2
Arginbaatar	?	?	?	1	?	0	0	0	0	0
Bryceomys	?	?	?	?	?	?	0	0	?	2
Boffius	?	?	?	?	?	?	?	0	?	?
Meniscoessus	1	2	?	1	2	1	0	0	2	2
Buginbaatar	?	?	?	?	?	?	?	0	?	2
Cimolodon	?	2	?	1	?	1	0	0	1	2
Ectypodus	1	2	?	1	0	1	0	0	1	2
Mesodma	1	2	?	1	?	1	0	0	?	2
Ptilodus	0	2	?	1	0	1	0	0	0	2
Neoliotomus	?	?	?	1	?	1	0	0	1	2
Filikomys	1	2	?	1	2	1	0	0	1	2
Pentacosmodon	?	?	?	1	?	?	0	0	?	2
Microcosmodon	1	2	?	1	0	1	0	0	1	2
Catopsbaatar	2	2	?	1	0	2	0	0	2	2
Kamptobaatar	2	2	?	1	0	1	0	0	1	2
Chulsanbaatar	2	2	?	1	0	1	0	0	1	2
Kryptobaatar	2	2	?	1	0	1	0	0	1	2
Nemegtbaatar	2	2	?	1	1	1	0	0	1	2
Eucosmodon	?	2	?	1	?	2	0	0	?	2
Stygimys	2	2	?	1	1	1	0	0	1	2
Taeniolabis	0	2	?	1	2	3	1	0	2	[2 3]
Lambdopsalis	1	2	?	1	2	3	1	0	2	3
Sphenopsalis	0	2	?	1	2	3	1	0	2	3
Prionessus	?	2	?	1	?	3	[1 2]	0	2	3
Catopsalis	0	2	?	1	2	3	1	0	2	[2 3]
Yubaatar	?	2	?	1	?	1	0	0	1	[2 3]
K.ungureanui	0	2	?	?	1	1	0	0	0	4
B.transylvanicus	0	2	?	1	1	1	0	0	0	4
B.oardaensis	?	?	?	?	?	1	0	0	0	4
K.radulescui	0	2	?	1	1	1	0	0	0	4
H.belgica	?	?	?	?	?	1	0	0	?	4
H.pyrenaica	?	?	?	?	?	?	0	0	?	4
Kielanodon	?	?	?	?	?	0	0	1	?	1
Iberodon	?	?	?	1	?	0	0	1	?	1
Pinheirodon	?	?	?	1	?	0	0	1	?	1
Bernardodon	?	?	?	1	?	0	0	1	?	1
New Fossil	?	?	?	1	?	?	?	?	?	?

	31	32	33	34	35	36	37	38	39	40
Sinoconodon	0	0	0	0	0	0	0	0	?	0
Morganucodon	0	0	0	0	0	0	0	0	?	0
Thomasia	0	1	?	?	0	0	0	0	?	0
Haramiyavia	?	?	0	0	0	0	0	0	?	0
Rugosodon	?	?	0	0	0	1	?	1	?	0
Paulchoffatia	?	?	0	0	0	1	0	1	0	0
Meketichoffatia	0	0	?	?	?	?	?	?	?	?
Henkelodon	0	0	?	?	?	?	?	?	?	?
Meketibolodon	?	?	0	0	0	1	0	1	0	0
Guimarotodon	?	?	0	0	0	1	0	1	0	0
Kuehneodon	0	0	0	0	[0 1]	1	0	1	0	0
Pseudobolodon	0	?	?	?	?	?	?	?	?	?
Ctenacodon	0	0	0	0	0	1	0	1	1	0
Glirodon	0	0	0	0	0	?	0	1	1	0
Bolodon	0	0	0	0	0	1	0	2	1	0
Plagiaulax	?	?	1	0	0	1	0	2	1	0
Zofiabaatar	?	?	0	0	0	1	0	1	1	0
Sinobaatar	0	[1 2]	1	0	0	1	1	2	1	0
Eobaatar	0	1	1	0	0	1	0	2	1	0
Jeholbaatar	0	1	1	0	0	1	1	2	1	0
Heishanobaatar	?	?	1	0	0	1	0	2	1	0
Liaobaatar	?	1	1	0	0	1	1	2	1	1
Hakusanobaatar	1	1	1	0	0	1	1	2	1	0
Arginbaatar	0	1	1	0	0	0	1	2	1	1
Bryceomys	1	1	?	?	?	?	?	?	?	?
Boffius	1	1	?	?	?	?	?	?	?	?
Meniscoessus	0	2	1	1	0	0	1	3	1	1
Buginbaatar	1	3	1	1	1	?	?	?	?	?
Cimolodon	1	1	1	1	0	0	1	3	1	1
Ectypodus	2	1	1	1	0	0	1	3	1	1
Mesodma	1	1	1	1	0	0	1	3	1	1
Ptilodus	2	1	1	1	0	0	1	3	1	1
Neoliotomus	2	1	1	1	0	0	1	3	1	1
Filikomys	1	2	1	1	0	0	1	3	1	1
Pentacosmodon	0	2	1	1	1	?	?	?	?	1
Microcosmodon	1	2	1	1	0	0	1	2	1	1
Catopsbaatar	1	3	1	1	0	0	1	3	1	1
Kamptobaatar	1	2	1	1	0	0	1	3	1	1
Chulsanbaatar	1	2	1	1	0	0	1	3	1	1
Kryptobaatar	1	2	1	1	0	0	1	3	1	1
Nemegtbaatar	1	2	1	1	0	0	1	3	1	1
Eucosmodon	?	?	1	1	1	?	?	?	?	?
Stygimys	2	1	1	1	1	?	?	?	?	?
Taeniolabis	0	3	1	1	1	?	?	?	?	?
Lambdopsalis	0	3	1	1	1	?	?	?	?	?
Sphenopsalis	0	3	1	1	1	?	?	?	?	?
Prionessus	0	3	1	1	1	?	?	?	?	?
Catopsalis	1	2	1	1	1	?	?	?	?	?
Yubaatar	0	[2 3]	1	1	1	?	?	?	?	?
K.ungureanui	0	2	?	?	?	?	?	?	?	?
B.transylvanicus	0	1	1	1	1	?	?	?	?	?
B.oardaensis	0	2	1	1	1	?	?	?	?	?
K.radulescui	0	2	1	1	1	?	?	?	?	?
H.belgica	0	2	1	1	1	?	?	?	?	?
H.pyrenaica	0	2	?	?	?	?	?	?	?	?
Kielanodon	0	2	?	?	?	?	?	?	?	?
Iberodon	?	1	?	0	0	1	?	2	1	?
Pinheirodon	?	0	?	0	0	1	0	1	?	?
Bernardodon	?	1	?	0	0	1	0	1	0	?
New Fossil	?	?	0	0	0	1	0	2	0	0

	41	42	43	44	45	46	47	48	49	50
Sinoconodon	0	0	?	0	0	1	0	0	?	?
Morganucodon	0	0	?	0	0	1	0	0	0	0
Thomasia	0	1	?	0	0	1	0	0	0	0
Haramiyavia	0	0	?	0	0	?	0	0	0	0
Rugosodon	1	1	0	0	1	?	?	1	1	1
Paulchoffatia	1	1	0	0	1	0	2	1	1	?
Meketichoffatia	?	?	?	?	?	?	?	?	?	1
Henkelodon	?	?	?	?	?	?	?	?	?	1
Meketibolodon	1	1	0	0	1	0	3	?	?	?
Guimarotodon	1	1	0	0	1	0	3	1	1	?
Kuehneodon	1	1	0	0	1	0	2	1	1	1
Pseudobolodon	?	?	?	?	?	?	?	?	?	?
Ctenacodon	1	1	0	0	1	1	2	1	1	1
Glirodon	1	1	0	0	1	1	2	1	1	1
Bolodon	1	1	0	0	1	1	2	?	1	1
Plagiaulax	1	1	1	0	?	1	2	?	1	?
Zofiabaatar	1	1	0	0	1	1	2	3	1	?
Sinobaatar	1	2	1	1	1	[1 2]	1	2	1	1
Eobaatar	1	2	1	1	?	2	1	?	1	1
Jeholbaatar	1	2	1	1	1	2	1	2	1	1
Heishanobaatar	1	2	1	1	1	1	1	2	1	?
Liaobaatar	1	2	2	1	1	2	1	3	1	?
Hakusanobaatar	1	2	1	1	1	2	1	?	1	?
Arginbaatar	1	2	2	1	1	2	0	3	1	1
Bryceomys	1	2	[1 2]	1	?	?	1	2	1	1
Boffius	?	?	?	?	?	?	?	?	1	?
Meniscoessus	1	2	1	1	0	3	0	0	1	1
Buginbaatar	1	2	0	0	0	?	0	0	1	1
Cimolodon	1	2	2	1	1	2	0	[1 2]	1	1
Ectypodus	1	2	2	1	1	3	0	3	1	1
Mesodma	1	2	[1 2]	1	1	3	0	[1 2]	1	1
Ptilodus	1	2	2	1	1	3	0	2	1	1
Neoliotomus	1	2	2	1	1	3	0	3	1	1
Filikomys	1	1	1	1	1	3	0	2	1	1
Pentacosmodon	1	2	0	1	0	?	1	0	1	1
Microcosmodon	1	2	0	1	0	?	1	0	1	1
Catopsbaatar	1	1	0	0	0	3	0	[0 1]	1	1
Kamptobaatar	1	2	1	1	0	3	0	1	1	1
Chulsanbaatar	1	2	1	1	0	3	0	1	1	1
Kryptobaatar	1	2	1	1	0	3	0	1	1	1
Nemegtbaatar	1	2	1	1	0	3	0	1	1	1
Eucosmodon	1	2	2	1	0	?	0	1	1	1
Stygimys	1	2	2	1	0	?	1	1	1	1
Taeniolabis	0	3	?	0	0	?	1	0	1	1
Lambdopsalis	0	3	?	0	0	?	0	0	1	1
Sphenopsalis	0	3	?	0	0	?	0	0	1	1
Prionessus	0	3	?	0	0	?	0	0	1	1
Catopsalis	0	3	?	0	0	?	1	0	1	1
Yubaatar	0	2	1	0	0	?	1	0	1	1
K.ungureanui	?	?	?	?	?	?	?	?	?	1
B.transylvanicus	1	2	1	0	1	?	1	3	1	1
B.oardaensis	1	2	[1 2]	0	1	?	1	2	1	1
K.radulescui	1	2	0	0	?	?	1	?	?	1
H.belgica	1	2	0	0	1	?	1	3	1	?
H.pyrenaica	?	?	?	?	?	?	?	?	1	?
Kielanodon	?	?	?	?	?	?	?	?	?	?
Iberodon	1	1	0	1	?	1	2	1	1	1
Pinheirodon	1	1	0	?	?	1	?	1	1	1
Bernardodon	1	1	0	1	?	1	2	1	1	1
New Fossil	1	1	0	1	?	1	2	?	?	?

	51	52	53	54	55	56	57	58	59	60
Sinoconodon	0	0	0	0	?	0	?	?	?	0
Morganucodon	0	0	0	0	?	0	?	?	?	0
Thomasia	?	?	1	0	?	0	0	?	?	0
Haramiyavia	0	0	1	0	?	0	0	?	?	0
Rugosodon	1	1	1	0	[0 1]	1	0	?	?	1
Paulchoffatia	?	1	1	0	0	?	?	?	?	?
Meketichoffatia	1	?	?	?	0	0	0	?	?	1
Henkelodon	1	?	?	?	0	1	0	?	?	1
Meketibolodon	?	?	?	?	0	?	?	?	?	?
Guimarotodon	?	1	1	0	?	?	?	?	?	?
Kuehneodon	2	1	1	0	0	1	0	?	?	1
Pseudobolodon	?	?	?	?	?	?	?	?	?	?
Ctenacodon	1	1	0	1	1	1	1	0	0	1
Glirodon	1	1	0	1	0	1	0	?	?	1
Bolodon	1	1	0	1	0	1	1	0	0	1
Plagiaulax	?	1	0	1	?	?	?	?	?	?
Zofiabaatar	?	1	0	1	?	?	?	?	?	?
Sinobaatar	1	2	0	1	1	1	1	1	0	1
Eobaatar	1	2	0	1	0	1	1	1	0	1
Jeholbaatar	1	2	0	1	1	1	1	1	0	1
Heishanobaatar	?	2	0	1	?	?	?	?	?	?
Liaobaatar	?	2	0	1	?	?	?	?	?	?
Hakusanobaatar	?	2	0	1	1	1	1	1	0	?
Arginbaatar	1	2	0	1	0	1	1	0	0	1
Bryceomys	?	?	0	1	4	1	1	1	2	?
Boffius	?	?	?	?	3	?	1	2	3	1
Meniscoessus	2	2	0	1	[2 3]	1	1	2	3	1
Buginbaatar	?	2	0	1	3	1	1	1	3	1
Cimolodon	2	2	0	1	2	1	1	2	2	1
Ectypodus	2	2	0	1	[2 3]	1	1	1	3	1
Mesodma	2	2	0	1	2	1	1	2	[2 3]	1
Ptilodus	2	2	0	1	[2 3]	1	1	1	3	1
Neoliotomus	2	2	0	1	3	1	1	2	3	1
Filikomys	2	2	0	1	2	1	1	2	2	1
Pentacosmodon	?	2	0	1	2	1	1	1	2	1
Microcosmodon	2	2	0	1	2	1	1	1	3	1
Catopsbaatar	3	2	0	1	2	1	1	2	3	1
Kamptobaatar	2	2	0	1	1	1	1	0	1	1
Chulsanbaatar	2	2	0	1	1	1	1	0	1	1
Kryptobaatar	2	2	0	1	1	1	1	1	2	1
Nemegtbaatar	2	2	0	1	[1 2]	1	1	2	2	1
Eucosmodon	2	2	0	1	2	1	1	?	?	1
Stygimys	2	2	0	1	2	1	1	1	[2 3]	1
Taeniolabis	3	2	0	1	3	1	1	2	3	1
Lambdopsalis	3	2	2	1	3	1	1	2	3	1
Sphenopsalis	3	2	2	1	3	1	1	2	3	1
Prionessus	3	2	0	1	3	1	1	2	3	1
Catopsalis	3	2	0	1	3	1	1	2	3	1
Yubaatar	2	2	0	1	2	1	1	2	3	1
K.ungureanui	2	?	?	?	4	1	1	2	2	1
B.transylvanicus	2	2	0	1	4	1	1	2	2	1
B.oardaensis	2	?	0	1	4	1	1	2	2	1
K.radulescui	2	?	?	?	4	1	1	2	2	1
H.belgica	?	?	0	1	4	1	1	2	3	1
H.pyrenaica	?	?	0	1	4	1	1	2	3	1
Kielanodon	?	?	?	?	1	?	?	?	?	0
Iberodon	?	?	0	0	4	1	0	?	?	1
Pinheirodon	?	?	0	0	4	1	0	?	?	1
Bernardodon	?	?	0	0	4	1	0	?	?	1
New Fossil	?	?	?	?	?	?	?	?	?	?

	61	62	63	64	65	66	67	68	69	70
Sinoconodon	1	0	0	?	?	0	0	0	0	?
Morganucodon	1	0	0	?	?	0	0	0	0	?
Thomasia	1	1	3	0	0	0	0	?	2	0
Haramiyavia	1	1	3	0	0	1	0	1	2	0
Rugosodon	0	1	1	1	1	2	0	2	2	1
Paulchoffatia	?	?	?	?	?	?	0	2	2	1
Meketichoffatia	?	1	1	?	?	?	?	?	?	?
Henkelodon	?	1	2	?	?	?	?	?	?	?
Meketibolodon	?	?	?	?	?	?	?	2	?	?
Guimarotodon	?	?	?	?	?	?	0	2	2	1
Kuehneodon	0	1	2	1	1	2	0	2	2	1
Pseudobolodon	?	?	?	?	?	?	?	?	?	?
Ctenacodon	0	2	3	0	0	1	0	1	1	0
Glirodon	0	2	3	0	0	1	0	1	1	0
Bolodon	0	2	3	0	0	1	0	?	1	?
Plagiaulax	?	?	?	?	?	1	0	1	1	0
Zofiabaatar	?	?	?	?	?	1	0	?	1	0
Sinobaatar	1	2	3	0	0	1	0	1	1	1
Eobaatar	1	2	3	0	0	1	0	1	1	1
Jeholbaatar	1	2	3	0	0	1	0	1	1	1
Heishanobaatar	?	?	?	?	?	?	0	1	1	1
Liaobaatar	?	?	?	?	?	?	0	1	1	1
Hakusanobaatar	?	?	3	?	?	?	?	?	?	?
Arginbaatar	0	2	3	0	0	1	0	1	1	0
Bryceomys	0	2	3	0	0	2	0	1	1	0
Boffius	?	2	3	?	?	1	?	?	?	?
Meniscoessus	2	2	3	0	0	1	1	?	1	0
Buginbaatar	2	2	3	0	0	1	2	?	1	0
Cimolodon	2	2	3	0	0	1	[0 1]	1	1	0
Ectypodus	1	2	3	1	0	1	2	1	1	0
Mesodma	1	2	3	0	0	1	[0 1]	1	1	0
Ptilodus	1	2	3	1	0	1	2	1	1	0
Neoliotomus	1	2	3	0	0	1	2	1	1	0
Filikomys	1	2	3	0	0	1	0	1	1	0
Pentacosmodon	0	2	3	0	0	0	0	1	1	0
Microcosmodon	1	2	3	0	0	1	[0 1]	1	1	0
Catopsbaatar	0	2	3	0	0	1	0	1	1	0
Kamptobaatar	1	2	3	0	0	1	0	1	1	0
Chulsanbaatar	1	2	3	0	0	1	0	1	1	0
Kryptobaatar	2	2	3	0	0	1	0	1	1	0
Nemegtbaatar	2	2	3	0	0	1	0	1	1	0
Eucosmodon	?	2	3	?	?	1	1	1	1	0
Stygimys	1	2	3	0	0	1	2	1	1	0
Taeniolabis	[1 2]	2	4	0	2	1	2	1	1	0
Lambdopsalis	0	1	3	0	0	1	0	2	2	0
Sphenopsalis	0	1	3	0	0	1	0	2	2	0
Prionessus	0	[1 2]	3	0	0	1	0	1	1	0
Catopsalis	1	2	4	0	[1 2]	1	[0 1]	1	1	0
Yubaatar	1	2	3	0	0	1	2	1	1	0
K.ungureanui	0	2	3	0	0	1	?	?	?	?
B.transylvanicus	0	2	3	0	0	1	0	1	1	0
B.oardaensis	0	2	3	0	0	1	0	1	1	0
K.radulescui	0	2	3	0	0	1	?	?	?	?
H.belgica	?	?	3	?	?	?	0	1	1	0
H.pyrenaica	?	?	3	?	?	?	0	1	1	0
Kielanodon	?	?	1	?	?	?	?	?	?	?
Iberodon	0	2	2	0	0	0	0	2	2	0
Pinheirodon	0	2	2	0	0	0	0	2	2	?
Bernardodon	0	2	2	0	0	0	?	?	2	0
New Fossil	?	?	?	?	?	?	?	?	?	?

	71	72	73	74	75	76	77	78	79	80
Sinoconodon	?	?	?	?	?	0	0	0	0	0
Morganucodon	?	?	?	?	?	0	0	1	1	0
Thomasia	0	2	0	0	0	0	?	1	?	?
Haramiyavia	0	2	0	0	0	0	1	1	?	?
Rugosodon	1	0	0	0	1	1	1	1	1	0
Paulchoffatia	1	0	0	0	2	1	1	1	?	?
Meketichoffatia	?	?	?	?	?	1	?	1	?	0
Henkelodon	?	?	?	?	?	1	?	1	1	0
Meketibolodon	?	0	?	?	2	1	?	1	?	?
Guimarotodon	1	0	0	0	2	1	1	1	?	?
Kuehneodon	1	1	0	0	[1 2]	1	1	1	1	0
Pseudobolodon	?	?	?	?	?	?	?	?	?	?
Ctenacodon	0	1	1	0	0	0	0	1	?	0
Glirodon	0	1	1	0	0	0	0	1	?	0
Bolodon	?	1	1	0	0	1	0	1	?	0
Plagiaulax	0	1	1	?	0	0	0	1	?	?
Zofiabaatar	0	1	1	0	0	0	0	1	?	?
Sinobaatar	0	1	1	0	0	1	0	1	1	0
Eobaatar	0	1	1	0	0	1	1	1	?	?
Jeholbaatar	0	1	1	0	0	1	?	1	?	1
Heishanobaatar	0	1	1	0	0	1	?	1	?	?
Liaobaatar	0	1	1	0	0	1	?	1	?	0
Hakusanobaatar	?	?	?	0	0	1	?	1	?	?
Arginbaatar	0	1	1	0	0	0	1	1	?	0
Bryceomys	0	1	1	0	0	1	?	1	?	?
Boffius	?	?	1	?	0	0	1	1	?	?
Meniscoessus	0	2	1	1	0	1	1	1	?	0
Buginbaatar	0	1	1	0	0	0	?	1	?	?
Cimolodon	0	2	1	0	0	1	1	1	1	?
Ectypodus	0	2	1	0	0	1	2	1	1	1
Mesodma	0	[1 2]	1	0	0	1	2	1	1	1
Ptilodus	0	2	1	0	0	1	2	1	1	1
Neoliotomus	0	2	1	1	0	1	2	1	?	?
Filikomys	0	1	1	0	0	1	?	1	1	1
Pentacosmodon	0	1	1	0	0	0	1	1	?	?
Microcosmodon	0	1	1	0	0	0	?	1	1	1
Catopsbaatar	0	1	1	0	0	0	1	1	?	1
Kamptobaatar	0	1	1	0	0	0	1	1	?	1
Chulsanbaatar	0	1	1	0	0	0	1	1	1	1
Kryptobaatar	0	1	1	0	0	0	1	1	1	1
Nemegtbaatar	0	1	1	0	0	0	1	1	1	1
Eucosmodon	0	2	1	0	0	0	1	1	?	1
Stygimys	0	1	1	0	0	0	1	1	?	1
Taeniolabis	0	2	0	2	0	0	1	1	1	1
Lambdopsalis	0	1	1	1	0	0	1	1	1	1
Sphenopsalis	0	1	1	1	0	0	1	1	?	?
Prionessus	0	1	0	0	0	0	1	1	?	?
Catopsalis	0	1	[0 1]	2	0	0	1	1	?	?
Yubaatar	0	2	0	0	0	0	?	1	1	1
K.ungureanui	?	?	?	?	?	0	1	1	?	1
B.transylvanicus	0	1	1	0	0	1	?	1	?	1
B.oardaensis	0	1	0	0	0	[0 1]	?	1	?	?
K.radulescui	?	?	?	?	?	[0 1]	?	1	?	1
H.belgica	0	1	0	0	0	0	1	1	?	?
H.pyrenaica	0	1	0	0	0	[0 1]	?	1	?	?
Kielanodon	?	?	?	?	?	?	?	1	1	?
Iberodon	1	1	1	0	2	[0 1]	?	1	?	?
Pinheirodon	1	1	1	0	2	[0 1]	?	1	?	?
Bernardodon	1	1	1	0	?	[0 1]	?	1	?	?
New Fossil	?	?	?	?	?	?	?	0	1	?

	81	82	83	84	85	86	87	88	89	90
Sinoconodon	0	0	0	1	0	0	0	0	1	0
Morganucodon	0	0	0	0	0	0	0	0	1	0
Thomasia	?	?	?	?	?	?	?	?	?	?
Haramiyavia	?	?	?	?	?	?	0	?	?	?
Rugosodon	?	?	?	?	0	?	?	?	0	?
Paulchoffatia	?	?	?	?	?	?	?	?	?	?
Meketichoffatia	0	0	0	?	?	0	0	?	0	0
Henkelodon	?	?	?	?	?	?	?	?	?	?
Meketibolodon	?	?	?	?	?	?	?	?	?	?
Guimarotodon	?	?	?	?	?	?	?	?	?	?
Kuehneodon	?	?	?	?	?	?	0	?	?	?
Pseudobolodon	?	?	?	?	?	?	?	?	?	?
Ctenacodon	?	?	0	?	?	0	?	?	?	?
Glirodon	0	0	0	1	1	0	0	?	?	0
Bolodon	0	?	?	?	1	?	?	?	?	?
Plagiaulax	?	?	?	?	?	?	?	?	?	?
Zofiabaatar	?	?	?	?	?	?	?	?	?	?
Sinobaatar	0	0	?	1	0	1	0	?	0	1
Eobaatar	?	?	?	?	?	?	?	?	?	?
Jeholbaatar	?	?	0	?	?	1	?	0	?	?
Heishanobaatar	?	?	?	?	?	?	?	?	?	?
Liaobaatar	?	?	?	?	?	?	?	?	?	?
Hakusanobaatar	?	?	?	?	?	?	?	?	?	?
Arginbaatar	?	?	?	?	?	?	?	?	?	?
Bryceomys	?	?	?	?	?	?	?	?	?	?
Boffius	?	?	?	?	?	?	?	?	?	?
Meniscoessus	2	0	0	?	0	1	?	?	?	?
Buginbaatar	?	?	?	?	?	?	?	?	?	?
Cimolodon	?	?	?	?	?	?	?	?	?	?
Ectypodus	1	?	0	?	0	1	0	?	0	?
Mesodma	?	?	?	?	?	?	?	?	?	?
Ptilodus	1	0	0	2	0	0	0	?	0	0
Neoliotomus	?	?	?	?	?	?	?	?	?	?
Filikomys	1	1	0	2	0	0	0	0	0	1
Pentacosmodon	?	?	?	?	?	?	?	?	?	?
Microcosmodon	0	0	1	?	0	0	0	?	?	?
Catopsbaatar	0	1	0	2	0	1	1	1	1	1
Kamptobaatar	0	1	0	3	2	0	1	0	0	1
Chulsanbaatar	0	1	0	2	2	0	1	0	0	1
Kryptobaatar	0	1	0	2	1	0	1	1	1	1
Nemegtbaatar	2	1	0	3	1	0	1	0	0	1
Eucosmodon	?	?	?	?	?	?	?	?	?	?
Stygimys	2	?	0	?	2	0	?	?	?	?
Taeniolabis	0	0	1	3	0	?	0	?	0	2
Lambdopsalis	0	0	1	3	0	1	0	1	0	2
Sphenopsalis	0	0	?	?	?	1	?	1	?	2
Prionessus	0	?	?	?	?	1	?	?	?	?
Catopsalis	?	?	?	?	?	?	?	?	?	?
Yubaatar	[1 2]	?	1	3	0	1	0	1	?	2
K.ungureanui	0	0	1	3	0	0	0	0	0	0
B.transylvanicus	?	0	1	3	0	0	0	0	0	0
B.oardaensis	?	?	?	?	?	?	?	?	?	?
K.radulescui	?	0	?	3	0	?	0	?	?	?
H.belgica	?	?	?	?	?	?	?	?	?	?
H.pyrenaica	?	?	?	?	?	?	?	?	?	?
Kielanodon	?	?	1	?	?	0	?	?	?	?
Iberodon	?	?	?	?	?	?	?	?	?	?
Pinheirodon	?	?	?	?	?	?	?	?	?	?
Bernardodon	?	?	?	?	?	?	?	?	?	?
New Fossil	?	?	?	?	?	?	?	?	?	?

	91	92	93	94	95	96	97	98	99	100
Sinoconodon	0	0	0	0	0	?	0	0	0	0
Morganucodon	0	0	0	0	0	?	0	0	0	0
Thomasia	?	?	?	?	?	?	?	?	?	?
Haramiyavia	?	?	?	?	?	?	?	?	?	?
Rugosodon	?	?	?	?	?	?	?	?	?	?
Paulchoffatia	?	?	?	?	?	?	?	?	?	?
Meketichoffatia	?	?	?	?	1	1	0	0	0	?
Henkelodon	?	?	?	?	?	?	?	?	?	?
Meketibolodon	?	?	?	?	?	?	?	?	?	?
Guimarotodon	?	?	?	?	?	?	?	?	?	?
Kuehneodon	?	?	?	?	?	?	?	?	?	?
Pseudobolodon	?	?	?	?	?	?	?	?	?	?
Ctenacodon	?	?	?	?	?	?	?	?	?	?
Glirodon	?	0	?	?	1	?	?	?	?	?
Bolodon	?	?	?	?	?	?	?	?	?	?
Plagiaulax	?	?	?	?	?	?	?	?	?	?
Zofiabaatar	?	?	?	?	?	?	?	?	?	?
Sinobaatar	?	0	?	?	?	?	?	?	?	?
Eobaatar	?	?	?	?	?	?	?	?	?	?
Jeholbaatar	?	0	?	?	?	?	1	?	?	1
Heishanobaatar	?	?	?	?	?	?	?	?	?	?
Liaobaatar	?	?	?	?	?	?	?	?	?	?
Hakusanobaatar	?	?	?	?	?	?	?	?	?	?
Arginbaatar	?	?	?	?	?	?	?	?	?	?
Bryceomys	?	?	?	?	?	?	?	?	?	?
Boffius	?	?	?	?	?	?	?	?	?	?
Meniscoessus	?	?	?	0	1	?	?	?	?	?
Buginbaatar	?	?	?	?	?	?	?	?	?	?
Cimolodon	?	?	?	?	?	?	?	?	?	?
Ectypodus	?	0	?	?	1	1	0	0	1	?
Mesodma	?	?	?	?	?	?	?	?	?	?
Ptilodus	0	0	0	0	1	0	0	0	1	0
Neoliotomus	?	?	?	?	?	?	?	?	?	?
Filikomys	0	0	0	0	1	0	0	?	1	0
Pentacosmodon	?	?	?	?	?	?	?	?	?	?
Microcosmodon	?	?	?	?	1	?	?	?	1	?
Catopsbaatar	1	0	1	1	0	?	1	1	0	0
Kamptobaatar	1	0	1	1	1	0	1	0	0	0
Chulsanbaatar	1	0	1	1	1	1	1	0	0	0
Kryptobaatar	1	0	1	1	1	1	1	1	0	0
Nemegtbaatar	1	0	1	1	1	0	1	0	0	0
Eucosmodon	?	?	?	?	?	?	?	?	?	?
Stygimys	?	?	?	1	1	?	?	?	?	?
Taeniolabis	0	1	0	0	?	?	?	?	?	1
Lambdopsalis	0	1	0	0	1	?	1	1	1	1
Sphenopsalis	0	?	?	?	1	?	?	1	?	?
Prionessus	?	?	?	?	?	?	?	?	?	?
Catopsalis	?	?	?	?	?	?	?	?	?	?
Yubaatar	0	0	1	0	?	?	1	1	1	1
K.ungureanui	0	0	?	?	1	?	1	?	1	?
B.transylvanicus	0	0	0	0	1	1	?	1	1	1
B.oardaensis	?	?	?	?	?	?	?	?	?	?
K.radulescui	?	0	?	0	1	?	?	?	?	?
H.belgica	?	?	?	?	?	?	?	?	?	?
H.pyrenaica	?	?	?	?	?	?	?	?	?	?
Kielanodon	?	?	?	?	?	?	?	?	?	?
Iberodon	?	?	?	?	?	?	?	?	?	?
Pinheirodon	?	?	?	?	?	?	?	?	?	?
Bernardodon	?	?	?	?	?	?	?	?	?	?
New Fossil	?	?	?	?	?	?	?	?	?	?

	101	102	103	104	105	106	107	108	109	110
Sinoconodon	0	0	?	?	?	?	?	0	0	0
Morganucodon	0	0	?	?	?	?	?	0	0	0
Thomasia	?	?	?	?	?	0	0	?	?	?
Haramiyavia	?	?	?	?	?	0	0	0	0	0
Rugosodon	?	?	2	0	0	0	0	0	0	0
Paulchoffatia	?	?	?	?	?	?	?	0	0	0
Meketichoffatia	1	0	0	0	0	0	0	?	?	?
Henkelodon	?	?	0	0	0	0	?	?	?	?
Meketibolodon	?	?	?	?	?	?	?	0	0	0
Guimarotodon	?	?	?	?	?	?	?	0	0	?
Kuehneodon	?	?	0	0	0	0	0	0	0	0
Pseudobolodon	?	?	0	?	?	?	?	?	?	?
Ctenacodon	?	?	0	0	0	0	0	0	0	0
Glirodon	?	?	0	0	0	0	0	?	?	?
Bolodon	?	?	0	0	0	0	0	0	0	0
Plagiaulax	?	?	?	?	?	?	?	1	0	0
Zofiabaatar	?	?	?	?	?	?	?	0	0	0
Sinobaatar	?	?	2	0	0	0	0	0	0	0
Eobaatar	?	?	0	0	0	0	0	?	?	?
Jeholbaatar	?	0	2	0	0	0	0	0	0	0
Heishanobaatar	?	?	?	?	?	?	?	0	0	0
Liaobaatar	?	?	?	?	?	?	?	0	0	0
Hakusanobaatar	?	?	0	?	?	?	?	?	0	?
Arginbaatar	?	?	1	?	?	?	?	0	0	0
Bryceomys	?	?	?	?	0	0	0	?	?	?
Boffius	?	?	2	2	0	0	?	?	?	?
Meniscoessus	?	?	?	3	1	0	0	?	?	?
Buginbaatar	?	?	?	?	1	1	1	?	?	?
Cimolodon	?	?	2	2	0	1	0	0	?	0
Ectypodus	1	0	2	2	0	1	[1 2]	0	1	0
Mesodma	?	?	?	?	0	1	?	0	1	?
Ptilodus	1	0	2	2	0	1	2	0	0	0
Neoliotomus	?	?	2	2	0	1	2	?	?	?
Filikomys	1	0	3	3	0	1	1	0	1	0
Pentacosmodon	?	?	?	?	?	?	2	0	0	1
Microcosmodon	?	?	?	?	0	0	?	?	?	?
Catopsbaatar	0	1	2	2	1	0	1	0	1	2
Kamptobaatar	1	0	3	3	0	0	1	0	1	1
Chulsanbaatar	1	0	2	2	[0 1]	[0 1]	2	1	1	1
Kryptobaatar	0	1	2	2	0	[0 1]	2	0	1	1
Nemegtbaatar	1	0	2	3	1	1	2	0	1	1
Eucosmodon	?	?	?	?	?	?	?	0	0	?
Stygimys	?	?	2	2	0	1	1	1	1	1
Taeniolabis	1	1	4	4	1	1	1	?	1	1
Lambdopsalis	1	1	4	4	2	1	1	0	1	1
Sphenopsalis	?	?	4	4	2	[0 1]	0	?	?	?
Prionessus	?	?	4	4	?	1	1	0	0	?
Catopsalis	?	?	4	4	1	0	1	0	0	?
Yubaatar	?	?	0	3	2	1	0	0	0	1
K.ungureanui	1	0	1	1	0	0	0	0	?	?
B.transylvanicus	1	0	1	1	0	0	0	0	0	?
B.oardaensis	?	?	1	0	0	0	0	?	?	?
K.radulescui	?	?	1	0	0	0	0	?	?	?
H.belgica	?	?	1	[0 1]	0	0	?	?	?	?
H.pyrenaica	?	?	1	0	0	0	?	?	?	?
Kielanodon	?	?	0	2	1	0	?	?	?	?
Iberodon	?	?	?	?	0	0	0	?	?	?
Pinheirodon	?	?	?	?	0	0	0	?	?	?
Bernardodon	?	?	?	?	0	0	0	?	?	?
New Fossil	?	?	?	?	?	?	?	?	0	?

	111	112	113	114	115	116	117	118	119	120
Sinoconodon	0	0	?	?	?	0	1	0	0	?
Morganucodon	0	0	?	?	?	0	1	0	0	?
Thomasia	0	?	?	?	?	?	?	?	?	?
Haramiyavia	0	?	?	0	?	?	?	0	0	?
Rugosodon	0	0	0	0	0	1	0	0	0	?
Paulchoffatia	0	0	0	0	?	?	?	0	0	?
Meketichoffatia	?	?	?	?	?	?	0	0	?	?
Henkelodon	?	?	?	?	0	1	0	0	?	?
Meketibolodon	0	0	0	0	?	?	?	0	0	?
Guimarotodon	0	0	0	0	?	?	?	0	0	?
Kuehneodon	0	0	0	0	1	?	0	0	0	?
Pseudobolodon	?	?	?	?	?	?	0	?	?	?
Ctenacodon	0	0	0	0	?	?	0	?	0	?
Glirodon	?	?	?	?	?	0	0	0	?	?
Bolodon	0	0	?	0	?	?	0	0	0	?
Plagiaulax	0	0	0	0	?	?	?	0	0	?
Zofiabaatar	0	0	0	0	?	?	?	0	0	?
Sinobaatar	0	0	0	0	?	2	0	0	0	?
Eobaatar	?	?	?	0	?	?	0	0	0	?
Jeholbaatar	0	0	0	0	0	2	0	0	0	?
Heishanobaatar	0	0	0	0	?	?	?	0	0	?
Liaobaatar	0	0	0	0	?	?	?	0	0	?
Hakusanobaatar	?	?	?	?	0	2	0	0	?	?
Arginbaatar	?	?	?	0	?	?	0	0	?	?
Bryceomys	?	?	?	?	?	?	?	0	0	?
Boffius	?	?	?	?	?	?	?	?	?	?
Meniscoessus	?	?	?	0	?	?	?	1	0	?
Buginbaatar	?	?	?	?	?	?	?	0	?	?
Cimolodon	0	0	?	0	?	?	?	0	?	?
Ectypodus	0	0	0	0	?	?	0	?	0	?
Mesodma	0	0	?	0	?	?	?	0	0	0
Ptilodus	0	0	1	0	?	?	0	0	0	1
Neoliotomus	0	?	?	?	?	?	?	?	?	?
Filikomys	0	0	1	0	?	2	0	0	0	0
Pentacosmodon	0	0	0	1	?	?	?	1	0	?
Microcosmodon	?	0	0	1	?	2	?	1	0	?
Catopsbaatar	1	1	1	0	?	0	0	0	0	?
Kamptobaatar	0	1	1	0	?	0	0	0	0	?
Chulsanbaatar	0	1	0	0	?	0	0	0	0	?
Kryptobaatar	0	0	0	0	?	0	0	0	0	0
Nemegtbaatar	0	?	1	0	?	0	0	0	0	0
Eucosmodon	?	?	?	1	?	?	0	0	?	?
Stygimys	1	0	0	1	0	?	0	0	0	?
Taeniolabis	1	1	0	0	?	0	?	0	1	?
Lambdopsalis	1	1	0	0	?	0	?	0	0	0
Sphenopsalis	?	?	?	?	?	?	?	0	0	?
Prionessus	?	?	?	0	?	0	?	0	0	?
Catopsalis	?	?	0	0	?	0	?	0	1	?
Yubaatar	0	0	0	0	?	?	0	0	0	?
K.ungureanui	?	?	?	?	?	2	?	0	?	?
B.transylvanicus	1	0	0	0	?	2	1	0	0	0
B.oardaensis	?	?	?	0	?	2	1	0	0	?
K.radulescui	?	?	?	0	?	2	1	?	0	?
H.belgica	?	?	?	?	?	?	1	0	0	?
H.pyrenaica	?	?	?	?	?	?	?	0	0	?
Kielanodon	?	?	?	?	?	?	1	?	?	?
Iberodon	?	?	?	?	?	2	?	0	0	?
Pinheirodon	?	?	?	?	?	[1 2]	?	0	0	?
Bernardodon	?	?	?	0	?	[1 2]	?	0	0	?
New Fossil	?	?	?	0	?	?	?	?	?	?

	121	122	123	124	125	126	127	128	129	130
Sinoconodon	0	0	0	?	?	?	?	?	?	?
Morganucodon	0	0	0	?	?	?	?	?	?	?
Thomasia	?	?	0	?	?	?	?	?	?	?
Haramiyavia	?	?	0	?	?	?	?	?	?	?
Rugosodon	?	?	0	0	0	0	0	?	0	0
Paulchoffatia	?	?	0	?	?	?	?	?	?	0
Meketichoffatia	1	0	?	0	0	0	0	?	0	?
Henkelodon	?	?	?	0	0	0	0	?	0	?
Meketibolodon	?	?	0	?	?	?	?	?	?	0
Guimarotodon	?	?	0	?	0	?	?	?	?	0
Kuehneodon	?	?	0	0	0	0	0	1	0	0
Pseudobolodon	1	2	?	0	0	0	?	?	0	?
Ctenacodon	?	?	0	1	0	1	0	?	0	0
Glirodon	?	?	0	0	0	1	0	?	0	0
Bolodon	?	?	0	1	0	1	0	?	0	?
Plagiaulax	?	?	0	?	?	?	?	?	?	0
Zofiabaatar	?	?	?	?	?	?	?	?	?	0
Sinobaatar	?	1	0	1	0	2	0	?	1	1
Eobaatar	?	?	0	1	0	2	0	?	1	1
Jeholbaatar	2	1	0	1	0	2	0	?	1	1
Heishanobaatar	?	?	0	?	?	?	?	?	?	1
Liaobaatar	?	?	0	?	1	2	0	?	?	1
Hakusanobaatar	?	?	0	0	0	1	1	?	1	?
Arginbaatar	?	?	1	0	0	1	0	?	1	0
Bryceomys	?	?	0	1	?	2	1	?	0	0
Boffius	?	?	?	?	1	0	1	?	?	?
Meniscoessus	1	?	0	1	?	1	0	0	0	0
Buginbaatar	?	?	0	?	?	2	1	?	?	?
Cimolodon	?	?	0	0	0	1	1	0	0	0
Ectypodus	1	?	0	0	0	1	1	0	0	0
Mesodma	?	?	0	0	?	2	1	0	0	0
Ptilodus	1	?	0	0	0	1	1	0	0	0
Neoliotomus	?	?	0	0	0	1	1	0	0	0
Filikomys	?	?	0	0	0	2	1	0	0	0
Pentacosmodon	?	?	0	0	?	[1 2]	0	?	0	0
Microcosmodon	?	?	0	0	?	2	1	?	0	0
Catopsbaatar	?	?	0	0	0	2	1	2	0	0
Kamptobaatar	1	?	0	0	0	2	1	0	0	0
Chulsanbaatar	1	1	0	0	0	2	1	0	0	0
Kryptobaatar	1	2	0	0	0	2	1	0	0	0
Nemegtbaatar	1	?	0	0	0	2	1	0	0	0
Eucosmodon	?	?	0	0	?	1	1	?	0	0
Stygimys	?	?	0	0	0	1	2	?	0	0
Taeniolabis	?	?	?	0	?	[1 2]	0	?	0	0
Lambdopsalis	2	1	0	0	?	0	0	?	0	0
Sphenopsalis	?	?	0	0	?	?	0	?	0	0
Prionessus	?	?	0	0	?	?	0	?	0	0
Catopsalis	?	?	0	0	0	[1 2]	0	?	0	0
Yubaatar	?	?	0	0	0	2	?	0	0	0
K.ungureanui	?	?	?	0	1	2	0	?	0	?
B.transylvanicus	?	?	0	0	1	2	0	0	1	0
B.oardaensis	?	?	0	0	1	[1 2]	0	0	[0 1]	0
K.radulescui	?	?	0	0	1	[1 2]	0	0	[0 1]	0
H.belgica	?	?	0	0	1	2	0	0	[0 1]	0
H.pyrenaica	?	?	?	0	1	1	0	?	0	0
Kielanodon	?	?	?	0	0	0	0	?	?	?
Iberodon	?	?	0	0	?	0	0	?	1	0
Pinheirodon	?	?	0	0	?	0	0	?	1	0
Bernardodon	?	?	0	0	?	0	0	?	1	0
New Fossil	?	?	0	?	?	?	?	?	?	?

	131	132	133	134	135	136	137	138
Sinoconodon	?	?	0	?	?	?	?	?
Morganucodon	0	?	0	?	?	?	?	0
Thomasia	?	?	?	?	?	?	?	?
Haramiyavia	?	?	?	?	?	?	?	0
Rugosodon	1	0	1	?	?	?	?	?
Paulchoffatia	?	0	0	0	0	0	0	0
Meketichoffatia	?	?	?	?	?	?	?	?
Henkelodon	0	?	?	?	?	?	?	?
Meketibolodon	?	0	1	0	0	0	0	1
Guimarotodon	?	1	0	0	0	0	0	1
Kuehneodon	0	0	0	0	0	0	0	2
Pseudobolodon	?	?	?	?	?	?	?	?
Ctenacodon	?	[0 1]	[0 1]	1	1	0	0	0
Glirodon	?	0	1	?	1	?	1	0
Bolodon	?	0	0	1	1	1	1	?
Plagiaulax	?	0	1	1	1	1	1	?
Zofiabaatar	?	1	1	0	1	0	0	2
Sinobaatar	0	2	1	?	1	?	0	1
Eobaatar	?	0	0	?	1	?	1	?
Jeholbaatar	?	0	1	?	1	0	1	?
Heishanobaatar	?	2	1	0	1	0	1	1
Liaobaatar	?	0	1	0	1	0	1	1
Hakusanobaatar	?	?	?	?	1	?	1	?
Arginbaatar	?	0	1	?	1	?	1	?
Bryceomys	?	?	?	?	?	?	?	?
Boffius	?	?	?	?	?	?	?	?
Meniscoessus	?	0	2	?	?	?	?	2
Buginbaatar	?	?	?	?	?	?	?	?
Cimolodon	0	0	?	?	?	?	?	?
Ectypodus	0	0	2	?	?	?	?	?
Mesodma	0	0	?	?	?	?	?	0
Ptilodus	0	0	2	?	?	?	?	2
Neoliotomus	?	?	?	?	?	?	?	?
Filikomys	?	0	?	?	?	?	?	?
Pentacosmodon	?	2	1	?	?	?	?	?
Microcosmodon	?	0	1	?	?	?	?	?
Catopsbaatar	?	2	2	?	?	?	?	2
Kamptobaatar	?	2	2	?	?	?	?	2
Chulsanbaatar	0	0	2	?	?	?	?	?
Kryptobaatar	0	0	1	?	?	?	?	?
Nemegtbaatar	0	1	2	?	?	?	?	2
Eucosmodon	?	0	1	?	?	?	?	?
Stygimys	?	0	2	?	?	?	?	?
Taeniolabis	0	1	2	?	?	?	?	2
Lambdopsalis	0	1	2	?	?	?	?	?
Sphenopsalis	?	?	?	?	?	?	?	?
Prionessus	?	?	?	?	?	?	?	2
Catopsalis	?	2	2	?	?	?	?	1
Yubaatar	0	2	1	?	?	?	?	?
K.ungureanui	?	?	?	?	?	?	?	?
B.transylvanicus	?	0	1	?	?	?	?	2
B.oardaensis	?	?	?	?	?	?	?	?
K.radulescui	?	0	1	?	?	?	?	?
H.belgica	?	?	?	?	?	?	?	?
H.pyrenaica	?	?	?	?	?	?	?	?
Kielanodon	1	?	?	?	?	?	?	?
Iberodon	?	?	?	1	1	1	1	?
Pinheirodon	?	?	?	1	1	0	0	?
Bernardodon	?	?	?	1	1	0	0	?
New Fossil	1	1	0	1	1	1	1	1

CAMBELAS QUARRY

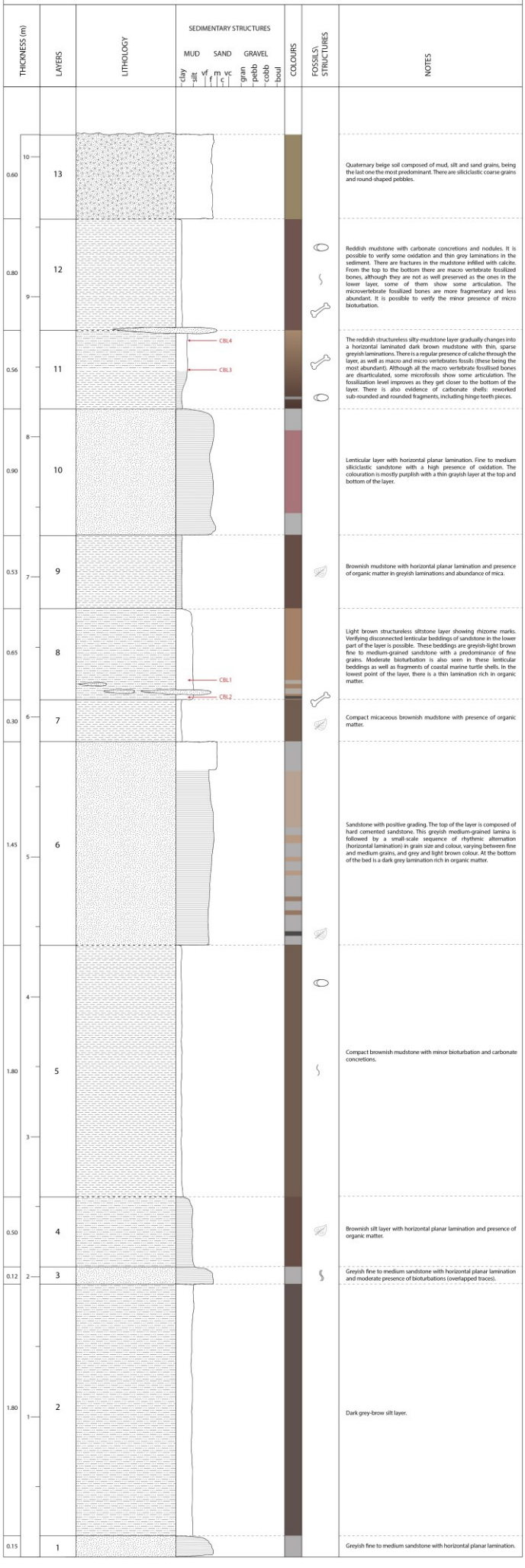

CAMBELAS QUARRY 2